Numerical modelling of autoignition chemistry kinetics in computational fluid dynamics

Ban, Marko

UNIVERSITY OF ZAGREB
FACULTY OF MECHANICAL ENGINEERING
AND NAVAL ARCHITECTURE

NUMERICAL MODELLING OF AUTO-IGNITION CHEMISTRY KINETICS IN COMPUTATIONAL FLUID DYNAMICS

DOCTORAL THESIS

Mentor:

Prof.dr.sc. NEVEN DUIĆ **MARKO BAN**

ZAGREB, 2011.

BIBLIOGRAPHY DATA:

UDC:	519.876.5
Keywords:	Computational fluid dynamics, combustion, auto-ignition, tabulation, chemical kinetics
Scientific area:	Technical sciences
Scientific field:	Mechanical engineering
Institution:	Faculty of Mechanical Engineering and Naval Architecture (FMENA), University of Zagreb
Principal supervisor:	Dr.sc. Neven Duić, Associate Professor
Number of pages:	140
Number of figures:	35
Number of tables:	10
Number of references:	144

Jury members:

Dr.sc. Zoran Lulić (FMENA, Zagreb), Associate Professor
Dr.sc. Neven Duić (FMENA, Zagreb), Associate Professor
Dr.sc. Želimir Kurtanjek (PBF, Zagreb), Full Professor
Dr.sc. Daniel Rolph Schneider (FMENA, Zagreb), Associate Professor
Dr. Peter Priesching (AVL AST, Graz)

Acknowledgments

This work was carried out at the Department of Energy, Power Engineering and Environment in the Faculty of Mechanical Engineering and Naval Architecture, University of Zagreb.

First, I would like to express my gratitude to the supervisor of this thesis, Professor Neven Duić, for the opportunity, guidance, patience and support throughout this work.

I would also like thank the AVL AST team in Graz, Dr. Reinhard Tatschl, Dr. Peter Priesching, and others in the CFD development group, for the continuous support and accessibility. Continuous meetings and their suggestions helped in a great deal to shape this dissertation. I would also like to acknowledge the financial support of AVL AST Zagreb. Very special thanks in this regard to its director, Mr. Goran Mirković.

I am very thankful for the valuable comments from jury members, Professors Zoran Lulić, Želimir Kurtanjek and Daniel Rolph Schnieder. I would also like to extend my appreciation to my collegues, Dr. Milan Vujanovic, who also played a part in finalizing this work, Dr. Mario Baburić, Luka Perković and Hrvoje Mikulčić for always helpful, and most often fun, discussions. Many thanks go to all members at the Department of Energy, Power Engineering and Environment.

My parents, who supported this venture, deserve also the deepest gratitude.

Last, but not least, I am extremely grateful to my wife, Ljiljana, for always being there for me.

Zagreb, June 2011.

Marko Ban

Prediction is very difficult, especially if it's about the future.

Niels Bohr

Contents

Preface

Energy crisis we are facing today is a result of constant population growth and industrial development, causing an enormous global energy demand coupled by fuel production stagnation. Combustion of fossil fuels is still the major driving force of energy production, but also the greatest source of pollution. The environmental downsides, being more and more visible each day are fought by prescribing more stringent regulations in nearly the same rate.

These regulations , combined with increased living standard, together put a high strain to the development of new combustion systems (using conventional-fossil fuel) requiring lower pollutant emission and performing at the same, but preferably higher, level to remain competitive in an economic sense. Such requirements demand a new, detailed, insight into the details of every aspect of the newly developed practical combustion systems. Mechanical design of key components on one side and combustion process regulation on the other, are now utilizing the increase of computer power to meet aforementioned demands. Methods developed in the last thirty years are becoming essential tool for anyone desiring to be competitive in the research and development field. Simulation tools are able to give a sound estimates to compare different designs but also providing a deeper insight into combustion related phenomena which can motivate the research of novel designs based on the new data. Experimental investigation and prototyping are usually time, and funds, consuming processes, and using any computer tools is now not simply a secondary commodity of the top research institutions, but a crucial step in the development process.

Computational fluid dynamics (CFD) has proved itself to be a reliable, versatile, tool with a broad spectrum of application. Combustion modeling, as a part of the CFD, is also being used at a basic research level for obtaining the crucial information used for increasing both the efficiency of the developed system and the environmental aspects.

Abstract

The research in this work aims at improving application of the simulation of fuel ignition, focusing on the low-temperature auto-ignition phenomenon. The simulation of low temperature ignition has been typically achieved by using computationally demanding calculations of complex chemistry kinetics. This work attempts to reproduce the effects of complex chemistry by developing the methodology of efficient database creation consisting of the relevant ignition data used by existing combustion models.

The research was separate in several phases: pre-processing, tabulation with data post-processing, and finally the implementation in the CFD software. In the pre-processing stage, available reaction mechanisms of most popular fuels have been thoroughly investigated and compared focused on their accuracy and complexity. Criteria for low- and high-temperature ignition were discussed as implemented into the tabulation application. In the post-processing part of the tabulation, several methods of data manipulation are suggested in forms of correlation functions and repair algorithms, used on the incomplete databases.

Additionally, an approach of using existing data for two fuels to calculate the ignition values for their blend dependant only on the previously stored values and the blending factor is presented for the case of a fuel with varying research octane number.

Finally, the database implementation into the CFD software is presented and validated. The validation was done in two stages. Initially the implemented data was compared against the results of the homogeneous reactor calculations using a comprehensive mechanism and in the final stage the model was used in a real-life case and successfully validated proving the viability of the entire process.

Sažetak

Glavna namjera istraživanja ovog rada je izvesti numerički učinkovite algoritme za modeliranje zapaljenja goriva s posebnim fokusom na fenomen niskotemperaturnog zapaljenja. Numerička simulacija niskotemperaturnog zapaljenja dosad se uglavnom postizala računalno zahtjevnim izračunima složene kemijske kinetike, dok će ovaj rad pokušati razviti nove postupke učinkovite izrade baza podataka koje sadrže informacije o efektima složene kemijske kinetike potrebne za simulaciju zapaljenja goriva.

Istraživanje je jasno podijeljeno u nekoliko faza: pred-procesiranje, tabelacija s post-procesiranjem podataka, te na kraju implementacija u CFD aplikaciju. U prvoj fazi, pred-procesiranju, detaljno su predstavljeni dostupni reakcijski mehanizmi za popularna goriva, te su isti međusobno uspoređeni prema njihovoj točnosti i kompleksnosti. Zatim je prikazan način modeliranja nula-dimenzijskog proračuna s kriterijima određivanja nisko- i visokotemperaturnog zapaljenja. U sljedećoj fazi, post-procesiranju, predloženi su alati za manipulaciju izračunatim podacima, s posebnim fokusom na popunjavanje krnjih baza podataka korelacijskim funkcijama i matematičkim algoritmima.

Dodatno, predložen je i način korištenja postojećih podataka za pojedina goriva pri izračunavanju karakterističnih veličina za njihovu smjesu. U tom se slučaju koriste samo vrijednosti za izgaranje svako goriva (čistog) i faktor miješanja. Princip je provjeren na gorivu varijacijom istraživačkog oktanskog broja.

Na kraju, prikazana je implementacija u CFD aplikaciju te je ista i validirana u dvije faze. Prvo je napravljena usporedba s proračunom homogenog kemijskog reaktora s kompleksnim reakcijskim mehanizmom a na samom kraju i primjer stvarne komore izgaranja što je pokazalo valjanost modela i cijele procedure.

Prošireni sažetak

Energetska kriza s kojom smo suočeni, posljedica je ubrzanog gospodarskog i populacijskog rasta u svijetu. Ista je uzrokovana velikom potražnjom za energijom dodatno potenciranom stagnacijom produkcije fosilnih goriva. Fosilna su goriva još uvijek glavni energent, no isto tako i glavni izvor onečišćenja. Negativne posljedice njihovog korištenja pokušavaju se smanjiti na globalnoj razini uvođenjem raznih regulacijskih odredbi.

Međunarodne odredbe posljednjih godina nameću sve stroža ograničenja na emisije polutanata i potrošnju goriva uređaja koji koriste izgaranje fosilnih goriva. Takve odredbe, u kombinaciji s rastom životnog standarda stavljaju dodatni pritisak na razvoj novih uređaja koji izgaraju konvencionalna goriva. Zadatak je inženjera u razvoju tih uređaja zadovoljiti propisane granice štetnih emisija, a isto tako zadovoljiti potražnju tržišta većom efikasnošću i boljim performansama. Ti strogi zahtjevi traže sasvim novi, detaljniji uvid u svaki aspekt dizajna i razvoja novih sustava izgaranja. Uobičajeno se to čini poboljšavanjem sustava regulacije procesa uređaja ili tehničkim dizajnom ključnih komponenata, koji se u današnje vrijeme sve više oslanjaju na rastuću računalnu snagu. Metode razvijene u posljednjih tridesetak godina postaju osnovni alati svakome tko danas iole želi biti kompetitivan u području istraživanja i razvoja. Simulacijski alati sposobni su dati kvalitetne procjene razlika pojedinih inženjerskih rješenja, ali također pružaju novi, detaljan uvid u fenomene vezane uz izgaranje koji može poslužiti kao dodatna motivacija i inspiracija za nove ideje. Eksperimentalna istraživanja i izrada prototipova najčešće su vremenski, ali i financijski, zahtjevni, te računalni alati s tog aspekta više ne predstavljaju privilegiju vrhunskih razvojnih timova, već su postali osnovni i, ponekad, ključni korak u razvojnom procesu.

Računalna dinamika fluida (RDF), računanjem usrednjenih Navier-Stokesovih jednadžbi, postala je nezaobilazan alat u današnje vrijeme. Ona omogućuje bolje razumijevanje procesa izgaranja u modernim inženjerskim sustavima, a usto se na brz i isplativiji način mogu ispitati promjene u dizajnu

uređaja. Da bi se što vjernije simulirao proces izgaranja potrebno je na neki način obuhvatiti sve kemijske fenomene koji se pri izgaranju događaju. Veći dio modela izgaranja koristi osnovni set kemijskih jednadžbi koji kvalitativno daje rezultate kada nije potreban detaljan uvid u srž fenomena izgaranja, dok se za detaljnije promatranje treba ipak osloniti na uvrštavanje što detaljnije kemijske kinetike, što povlači i veće korištenje računalnih resursa. Stoga se noviji modeli izgaranja koriste postupcima pred-tabeliranja pojedinih fenomena koje donosi kompleksna kemijska kinetika. U ovom slučaju pažnja se posvećuje fenomenu samozapaljenja koji je u mnogo slučajeva jedan od glavnih pokretača izgaranja (kako poželjan, tako i neželjen). Analizom samozapaljenja goriva dolazi se do daljnje problematike nisko-temperaturnog zapaljenja koje je i glavna motivacija ovog rada. Dosad se nisko-temperaturno zapaljenje uglavnom promatralo u modeliranju kemijske kinetike pri razvoju reakcijskih mehanizama, no vrlo rijetko kao praktična primjena u poboljšanju modela izgaranja koji se koriste za simuliranje konkretnih problema.

Kada se razmatra razvoj modela izgaranja koji pokušavaju reproducirati realne efekte, pregled dosadašnjih istraživanja postaje dvojak. S jedne strane treba promotriti sam razvoj modela izgaranja, dok je s druge strane znanost koja se bavi razvojem reakcijskih mehanizama izgaranja pojedinih goriva. Naravno, obje teme se međusobno isprepliću.

Sam proces izgaranja ugrubo se može podijeliti na predmiješano i nepredmiješano izgaranje. Prvi se dijeli na izgaranje koje je vođeno zapaljenjem uslijed povoljnih uvjeta u gorivoj smjesi (tlak, temperatura, sastav) te ono koje započinje vanjskim utjecajem u određenoj točki prostora (iskra). Nepredmiješano izgaranje se događa kada postoje razdvojene zone goriva i zraka te reaktivna zona između njih. Naravno, samo izgaranje snažno ovisi u uvjetima unutar komore izgaranja te su razvijeni modeli koji pokušavaju obuhvatiti što je veći broj različitih stanja unutar tog sustava. Dvo-zonski *flamelet* model, primjerice, predlaže opisivanje nepotpunog miješanja u kontrolnom volumenu razdvajanjem neizgorenih plinova u odvojena područja nemiješanog goriva i zraka te potpuno

izmješanih koje tada preuzima model samozapaljenja i propagirajućeg plamena. Eulerian Particle Flamelet model (EPFM) dopušta istovremeno promatranje više nestacionarnih *flamelet*-a, uz simultano računanje Navier-Stokesovih jednadžbi u RDF kodu, te je napose primjenjiv u slučaju turbulentnih nepredmiješanih plamenova. U novije vrijeme vrlo je rasprostranjena upotreba funkcije gustoće vjerojatnosti (*probability density function approach*) u obliku transportiranih *pdf* gdje se ne rade pretpostavke glede oblika funkcije gustoće vjerojatnosti miješanja (mixture fraction) već se ona direktno prenosi koristeći Monte-Carlo postupak. *Flame surface density* modeli (FSD) – općeniti model gustoće plamena uključuje sve moguće vrijednosti udjela goriva, dok su brzine reakcije dane kao baza podataka tranzijentnih difuzijskih plamenova.

Presumed Conditional Moment pristup (PCM), te u novije vrijeme razvijen i DF-PCM (difuzijski plamen + PCM), predstavljaju pojednostavljenu verziju *Conditional Moment Closure* pristupa (CMC) gdje se pretpostavlja uvjetovani moment varijable napredovanja reakcija a uvjetovane brzine reakcija dane su posebnim izračunom baza podataka predmiješanih i nepredmiješanih stacionarnih *flamelet*-a. Kao posljednji model izgaranja, tro-zonski *Extended Coherent Flame Model* (ECFM-3Z) pretpostavlja dvije zone izgoreno-neizgoreno i tri zone miješanja (čisti zrak, čisto gorivo te zona potpunog miješanja), čime omogućuje kvalitetan opis kako samozapaljenja, tako i propagirajućeg i difuzijskog plamena uz korištenje tabeliranih vrijednosti za korektnu simulaciju trenutka zapaljenja.

Velik dio spomenutih modela izgaranja u nekom obliku koristi pred-tabelirane vrijednosti specifičnih kemijskih efekata. Za to su pak potrebni kvalitetni reakcijski mehanizmi. Tri su razine složenosti reakcijskih mehanizama - složeni, reducirani i skeletalni. Složeni mehanizmi pokušavaju za određeno gorivo (ili smjesu goriva) uključiti što je moguće više poznatih kemijskih reakcija da bi se proces izgaranja što vjernije reproducirao. Primjerice, reakcijski mehanizmi korišteni za izgaranje velikog broja ugljikovodika višeg reda nisu primjereni za direktno korištenje u računalnoj dinamici fluida zbog prevelikog broja dodatnih jednadžbi koje nameću. U tu svrhu razvijaju se reducirani mehanizmi koji

pokušavaju što je više pojednostaviti složene, zadržavajući fizikalno/kemijsku relevantnost pojedinih reakcija (s obzirom na ciljani efekt redukcije). Na kraju, skeletalni modeli su najjednostavniji (brojem reakcija i kemijskih vrsta) ali su najčešće napravljeni matematički, bez obzira na važnost pojedinih reakcija, i usko su „specijalizirani“ za reprodukciju točno određenih efekata.

Hipoteza rada i opis istraživanja

Modeliranje samozapaljenja jedan je od važnih elemenata svakog modela izgaranja. Poboljšavanjem istog, primjerice dodavanjem detaljnog opisa nisko-temperaturnog zapaljenja, moguće je popraviti i rezultate cjelokupnog modela. Isto tako, bitno je proceduru tabeliranja podataka za izračunavanje objediniti postupkom koji će omogućiti pojednostavljenu izradu baze podataka efekata samozapaljenja neovisno o složenosti reakcijskog mehanizma koji se želi koristiti, čineći tako integrirani pristup relativno jednostavnim za korištenje u širem spektru primjene u praktičnim problemima.

Istraživanje obuhvaćeno ovim radom podijeljeno je u nekoliko koraka. Kao što je ranije naznačeno, cilj je poboljšanje reprodukcije efekata složene kemijske kinetike u obliku koji je praktično primjenjiv – kako u pogledu brzine izvođenja tako i sa stanovišta korištenja računalnih resursa.

U prvom dijelu istraživanja, provedena je analiza mogućih pristupa automatskoj i samostalnoj proceduri izrade tablica koje sadrže potrebne podatke za kasnije uvrštavanje u matematički model izgaranja. Tu su promatrani dostupni matematički modeli i računalna rješenja, i na kraju prikazana metodologija primijenjena u samostalnom kodu za automatsku tabelaciju. Problematika samozapaljenja inicijalno je promatrana u nula-dimenzijskom okruženju, dakle ovisno samo o temperaturi, tlaku, sastavu u pojedinom vremenskom trenutku, da bi se jednoznačno odredili postupci za dva ključna elementa tokom zapaljenja. Prvo, bitno je kvalitetno i točno „uhvatiti“ trenutak samozapaljenja (kako nisko-temperaturnog, tako i visoko-temperaturnog), te sa stanovišta automatske

tabelacije podataka, kvalitetno odrediti kriterij zaustavljanja pojedinog izračuna. Pri izradi su se koristili matematički modeli koji računaju parametre Arrheniusovog modela, koeficijent brzine i energije aktivacije, brzine proizvodnje (ili potrošnje) kemijskih vrsta , te su isti iskorišteni pri izračunu izgaranja u sustavu energetskih jednadžbi u slučaju problema s konstantnim volumenom. Nakon analize trenutačnih dostignuća na ovom području, ispitano je nekoliko kriterija za praćenje trenutka zapaljenja. Kao najčešće korišteni kriterij, praćenje fiksnog povećanja temperature u nekom vremenskom intervalu, zbog činjenice da u nekom slučajevima ne uspijeva „uhvatiti“ nisko-temperaturno zapaljenje, zamijenjen je drugim pristupom. Kriterij infleksije na krivulji temperatura/vrijeme pokazao se kao robusno rješenje koje dovoljno precizno „hvata“ i nisko- i visoko-temperaturno zapaljenje, ali se nakon analize podataka koji se koriste u RDF rješavaču i modelu izgaranja, vidjelo da se s tim pristupom dobivaju kasnija vremena zapaljenja (objašnjeno detaljnije kasnije u tekstu). Konačni kriterij, detaljnije prikazan u poglavlju 2.2, predstavlja kombinaciju ova dva pristupa te je i jednako robustan za primjenu u tabelaciji, a daje i rješenja koja primijenjena u modelu izgaranja daju točnije rezultate. U istom je poglavlju dana i usporedbena analiza utjecaja pojedinih parametara na samozapaljenje i to na primjeru nekoliko goriva. Ova analiza kasnije će biti iskorištena za formuliranje algoritama popravljanja nepotpunih tablica.

U ovom dijelu istraživanja također je provedena opsežna usporedbena analiza dostupnih reakcijskih mehanizama, u poglavljima od 2.10.1 do 2.10.6, kako sa stanovišta samog procesa zapaljenja tako i sa stanovišta brzine izgaranja. Najveći je fokus bio na dizelskim gorivima, koja su inicijalno i motivirala ovo istraživanje, odnosno n-heptan kao kemijski surogat. Osim n-heptana,komparativno su prikazani i reakcijski mehanizmi za izo-oktan, etanol, dimetil-eter i metan, kao vrlo interesantna alternativna goriva. Ova analiza ukazala je na važnost poznavanja tematike od strane korisnika, jer odabir pravog mehanizma znači popriličan kompromis između veličine istog (što se može izjednačiti s brzinom izvođenja tabelacije), te točnosti rješenja koja se dobivaju.

Kao grubo pravilo postavljeno uzeta je činjenica ad kompleksnost pojedinog mehanizma ujedno znači i njegovu točnost. Ovo ne mora nužno značiti da se jednostavnijim mehanizmima dobivaju rezultati koji se ne mogu koristiti, ali daje mogućnost da se, uz pregled literature, kompleksni mehanizmi mogu koristiti kao referenca pri izboru optiomalnog. Automatska tabelacija ovisi i o numeričkoj stabilnosti izračuna korištenjem pojedinih mehanizama te je analiziran i taj aspekt.

Svi aspekti vezanu uz tabelaciju prikazani su u poglavlju 2.11. Izrađene tablice će sadržavati četiri podatka važna za kasniju implementaciju u RDF kod: vrijeme nisko- i visoko-temperaturnog zapaljenja te oslobođene topline u oba trenutka. Tablica za svako gorivo je izrađena sekvencijalnim izvođenjem proračuna koncentriranog modela varijacijom četiri parametra: temperature, tlaka, sastava određenog koeficijentom pretička zraka i eventualnog udjela recirkulirajućih produkata izgaranja (exhaust gas recirculation - EGR). Tablica je na kraju sačuvana kao četvero-dimenzionalna matrica sačinjena od gore navedena četiri elementa zapaljenja (AI = AI (T, p, l, egr)).

Numeričke nestabilnosti uslijed varijacija pojedinih parametara, što proračune za pojedina goriva (odnosno, reakcijske mehanizme) dovodi u područje za koje nisu predviđeni, dovode do nepotpunih podataka. Zbog takvih slučajeva provedena je analiza postojećih rezultata, te su predloženi algoritmi i korelacijske funkcije kojima se postojeći rezultati, izračunati u stabilnim režimima, koriste za popunu nedostajućih, kako je prikazano u poglavljima 2.11.5 i 2.11.6. Ovi algoritmi, odnosno korelacijske funkcije, koriste saznanja dobivena iz ranijih analiza utjecaja pojedinih parametara na rješenja te se poštivanjem propisanih trendova relativno jednostavno može izračunati čak i veća količina podataka koja nedostaje. Kod korelacijskih funkcija, primjerice, korištena je činjenica da povećanje količine produkata izgaranja (kao rpiblizni model recirkuliranja ispušnih plinova) negativno utječe na brzinu samog izgaranja te je predložena jednostavna funkcija koja se može koristiti ne samo za popravak manjkave tablice, već unaprijed i za smanjenje potrebne količine proračuna.

Kao važan doprinos pojednostavljivanju procesa tabelacij kompleksnijih goriva, u poglavlju 2.11.7, analizirana je mogućnost korištenja postojećih tablica za dva različita goriva i korištenje istih za izračunavanje vrijednosti trenutaka zapaljenja za slučaj njihove smjese. Kao rezultat analize predložena je funkcija ovisnosti trenutka zapaljenja smjese samo o vrijednostima za čista pojedina goriva te koeficijent njihova miješanja (0-1). Važno je napomenuti da je ova funkcija razvijena uz pomoć vrlo kompleksnog reakcijskog mehanizma koji specifično sadrži i paralelni oksidacijski mehanizmi za smjesu goriva, te se ista ne može koristiti za drugu kombinaciju goriva. Ovakav pristup omogućuje brzo i relativno točno ispitivanje utjecaja mješavine goriva u sustavu, bez potrebe za prethodnom, dugotrajnom tabelacijom za pojedinu kombinaciju goriva.

Nakon izrade koda koji obuhvaća sve gore navedene elemente napravljene su tablice za sva promatrana goriva, uz, primjerice za n-heptan tabelacija s tri reakcijska mehanizma s različitim stupnjevima kompleksnosti, kako je prikazano u poglavlju 3.1. Iste su zatim implementirane u postojeći RDF kod koji koristi ECFM-3Z model izgaranja (kratko opisan na početku ovog poglavlja). Model izgaranja je detaljnije opisan u poglavlju 2.13, nakon što su osnovne informacije o modeliranju strujanja dane u prethodnom (2.12). U ovom modelu izgaranja, tabelirani podaci, u binarnom obliku, ulaze u transportnu jednadžbu predkursora zapaljenja. U trenutku kad je rad započeo verzija ECFM-3Z modela u softverskom paketu FIRE uključivala je samo trenutak visoko-temperaturnog zapaljenja. Autori modela su efekt nisko-temperaturnog zapaljenja dodali uvodeći još jednu varijablu u tabelaciju (varijablu napredovanja reakcija – *progress variable*) čime se čitav sustav dodatno komplicira. Jedna od hipoteza ovog rada je i da se princip po kojem se računa trenutak visoko-temperaturnog zapaljenja može uspješno iskoristiti za kvalitetnu reprodukciju i nisko-temperaturno zapaljenja tako da se zadrži jednostavnost i procesa tabelacije a i same implementacije u model izgaranja. U ovom slučaju dodan je još jedan pred-kursor zapaljenja koji u obzir uzima tabelirani trenutak nisko-temperaturnog zapaljenja, te kada dostigne vrijednost lokalnog udjela neizgorenog goriva pokrenuti proceduru izgaranja u kojoj sudjeluju

tabelirane vrijednosti oslobođene topline. Pošto se pri nisko-temperaturnom zapaljenju ne potroši svo gorivo u kontrolnom volumenu, ove vrijednosti se koriste za određivanje količine goriva koja se konzumira nakon čega se privremeno prekida proces izgaranja. Slijedi praćenje pred-kursora za visoko-temperaturno zapaljenja koji, kada kao i ovaj prethodni ne dostigne određenu razinu, pokreće daljnje elemente modela izgaranja kojima se konzumira preostalo gorivo.

Nakon implementacije niskotemperaturnog zapaljenja u ECMF-3Z model, uslijedila je provjera iste kako je prikazano u poglavlju 3.2. Provjera se radila u na jednostavnoj mreži kontrolnih volumena u nekoliko koraka. Kao početni uvjeti prvo su postavljeni parametri korišteni pri tabelaciji. Prikaz vremenske raspodjele temperature na kojem se jasno vide trenuci nisko-temperaturnog i visoko-temperaturnog zapaljenja biti će glavni kriterij pri određivanju valjanosti prethodno opisanog unapređenja modela izgaranja. Ista mreža i isti parametri biti će korišteni s postojećim modelom izgaranja da bi se pokazala kvalitativna razlika u rezultatu. Razvijeni model provjerit će se na nekoliko karakterističnih točaka, prvo s vrijednostima parametara koje su korištene u tabelaciji, da bi se ispitala točnost implementacije, zatim s pojedinim parametrima izvan tabeliranog spektra da se ispita valjanost četverodimenzionalnog interpolacijskog algoritma, te najzad variranjem svih parametra da se provjeri osjetljivost modela.

Kao završni korak, modificirani model je ispitan na kompleksnijoj geometriji praktičnog sustava izgaranja, te su rezultati uspješno validirani, kako je prikazano u poglavlju 3.3.

Doprinos rada

Ovaj je rad rezultirao poboljšanjem postupaka kojima se opisuje izgaranje u nepredmiješanom i predmiješanom režimu, dodavanjem efekta nisko-temperaturnog zapaljenja postojećem matematičkom modelu zadržavajući jednostavnost implementacije i korištenja.

Također, prikazan je i opsežan kvalitativan pregled i usporedba dostupnih reakcijskih mehanizama za nekoliko danas važnih goriva, te je time olakšan izbor reakcijskog mehanizma za različite potrebe. Razvijena je aplikacija koja je dovoljno robusna i točna da izračuna karakteristične veličine nisko- i visoko-temperaturnog zapaljenja neovisno o vrsti goriva i kompleksnosti reakcijskog mehanizma koji se koristi. Na ovaj se način omogućuje relativno brzo i jednostavno korištenje modela s gorivom za koje trenutačno ne postoji tablica. U sklopu rada napravljene su tablice za nekoliko karakterističnih goriva, od tekućih konvencionalnih do alternativnih i plinovitih.

Razvijena je jednostavna procedura za tabelaciju te su predloženi alati kojima se eventualne numeričke greške jednostavno uklanjaju.

Dodatno, predložena je i funkcija za računanje karakterističnih veličina za smjesu goriva koja koristi samo postojeće vrijednosti prethodno izračunate za slučaj izgaranja svakog pojedinog čistog goriva te faktor miješanja. Ovim pristupom značajno se ubrzava proces ispitivanja utjecaja mješavine goriva, pošto se preskače cjelokupni postupak tabelacije (koji za slučaj mješavine nužno iziskuje korištenje kompleksnijeg mehanizma).

Keywords

Computational fluid dynamics, combustion, auto-ignition, tabulation, chemical kinetics

Ključne riječi

Računalna dinamika fluida, izgaranje, samozapaljenje goriva, tabelacija, kemijska kinetika

List of figures

List of tables

Nomenclature

Roman	Description	Unit
a	Coefficient in Troe form	
	polynomial coefficient	
A	Pre-exponential constant in the Arrhenius equation	
	Surface	m^2
	Model constant	
b	Coefficient in Troe form	
B	Model constant	(s)
c	Coefficient in Troe form	
	progress variable	
$C_{\varepsilon 1}, \ldots$	empirical constants	
C_M	Effective third body concentration	$kmol/m^3$
$\overline{C_p}^0$	Mean standard statemolar heat capactity at constant pressure	J/kmol K
c_v	Mean specific heat capacity	J/kg K
d	Coefficient in Troe form	
D	Diffusion rate	kmol/s
	Sink in the flame surface density transport equation	
D_{ij}	Strain rate tensor component	1/s
e	Specific energy	J/kg
E	Activation energy in the Arrhenius equation	J/kmol
F	Broadening factor in Lindemann form	
	Function (of ignition delay)	
F_{cent}	Falloff parameter in Troe equation	
f_i	Cartesian component of the force vector	m/s^2
G	Production term in equation for the turbulent kinetic energy	$kg/(ms^3)$
$\overline{H}^0$	Mean molar standard state enthalpy	J/kmol K
h_k	Specific enthalpy	J/kg
I	Total number of reactions	
K	Number of species in a reaction	
K_t	Intermittent turbulence net flame stretch	kg/m^3s

k	Thermal conductivity	W/(mK)
	Turbulent kinetic energy;	m^2/s^2
k_0	Forward rate coeff. in Lindemann form (low press)	m^3/kmol s
k_∞	Forward rate coeff. in Lindemann form (high press)	1/s
k_f	Forward rate coefficient of a reaction	J/kmol K
m	Mass	kg
$\dot{M}$	Mass flux	kg/s
n	amount	kmol
n_j	Cartesian component of the unit normal vector	
N	Variable in Troe form	
O_{stoich}	Stoichiometric amount of oxidizer needed for combustion	
p	pressure	Pa
P	Production term in equation for the turbulent kinetic energy	kg/(ms^3)
	Source terms in flame surface density transport equation	
P_r	"reduced pressure" in Lindemann form	
R	Universal gas constant (R = 8314.4)	
q_i	Rate of progress of reaction i	kmol/m^3s
q_j	Cartesian component of the heat flux vector	W/m^2
S	Surface	m^2
	Source term	
$\bar{S}^0$	Mean molar standard state entropy	J/kmolK
Sc	Schmidt number	
S_L	Laminar flame velocity	m/s
t	time	s
T	Temperature	K
u	Velocity	m/s
u_j	Cartesian velocity	m/s
V	Volume	m^3
V_k	Diffusion velocity	m/s
W_k	Molar weight	kg/kmol
x	Co-ordinate direction	
	Number of carbon atoms in species	
x_j	Cartesian co-ordinate	
X_k	Molar fraction of kth species	
y	Co-ordinate direction	

	Number of hydrogen atoms in species	
	Mass fraction	
Y_k	Mass fraction of kth species	
z	Number of oxygen atoms in species	

Greek	Description	Unit
α	Model constant	
β	Temperature exponent in the Arrhenius equation	
	Model constant	
Γ	Diffusion coefficient	
ε	Dissipation rate of the turbulent kinetic energy	m^2/s^3
v	Specific volume	$1/m^3$
υ_{ki}	Stoichiometric coefficient for species k in reaction i	
λ	Thermal conductivity	W/m K
$\dot{\omega}_k$	Chemical production rate of species k	$kmol/m^3$ s
	Combustion source term	kg/s
φ	Equivalence ratio	
	Intensive (scalar) property	
μ	Dynamic viscosity (molecular);	Pa s
ρ	Density	kg/m^3
Σ	Flame surface density	1/m
σ_{ji}	Stress tensor component	N/m^2
$\sigma_k, \sigma_\varepsilon$	empirical constants	
τ_d	Ignition delay	s
τ_{ij}	Tangential stress tensor component	N/m^2

Subscript	Description
o	standard state
	low pressure limit (in Lindemann form)
	state with no residual gases
d	delay

EGR	residual gases
f	forward (in reaction rate coefficient)
	fuel
HT	high temperature
i	reaction
k	species
L	laminar
L,o	laminar - no residual gases
LT	low temperature
M	mixture
ox	oxidizer
react	reactant
S	surface
stoich	stoichiometric
t	turbulent
V	volume
φ	Intensive (scalar) property
∞	High pressure limit (in Lindemann form)

Superscript	Description
$'$	Reynolds fluctuation
$''$	Favre fluctuation
$\sim$	Favre average
$\bar{}$	Reynolds average
o	standard state
	no residual gases
b	burned
u	unburned

Math. symbol	Description
e	= 2.718281828…
exp	Exponential function (e^x)
$\prod$	Product

$\sum$	Summation
$\frac{d}{d}$	Derivation
$\int$	Integration
δ_{ij}	Kronecker tensor component

Abreviation	Description
0D, 1D, 2D, 3D	Zero-, one-, two-, three-dimensional
AI	Auto-ignition
ASCII	American Standard Code for Information Interchange
BDF	Backward Differentiation Formula
CA	Crank Angle
CAI	Controlled Auto-Ignition
CFD	Computational Fluid Dynamics
CFM	Coherent Flame Model
CSP	Computer Singular Perturbation
DF	Diffusion Flame
DGREP	Directed Relation Graph Method with Error Propagation
DME	Dimethyl – Ether
DNS	Direct Numerical Simulation
ECFM(-3Z)	Extended Coherent Flame Model (with three zones)
EGR	Residual gasses
EHVA	Electro Hydraulic Valve Actuation
EPFM	Eulerian Particle Flamelet Model
FGM	Flamelet Generated Manifolds
FSD	Flame Surface Density
FPI	Flame Propagation of ILDM
GRI	Gas Research Institute
HCCI	Homogeneous Charge Compression Ignition
HT	High Temperature
ICE	Internal Combustion Engine
ILDM	Intrinsic Low Dimensional Manifold
ISAT	In Situ Adaptive Tabulation
LES	Large Eddy Simulation
LT	Low Temperature

NTC	Negative Temperature Coefficient
ODE	Ordinary Differential Equation
PDF	Probability Density Function
PF	Propagating Flame
RANS	Reynolds Averaged Navier-Stokes
RON	Research Octane Number
TDC	Top Dead Centre
TKI	Tabulated Kinetics of Ignition

1 Introduction

1.1 Motivation and General Overview

International regulations are becoming more and more stringent regarding pollutant emissions and fuel consumption of fossil fuel combusting devices. The main task of the engineers designing these devices is bringing them within these regulations by improving the efficiency, either by a process upgrade or by changing the physical design of key components.

Computational fluid dynamics (CFD), calculating the averaged Navier-Stokes equations, has become one of the key tools in modern engineering. It facilitates a better understanding of combustion processes in new design concepts, and provides a fast and relatively inexpensive way to test the design variations. To make the combustion simulation as tenable as possible, it is necessary to comprehend all chemical phenomena occurring during the combustion process. A good part of the mathematical combustion models use a basic set of chemical equations that qualitatively provide a result when detailed insight in the core combustion processes is not needed. For more extensive insight, one needs to include as much detailed information of chemistry kinetics as possible. This also means a subsequent increase of computer power demand. Therefore, some of the new combustion models use various methods of pre-tabulation of complex chemistry kinetics. The focus of this work is the phenomenon of auto-ignition, which in many cases is the main governing process of combustion (whether desired or not). Analysis of fuel auto-ignition opens new fields of interest regarding low temperature ignition, which is the main motivation of this work. Until recently, low temperature ignition was mainly contemplated during the development of chemical kinetics models, but not with a practical application that would improve combustion models to better represent real-life problems.

When one considers the development of combustion models aiming to replicate realistic effects, there is a need to look at two sides of the state-of-the-art research. On one hand, there is the development of mathematical combustion models, and on the other hand there is a completely separate science of developing new reaction mechanisms for different fuels, with the two sides are constantly interweaving. The first part of the survey focuses on the combustion models currently being used, followed by a short look at the current state of kinetic of development of chemistry reaction mechanisms.

The combustion process itself can be roughly divided into two basic concepts: premixed and non-premixed combustion. The first concept can be further divided into combustion governed by ignition due to favourable conditions of the species mixture (pressure, temperature, composition), and combustion started by an external source in an exact portion of the domain (spark ignition). Non-premixed combustion occurs when there is a clear separation between the fuel and air zones with a reactive zone between the two. Clearly, combustion is heavily dependant on the conditions inside the combustion chambers, and the developed mathematical models try to properly predict the combustion for as many of these conditions as possible.

A two-zone flamelet model, for instance, suggests the approach of defining the partially premixed behaviour inside a computational cell by separating the unburned gasses in separate regions of unmixed fuel and air, and regions with fully mixed fuel and air in which a model of autoignition takes place followed by a propagating flame combustion. The Eulerian Particle Flamelet Model (EPFM) allows simultaneous tracking of more unsteady flamelets, solving Navier-Stokes equations at the same time in the CFD code, making it especially applicable in the case of turbulent non-premixed flames. Also, a widely used approach is the usageof Probability Density Functions (PDFs), recently in a Transported pdf approach where one does not presume the shape of the probability density function of the mixture fraction but rather directly transports it using Monte-Carlo method. Flame surface density models (FSD) represent a generalized flame surface density model

including all possible values of mixture fraction, with reaction rates presented in database form for transient diffusion flames.

The Presumed Conditional Moment approach (PCM), as well as recently developed Diffusion-Flame PCM (DF-PCM) present a simplified version of the Conditional Moment Closure approach (CMC), whereby one assumes the conditional moment of a reaction progress variable. Reaction rates are also supplied by a database created for premixed and non-premixed stationary flamelets. The last modelling approach taken into consideration here is the Three Zone Extended Coherent Flame model (ECFM-3Z), which assumes two zones of burned-unburned and three zones of mixing (pure air, pure fuel, and completely mixed zone), enabling a good qualitatively description of autoignition, propagating flame and diffusion flame.

Most of these approaches in some way use pre-tabulated values for specific combustion effects. To calculate these values one needs quality chemical reaction mechanisms. There are three levels of chemical kinetics mechanism complexity. Complex (or comprehensive) mechanisms try, for a specific fuels (or set of fuels), include as much as possible known chemical reactions to reproduce the combustion process of a certain fuel to the fullest extent possible. For example in [1][2], such mechanism are described which are used for combustion of a number of higher order carbohydrates, but are not suitable for direct use in a CFD simulation due to the amount of added transport equations needed to be solved. For this purpose, reduced mechanisms for a single fuel, with specific effects taken into consideration, are developed, reducing the amount of chemical reactions but preserving the physical/chemical relevancy of the remaining reactions. Skeletal mechanisms, on the other hand, reduce the complex mechanisms purely mathematically, disregarding the low impact reactions and species (for a desired property) which does not conserve the chemical importance of the remaining reactions. As a result, this model is “specialized” for reproducing specific effects. In [3][4] all major, recently developed mechanisms representing higher order hydrocarbon fuels are briefly described, but one needs to mention also a very

popular mechanism for lower order hydrocarbons, also used in this work [5]. One of the fuels recently in focus, ethanol, has appeared as a part of the aforementioned primary reference fuel (PRF) mechanisms, but it has also been widely used in a specially developed mechanism (also incorporated into PRF mechanisms)[6], and a recently developed one [7].

1.2 Literature Review

In hydrocarbon combustion, different oxidizing schemes can become effective depending on the air–fuel mixture temperature. In the transition stage between low and high temperature oxidation, manifestation of cool flames for some fuels can be observed. These are governed by oxidative mechanisms dominated by exothermic degenerately branching chain reactions involving a number of important long-lived intermediates [8] with competition between termination and branching reactions taking place. The first exhibiting higher activation energies than the latter [9] results in a negative temperature coefficient (NTC) of the reaction rate with the overall reaction rate decreases with increasing temperature[10]. This region is clearly depicted in following chapters along with more detailed insight into the reaction mechanism behaviour under various conditions.

Work on hydrocarbon fuel oxidation kinetics is confined primarily to single-component reference fuels, such as n-heptane and isooctane, and there are no chemical kinetic schemes currently available for more complex, real-life multicomponent mixture fuels (e.g. “actual” diesel fuel)[8]. It is a common practice to use a simulant species to represent a certain complex fuel (e.g. n-heptane for diesel fuel [11]), especially considering autoignition modeling (cetane number is the property of interest here, and with n-heptane’s having a cetane number close to that of diesel[12][13], it is clear why this specific species has been chosen as a surrogate). There is a broad body of literature dealing with the

development of chemical kinetic mechanisms for hydrocarbon fuels, also many covering low-temperature oxidation and autoignition phenomena; examples are the reviews of the existing reduced [4] and detailed [4][14] mechanisms for n-heptane. The detailed autoignition chemical kinetic mechanisms for complex fuels such as n-heptane, described in greater detail in chapter 2.10.1, usually involve hundreds of chemical species and thousands of reactions[15][16][2].

As a result, incorporating such mechanisms into a CFD combustion simulation also involving turbulence or multiphase flow provides a stiff system of nonlinear differential equations imposing a great strain to available computer power with it's own hardware limitations [17]. Therefore, more and more methodologies are being proposed to simplify such detailed mechanisms without losing the essential chemical information [17]. They are either aimed at reducing the mechanism to a size reasonable to be included as a part of CFD simulation, or at developing techniques to use the more complex mechanisms for gathering specific data for use in subsequent computer simulations, simplifying the direct integration process [8]. As it was done during this work, the time-consuming chemical numerical calculations are performed a priori in pre-processing stage and the respective results, after being stored in a multidimensional database ("lookup table"), are easily retrieved by a CFD code [18].

The direct use of complex chemistry in CFD is possible, but it still remains very computationally expensive [18]. Other approaches also exist, such as flamelet [19][20][21][22] and RIF models [18][23][24] but also pose a relatively high computational demands. Mathematical reduction techniques have, therefore, been suggested, such as ILDM (Intrinsic Low-Dimensional Manifolds)[19][25][26] or ISAT (In Situ Adaptive Tabulations [27]). Even if the methods show promising progress in terms of efficient chemistry phenomena representation, they are still under development and also remain intensely computationally demanding[18]. Finally, an approach, benefiting from a full pre-tabulation of complex chemistry was proposed, and is the basis of this work. It is also utilized in techniques such as FPI (Flame Prolongation of ILDM) [26][28][29] or FGM (Flamelet Generated

Manifolds) [30]. The FPI approach, as reported by the literature sources, was initially developed in the context of stationary constant pressure adiabatic combustion devices but was then extended to non adiabatic constant pressure cases [29].

In the scope of the most complex domains, in terms of computational grid constantly changing affecting the chamber contents properties, the piston engine, the TKI (Tabulated Kinetics of Ignition) approach was used, tabulating the auto-ignition delay and heat release at constant pressures[31]. It was used in the framework of the ECFM3Z (Extended Coherent Flame Model 3 Zones) combustion model allowing successful predictions of auto-ignition in Diesel engines and more particularly in representing the influence of fuel composition[32][33][34]. This approach was extended further to a full FPI tabulation based on constant volume homogeneous reactors was proposed [35] to also include the description of species mass fractions during auto-ignition and after, showing that the species mass fractions predictions were accurate during auto-ignition occurring close to top dead centre (TDC) when there is practically no combustion chamber volume variation.

The CFD techniques used to solve the Reynolds Averaged Navier-Stokes (RANS) equations, as in more detail described in following chapters, have become nowadays a useful tool for manufacturers of any kind of combustion systems as they allow a better understanding of how combustion takes place in new combustion concepts and allowing rapid and low cost testing of different combustion chamber geometries and concepts in order to design the final product.
Classically, RANS combustion models have been clearly divided into premixed combustion models (e.g. gas turbines or spark ignition engines with gasoline fuel) and non-premixed combustion models (e.g. majority of industrial burners or Diesel engines)[32][36][37].
Basically, three main combustion modes encountered in industrial devices can be defined [38]. The first two modes are of the premixed type; a premixed charge of air and fuel can auto-ignite after a finite amount of time (called auto-ignition

delay), and is essentially controlled by temperature, pressure, fuel/air equivalence ratio and residual gases mass fraction. This type of combustion controls the beginning of combustion in, e.g., Diesel engines and can also be found in spark ignition engines as an undesirable combustion commonly called knock. The second premixed combustion mode is the premixed Propagation Flame (PF) used in spark ignition engines which occurs in the combustion chamber filled with a premixed blend of fuel and air ignited by a spark plug generating a small spherical propagation flame between the electrodes. The flame afterwards propagates in the combustion chamber until the fuel/air mixture has been totally consumed. The third combustion mode is the non-premixed combustion, also referred to as Diffusion Flame (DF). In this case, fuel and air are separated by a thin reaction zone in which burned gases are formed. The chemical time in the reactive zone is usually considered much smaller than the diffusion time involved in the diffusion of fuel and air towards the flame region, which is why this combustion mode is also called mixing controlled combustion [32][38].

In a real Diesel engine, for example, combustion process cannot be solely considered as non-premixed: the onset of combustion is controlled by partially premixed autoignition which is responsible for the rapid initial pressure rise in the chamber. This type of combustion can represent an important part of the total heat release in the cycle, depending on the engine operation point. Also, the new combustion concepts such as Controlled Auto Ignition (CAI) or Homogeneous Charge Compression Ignition HCCI are not clearly identified as premixed or nonpremixed combustion [32][39]. For both concepts auto-ignition is responsible for the start of combustion, but as the experiments have shown, afterwards, during combustion, the charge is not perfectly mixed [40], thus allowing the possibility of combustion proceeding simultaneously through propagating and diffusion flame.
Therefore, a need to develop combustion models with the ability to simultaneously take into account more than one type of combustion (preferably all three) has led to the development of the new generation combustion models.

Initially, an extended characteristic-time model accounting for chemical and turbulent time scales simultaneously has been proposed [41]; for example, in a classical Diesel engine, combustion is first controlled by the chemical time (AI period), and then by the turbulent time (diffusion flame combustion)[32]. In this model both premixed and non-premixed combustion modes are reported to be taken into account, but the mixing of the species is represented solely by a mixing time scale. This way, the history of mixing is not represented correctly and the transition between the chemically controlled and mixing controlled combustion is monitored by an empirical function, not really accounting for the premixed flame combustion. Mentioned as a next approach is the two zone flamelet model (referenced earlier) [22] which separates the computational cell into two zones in terms of unburned gases – separate regions therefore exist containing unmixed and fully mixed fuel and air. The latter region is the one being consumed in the model definition by autoignition and propagating flame. This model has been reported to correctly represent the initial mixing of unburned fuel and air used to rapidly ignite [42]. After this initial mixing occurs, the second phase takes place, with the chemical time being smaller than the mixing time leading to non-premixed combustion. However, even with including the representation of the mixing zone, this model only roughly estimates the volume occupied by this region not really allowing most accurate computation of species mass fractions, temperature or density. This causes some of the properties being also approximately estimated (e.g. laminar flame velocity, auto-ignition delay) finally causing difficulties when post-flame kinetics in the burned gases need to be performed.

In the flamelet approach, developed initially by [43][44][45], these properties have been represented in more rigorous manner, with reaction rate being tabulated (for a laminar diffusion flame against the mixture fraction for different scalar dissipation rates). Also probability density function (pdf) approach is being utilized here to integrate the reaction rate over all possible values of mixture fraction. Finally, this model incorporates the influences of the local

mixture fraction gradients from the flow field but also providing the representation of the finite rate chemistry.

The flamelet approach was consecutively extended by [46][47] developing the Eulerian Particle Flamelet Model (EPFM) which is able to simultaneously calculate a couple of unsteady flamelets which are solved in a separate, dedicated, flamelet code having the Navier-Stokes equation solved as a part of the CFD solver at the same time [48]. This model averages the mixing and combustion since the flamelets are also based on the averaged properties in the entire domain. Increasing the number of flamelets involved in the calculation also rapidly increases the computational cost. Additionally, this model does not account the propagating flame combustion.

The computational cost is the limiting factor also for the Conditional Moment Closure approach, initiated by [49][50][51]. In this approach mixture fraction is also the centre point of the model, but unlike in the other approaches it is not represented solely by the mean value and fluctuation, but in a discretized space. Mixing processes and combustion are solved conditioned for different values of mixture fraction. This approach, used mainly for non-premixed combustion cases can also be used for calculation of premixed flame combustion, but another dimension must be added (the reaction progress) which would further add to the complexity and computational demand.

Further approach considered is the transported pdf approach, which, as it could be assumed from its name, does not imply an assumption on the shape of the mixture fraction probability density function, but it is rather directly transported using Monte-Carlo methods. These models are also computationally demanding, and also relatively complex to develop, but have gained some interest and have been used to some extend [52][53].

Finally, recent approaches have tried to propose the models with lower computational demand compared to the ones presented earlier, and also to accurately represent the properties of auto-ignition delays and diffusion flames relying also on the flamelet libraries [54]. They consider only the dimensions of

mixing, which is represented by mean mixture fraction and its fluctuation and the mean progress variable and its fluctuation (which represents the dimension of advancement of reaction). The group of approaches interesting to this study are the flame surface density models, the presumed conditional moment approach (PCM) and the coherent flame models, one of which being also the ECFM-3z model in more detail described later in the text. The approach is not a novelty, being initially proposed by [55] in context of diffusion flames [56]. Later on, the idea has been extended by the work of [57] proposing the exact balance equation for the flame surface density, and also by considering a generalised flame surface density, proposed by [58] which includes all possible values of mixture fraction, and reaction rates (per unit of flame surface) calculated from a library of transient diffusion flames.

The presumed conditional moment approach from [59][60] is not an extension of the conditional moment approach, but rather a simplification presuming the conditional moments of the progress variable and calculating the conditional reaction rates and species utilizing the flame prolongation of the ILDM (FPI) approach [61]. This was based on the pre-tabulation of premixed and non-premixed stationary flamelets.

In practical applications, especially for new low emission combustion concepts such as HCCI engines, the cool flame heat release significantly contributes to the total heat release [31]. The mixture in this case is implied to be nearly homogeneous at an early time in the engine cycle having a temperature not high enough to trigger fast auto-ignition. Considering only a single delay ignition (not taking the low temperature ignition into consideration without its heat release) may draw an erroneous calculation of the main auto-ignition.

As it has been shown in [62], this approach would only be valid if calculations were made at constant pressure since the complex chemistry database has been built with constant pressure simulations [31]. In the second case, regarding the constant volume system, also including the variation of the volume in a deforming computational domain, the main ignition delay is clearly shortened

with the heat released during the cool flame period significantly modifying the thermodynamic conditions (pressure and temperature increase) and composition of the mixture. Consequently, this increases the rates of chemical reactions after the delay both in the constant volume and in the constant pressure case (evenwithout early heat release), but this effect is strongly enhanced by the existence of the low temperature ignition.
The necessity to take into account the heat released during the cool flame period is highlighted if the main ignition delay is to be correctly estimated in all situations [62].

1.3 Hypothesis and Work Outline

Autoignition modelling is a one of the important elements of every combustion model. Improving it, by adding a separate description of low temperature combustion makes it possible to improve the results of an entire model. It is thus important to develop an effective tabulation procedure independent of chemical kinetics model complexity, making it an integrated approach simple to use in a wider spectrum of practical applications.

The research involved in this work is divided into several phases. As mentioned earlier, the goal is to improve the reproduction of the complex chemistry effects in a form which is practically applicable, both in terms of required computational demands and time.

In the first phase of the research, an analysis of the possible approaches to automatic and autonomous methodology of database creation was carried out. Available mathematical models and software was surveyed at this stage, which resulted in a stand-alone application able to compute an ignition process regardless of the initial data and chemistry complexity. The ignition issue was observed in a dimensionless environment, dependant only on current temperature, pressure, composition and time, to unambiguously define the methods used for two key points in the ignition calculation. First, it is important to correctly capture the moment of ignition (both low- and high-temperature) and from a point of

automatic tabulation, devise a quality calculation stopping criterion for a single computation. The mathematical library used to calculate chemistry kinetics from mechanisms using Arrhenius coefficients for calculation of species production (destruction) will be used in a constant volume case.

In this phase of the research, a comprehensive comparative analysis of the available chemical reaction mechanisms was also performed, both from the point of the simulation of the ignition process, and also from the point of obtaining the flame velocity. As the automatic tabulation heavily depends on the numerical stability of the calculations, this aspect of the chemical reaction mechanism was analysed in addition to developing a mathematical procedures to complete the partially filled tables. Created tables store four items necessary for further inclusion in the CFD code: low and high temperature ignition, and heat releases respectively. The tables are created varying four initial parameters: temperature, pressure, composition defined by the fuel equivalence ratio and residual gas mass fraction. A final table will thus be represented as a four-dimensional matrix (AI = AI(T,p,f,egr)).

In the case of an incomplete table creation procedure (due to the mathematical instability in some cases), an analysis of existing data was performed, using mathematical methods to complete the tables with interpolation procedures or correlation functions developed aiming to link the existing data from a stable tabulation regime (i.e. higher residual gas mass fraction could be expected to cause the instabilities) with the rest of the table. Also, an effort to interconnect existing tables for pure fuels in a case of a fuel blend was made to get the ignition time of a blend as accurately as possible, without the need to use a complex mechanism combining both fuels and adding another initial parameter thus heavily increasing the computation demand and overall time of table creation procedure.

After all methods and procedures mentioned above have been developed and validated by creating an ignition tables for several different fuels (with different levels of chemistry mechanism complexity), an effort was made to

implement them into an existing CFD code using the ECFM-3Z model[32] where tabulated data are a part of transport equation of a combustion precursor variable. The current version of ECFM-3Z in the CFD solver of choice for this work had only a high-temperature ignition. The existing approach used for calculating the high temperature precursor was also used for adding the low-temperature precursor with a prescribed amount of fuel consumed after the ignition delay value is reached. After this amount of fuel is consumed, only the high temperature precursor is calculated until the high temperature ignition is reached and the remainder of the fuel is consumed.

After the implementation of low-temperature ignition effects into the ECFM-3Z model, it was tested, debugged and validated on a simple computational grid. The temperature/time dependence was the main criteria to determine the quality of implementation and results. Also, the existing model will be used with the same initial conditions on the same computational grid to display the differences. Validation will be performed in several steps to thoroughly validate the implementation of the model. First, the initial conditions will be exactly the same as the ones used for tabulation to validate the technical quality of implementation. Afterwards, one parameter was set outside the values used for tabulation, varying the parameters. Next, all parameters were set outside the values used for tabulation with several variations to analyze the sensitivity of the model. Finally, a full scale test on a more complex example (with available previously validated data for comparison) was performed.

1.4 Expected Scientific Contribution

It is expected that this work will improve the methodology describing the combustion in premixed and non-premixed mode by adding the effect of low temperature ignition to existing combustion model. Also a qualitatively extensive insight and comparison of existing chemical reaction mechanisms is provided, for several fuels of interest today, helping the selection of reaction mechanism for

wider scope of applications. A robust application for ignition data tabulation, providing valid low- and high-temperature ignition results, regardless of the fuel used, or the complexity of selected reaction mechanism. It enables a relatively quick and straightforward use of a fuel species for which there is no created table yet. During the work on this thesis ignition databases for several specific fuels of interest have been created, ranging from conventional liquid to alternative and gaseous.

A straightforward workflow for ignition tabulation has been developed, including tools for post-processing data with new correlation functions and algorithms for filling incomplete tables.

Additionally, a function for calculating the ignition values for fuel blends is suggested, using only the existing values for two pure fuels and the blending coefficient. This approach significantly speeds up the process of testing the influence of different blends of two fuels (in this case variation of fuel research octane number), since it does not require completely new tabulation by adding a new parameter (and necessary usage of complex mechanism specifically intended for such purpose).

2 Methodology

2.1 General 0D Approach

2.1.1 CHEMKIN basics

In this study of auto-ignition phenomenon, a FORTRAN subroutine library CHEMKIN™ II was used assuming zero dimension and adiabatic changes. It is generally used to predict the time-dependent kinetics behaviour of a homogenous gas mixture in a closed system [63]. There are many possibilities for the chemical kinetics problems that one may need to solve for various applications using this package. The problems interesting to this study are:

- An adiabatic system with constant pressure;
- An adiabatic system with constant volume.

During the calculation of a homogeneous reactor case, the net chemical production rate of each species results from a competition between all the chemical reactions involving that species. Each forward reaction coefficient is in the modified Arrhenius form [63][64][65][66][67]:

$$k_f = AT^{\beta} \exp\left(\frac{-E}{RT}\right), \qquad (2\text{-}1)$$

where the activation energy E, the temperature exponent β and the pre-exponential constant A represent the parameters in the model formulation. These parameters are obtained from a binary file, created by a special interpreter code reading in the values assembled in a textual file in the following standard format used by most reaction mechanism developers :

```
h+o2 = o+oh    1.915E+14   0.00  1.644E+04
         rev /  5.481E+11   0.39 -2.930E+02 /
```

The above example shows one reversible reaction with all parameters for the equation (2) both for forward and reverse case. Total chemical production rate is calculated from all competing reactions by the equation:

$$q_i = k_{f_i} \prod_{k=1}^{K} [X_k]^{\upsilon_{ki}'} - k_{r_i} \prod_{k=1}^{K} [X_k]^{\upsilon_{ki}''}, \qquad (2\text{-}2)$$

where υ_{ki} represents sroichiometric coefficient for the species k in the reaction i (in the above equation marked differently for forward and backward reactions) . Finally the expression for molar production/destruction of each species in each step of temporal discretization (summed for all reactions in which the species k is participating) is:

$$\dot{\omega}_k = \sum_{i=1}^{I} \upsilon_{ki} q_i. \qquad (2\text{-}3)$$

In the above reaction υ_{ki} represents the total stoichiometric coefficient calculated as a difference of forward and reverse ones.

All the species who enter a reaction, but are not actively participating (being produced or consumed) are called “third bodies” and the reactions therefore addressed to as “third body reactions”, usually representing a dissociation or recombination processes. It also covers catalytic species (such as Pb) which participate, but do not change the reaction. The “third body” species are represented with the letter ***M*** in the reaction.

A specific case regarding the determination of forward/backward rate coefficients is pressure dependence. CHEMKIN library distinguishes two types of reactions: the ones with molar rates increasing with the pressure (unimolecular/recombination fall-off) and the one with the opposite pressure influence (chemically activated bimolecular). For example, one could encounter a reaction which has a one form at a specific higher pressure values, and on the other

hand, for low pressures demands the existence of a third body. In this case, it is necessary to determine the behavior between these two cases. Two methods are used, *Lindemann* and *Troe* forms. The first one incorporates the approach of defining the rate constants for low and high pressures in the following forms:

$$k_0 = A_0 e^{\frac{-E_0}{RT}}, \qquad k_\infty = A_\infty e^{\frac{-E_\infty}{RT}}. \tag{2-4}$$

For the intermediate pressures, rate constant is defined as

$$k = k_\infty \left[\frac{P_r}{1+P_r}\right], \tag{2-5}$$

with P_r denoting a "reduced pressure" given by

$$P_r = \frac{k_0 C_M}{k_\infty}, \tag{2-6}$$

where C_M is the effective third body concentration (it would present the total concentration if all third body efficiencies are equal to 1 and different from the total concentration if there are non-unity efficiencies for at least one species). One should note that the units of k_0 and k_∞ differ from each other (k_0 has units of $\frac{l}{mol\ s}$ while k_∞ has units of $\frac{l^2}{mol^2\ s}$ which accounts for the third body concentration term). Subsequently, Troe developed a more complex pressure dependence definition based on an extensive experiments and analytical work, which is finally introduced in a form of the falloff parameter F_{cent} dependant on the four constants (also provided in the mechanism definition file):

$$F_{cent} = (1-a)e^{-\frac{T}{b}} + ae^{-\frac{T}{c}} + e^{-\frac{d}{T}}, \tag{2-7}$$

giving the temperature dependence of F_{cent}, the factor by which the rate constant of a given unimolecular reaction at temperature T and reduced pressure Pr (defined above in equation (2-6)) is less than the value of $\frac{k_\infty}{2}$ which it would have if the unimolecular reactions behaved according to the Lindemann formulation. The Lindemann form is further extended by introduction of a broadening factor F (in Lindemann case it is equal to 1) computed from F_{cent} by the equation:

$$logF = \frac{logF_{cent}}{1 + \left[\frac{logP_r + C}{N - 0.14(logP_r + C)}\right]^2}, \qquad (2\text{-}8)$$

with following variables

$$N = 0.75 - 1.27logF_{cent} \text{ and } C = -0.4 - 0.67logF_{cent}.$$

Finally, the rate coefficient k is calculated by multiplying the Lindemann formula with F.

In the chemistry mechanism it could happen that there two chemical reactions exist having the same reactants and products. CHEMKIN library interpreter would normally interrupt the operation and exit with an error, unless the difference between the reactions (they would usually have a different rate parameters) is implied by the reserved keyword (DUP).

Besides the mechanism data, the homogeneous reactor also requires the thermodynamic properties for all species defined in the mechanism. Thermodynamic properties are calculated using the widely used NASA polynomials with polynomial constants usually given in a separate file (in the CHEMKIN version used in this work, older form of the polynomials, with seven constants is applied). The polynomial form is defined as:

```
h                120186h   1              g  0300.00   5000.00  1000.00      1
 0.02500000e+02 0.00000000e+00 0.00000000e+00 0.00000000e+00 0.00000000e+00    2
 0.02547163e+06-0.04601176e+01 0.02500000e+02 0.00000000e+00 0.00000000e+00    3
```

```
 0.00000000e+00 0.00000000e+00 0.02547163e+06-0.04601176e+01                4
```

Low and high temperature regions each have their own sets of constants. The enthalpy, entropy and heat capacities (at the standard state) are, respectively, calculated using the following equations:

$$\frac{\overline{C_p}^0}{\mathcal{R}} = a_1 + a_2 T + a_3 T^2 + a_4 T^3 + a_5 T^4, \tag{2-9}$$

$$\frac{\bar{H}^0}{\mathcal{R}T} = a_1 + a_2 \frac{T}{2} + a_3 \frac{T^2}{3} + a_4 \frac{T^3}{4} + a_5 \frac{T^4}{5} + \frac{a_6}{T}, \tag{2-10}$$

$$\frac{\bar{S}^0}{\mathcal{R}} = a_1 lnT + a_2 T + a_3 \frac{T^2}{2} + a_4 \frac{T^3}{3} + a_5 \frac{T^4}{4} + a_7 . \tag{2-11}$$

Other thermodynamic properties can be easily calculated from the ones defined above.

2.2 Autoignition

Autoignition calculations, as the basic phenomenon investigated in this work were performed using the homogeneous constant volume reactor. The governing equations in this case are the energy equation which simplified to the following form [63]:

$$c_v \frac{dT}{dt} + v \sum_{k=1}^{K} h_k \dot{\omega}_k W_k = 0 , \tag{2-12}$$

and species conservation equation with constant mass:

$$\frac{dY_k}{dt} = v \dot{\omega}_k W_k, \tag{2-13}$$

with the mean specific heat of the mixture of c_v, temperature T, specific volume v, enthalpy h_k and molar weight W_k. Molar production rate $\dot{\omega}_k$ is calculated as defined in the equation (2-3).

Since monitoring the cool flame phenomenon was one of the main topics of this work, a methodology to create a general routine to be able to recognize both the cool flame and main ignition had to be developed. Available literature suggests several methods to determine the main ignition time, which will also be mentioned here, but finally a combination of criteria has been implemented to also sustain the subsequent implementation of the calculated values into the CFD combustion model. There are basically three types of ignition determination methods:

- predefined temperature, or pressure (in constant volume case) increment ΔT (Δp);
- temperature inflexion criteria;
- tracking the changes of an intermediate species.

The latter method was disregarded in this work, sine the aim was to develop a sturdy routine to be used as a part of the tabulation procedure with as little user required intervention as possible. In the case of intermediate species tracking the user should first run series of calculations to determine the species suitable for the task, dependant on the mechanism used. Also, even after determination of such a species it wouldn't guarantee a correct determination of the ignition delays in the entire desired initial parameter spectrum[68]. Furthermore, to also obtain the low temperature ignition delays, in most cases one should use a different tracking species (and additionally perform initial investigation to find which species to use in this case).

A useful basic definition of the ignition delay time was obtained from [69] which states that it could be presented as the time at which the temperature theoretically becomes infinite (the asymptote of the temperature curve). This definition, regarded in the lights of a real ignition calculation transforms to the

criteria of the temperature/time inflexion. In this work, in terms of a mixture property which is used to determine the ignition time, the temperature is selected, making the selection of the chemical reactor type (constant pressure or constant volume) not important, and the procedure entirely generalized. The inflexion criteria between two consecutive temporal discretization steps could generally be represented by the equation[70]:

$$sign\left(\frac{d^2T}{dt^2}\right)_t = -sign\left(\frac{d^2T}{dt^2}\right)_{t-dt}. \qquad (2\text{-}14)$$

This equation tracks the change of direction of the temperature curve slope and, at the occurrence of the sign change, triggers the ignition flag and stores information in the database. Inflexion criteria proved to be relatively stable and reliable from the purely numerical perspective, with the calculations providing smooth temperature curve valid for an inflexion criteria testing even between two consecutive temporal points. The only problem in this respect was encountered in several cases, usually mechanism related, in specific range around 1000 K where the temperature curve would provide several misleading ignition delay candidates. This problem is easily solved, first by filtering out the erroneous values and, as explained later in the text, the manner in which the values as stored in the tabulation database.

Second approach to ignition determination utilizes the predefined temperature increment, monitoring the temperature/time curve, and when found it is also, as in the previous case, stored in the database. However, in certain cases, usually in borderline values of the parameters (especially the higher values of residual gasses) temperature curve has lower gradients thus making the real ignition delay (determined by the inflexion) higher than the one indicated by the temperature increase. Having in mind the methodology behind the usage of stored values in the CFD combustion model, this approach proved to be very useful despite the mentioned flaws.

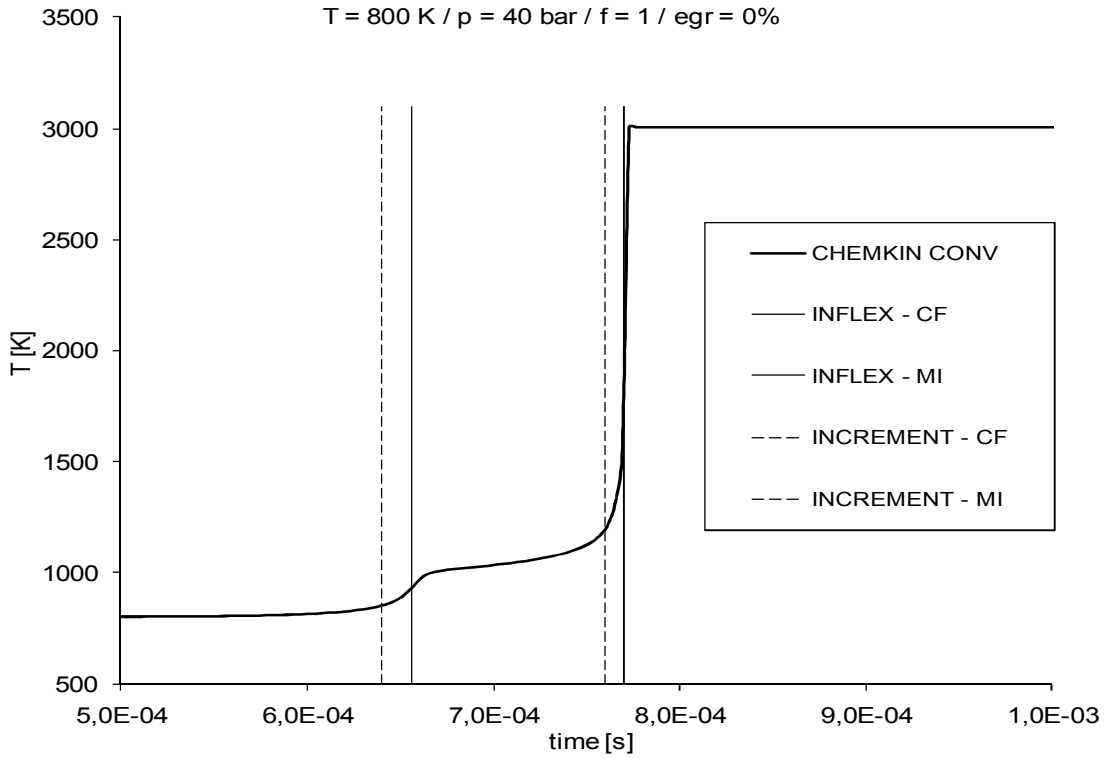

Figure 2-1 Ignition tracking criteria compared

Several different criteria was finally implemented in the code to make it possible to get both the low temperature and main ignition delay times, as well as to filter out the misleading ignition-time candidates at the beginning of the calculation and around 1000 K. Fist approach was to use the temperature gradient which is checked at each time step according to equation (2-14) and if an inflexion occurred the current time-step value was stored into a resulting variable. Also, to comply to the methodology used by combustion mechanism, inflexion criteria was not the most correct approach in terms of final 3d implementation, and the temperature increment criteria also had to be used. This topic is in detail explained in chapter 3.2.

Furthermore, stopping criteria is also an issue that had to be considered. Since the tabulation calculations had to be performed over a number of initial parameter values, simply setting the fixed time-step value at which the calculation

would stop wasn't the right solution for two main reasons. First is the fact that having lower values for most of the parameters (except the EGR) compared to the other end of the range would provide differences in ignition delay values of almost several orders of magnitude. Making the stopping criteria a value of, for example, 1 second (in terms of internal combustion engine dynamics representing basically a case of "no ignition") would on the other hand make majority of calculations run beyond the main ignition, thus wasting valuable computational time. Solver, used by SENKIN application, DASSL, employs an internal time-step recalculation making it possible to stop the calculation at the predefined value of the time-step, since at the equilibrium state (or near it) no heavy chemical production is occurring (usually a small dissocitation/recombination reactions take place, if any) therefore providing the solver a matrix easily solved even with a higher time-step. DVODE, used finally in this work, uses predefined time-step, with the matrix solving done with an internal iteration procedure. One could possibly get the values from DVODE regarding the number of necessary iterations for the last time step – reasonably equal to using the automatic time-step value provided by DASSL, but the methodology is not so clear and could possibly provide wrong termination triggers, either stopping the calculation too soon, giving false values for ignition data, or running indefinitely, again, wasting tabulation time. One could also try to use a certain characteristic species to track the behaviour of the calculation, e.g. fuel or oxidizer species should at the equilibrium become near zero values. But, for some initial parameter sets this is hardly the case, and again would require additional input for tracking such species. Finally, a criterion, easily implemented to be used by both solvers, utilizes the simplest approach, tracking the temperature behaviour in time, waiting for temperature to reach its maximum value and stagnate for a predefined temporal period (or decrease due to dissociation or other reactions among the product species). A fixed time interval, e.g. a value order of magnitude greater than the time step used for temporal discretization, is defined for tracking the temperature change. If the temperature value remains the same, or decreases, the stopping criterion is met and the calculation stops storing the

ignition data to database. Numerically, the method has been proved to work with few flaws. It is also important not to impose the criterion at the beginning of the calculation, since it could cause the calculation to finish even before the first ignition criterion is met (some mechanisms, with certain combinations of initial parameters would yield a small temperature drop at the start). The methodology used in this work implemented the stopping criterion monitoring only after the first temperature inflexion.

Another issue closely related to stopping criterion is the case of "no ignition" and a way to track it. Simply put, the "no ignition" case was in this work dealt simply imposing a maximum allowed temporal variable to a predefined value (1 second). In most real-world cases the combustion process is very fast and tabulation of the high ignition delay values would make no sense in terms of using them in the unsteady CFD calculations involving combustion with, usually, very fine temporal discretization and low calculation termination time (possibly lower than the one obtained by the 0D homogeneous reactor calculation). In the experience gathered during this work the occurrence of "no ignition" cases is rather rare, and, as expected, occurs in borderline values of certain parameters (depending of the reaction mechanism used). Temperatures and pressures usually perform well at higher values, but for lower values should be subdued to testing to gain an insight into the mechanism's ability to provide viable results under such conditions. On the other hand, higher EGR values usually proved to yield non-consistent data and they should be retained at a reasonable level. The same applies to the equivalence ratio, for extremely lean and rich mixtures. If one would desire to have such extreme values in the database, it could prove to be more efficient (or even more correct) to extrapolate the values from the ones in the stable spectrum (second order extrapolation usually provides reliable results with low computing power needed).

Finally, after the calculation is finished, all (or none) values stored in the result vector variable can be additionally used to check the success of the calculation.

If there is only one record in the vector variable at the end of the calculation, no cool flame ignition had occurred. In other case the first record is taken to be the cool flame ignition delay, and the last one is taken as main ignition delay. This approach provides efficient, general and robust way of monitoring the ignition delay at real time.

The used approach used (partly) all of the mentioned methods. The temperature increase was set to 10 degrees at the start to catch the eventual cool flame ignition. After the criterion has been met, the inflexion point is also sought for, in order to have an insight in the overall gradient of the temperature curve (the case of low gradients where the actual ignition occurs slowly and fixed temperature criterion is no longer valid). The next inflexion point is used to reset the tracking variables, and also to set the second predefined value for main ignition tracking to 30 degrees. One should be aware of the fact that the inflexion point used to reset the tracking is the temperature gradient changing its direction once again, indicating the end of ignition and providing a sound point at which the intermediate heat release values could be calculated.

2.3 Temperature influence on autoignition

In the next few chapters the influences of the initial parameters on the autoignition delay times will be discussed. Any regularities observed at this stage could provide important information for later application in developing the algorithms for data post-processing, especially regarding database repair.

Dependence of temperature variation on the ignition delay times is presented in Figure 2-2. Some of the fuels of interest have been selected (in more detail discussed in later chapters) and compared. Traditionally, temperature/ignition delay plot is made with logarithmic scale on the ordinate, and instead of using temperature the 1000K/T is used on the abscissa.

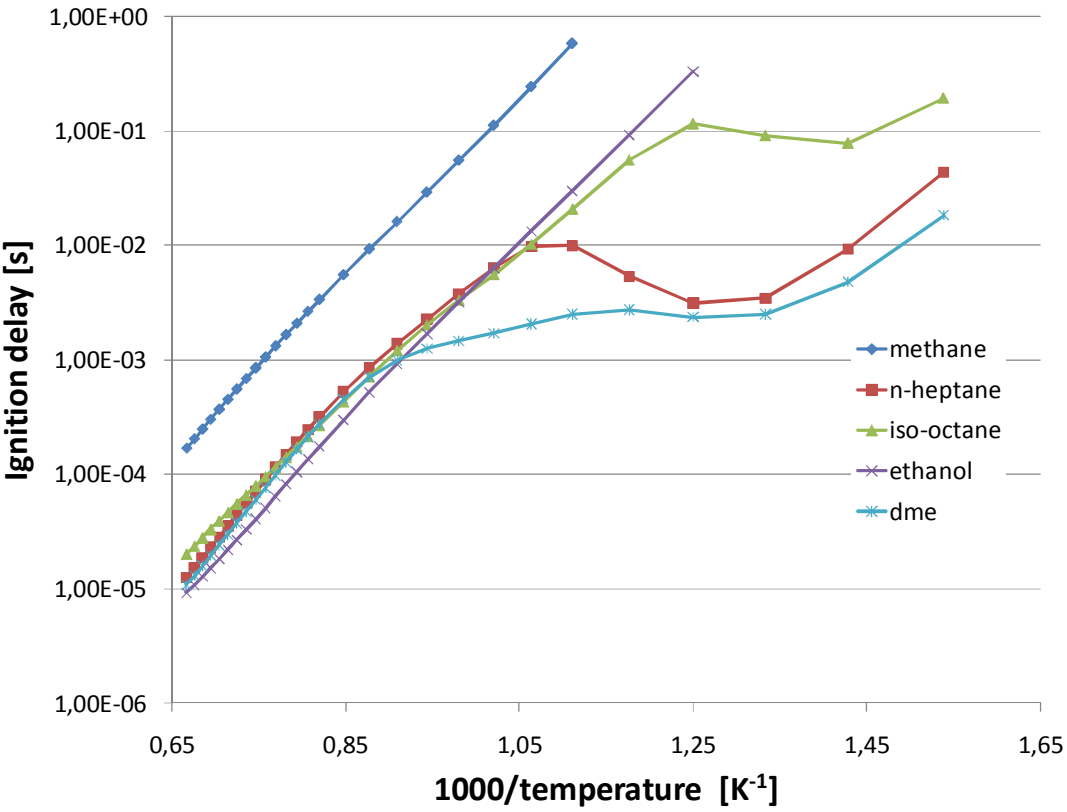

Figure 2-2 Temperature dependence of autoignition of selected fuels

The above figure shows exponential dependence of ignition delay against the temperature in case of simple fuels (methane and ethanol), and a more complex behaviour of iso-octane and n-heptane. Dimethyl-ether, having the same atom count as the ethanol displays completely different behaviour, closer to the two higher hydrocarbon fuels. Those exhibit a negative temperature coefficient (NTC) region, which is a result of the reaction mechanism including both low and high temperature branches. The complex low-temperature path includes several sub-mechanisms, which depend sensitively on temperature as described in more detail in [16] and [71]. This NTC region, for these fuels, creates a second maximum and minimum in the ignition delay /temperature curve making it difficult to use as one of the criteria for data manipulation. In case of ethanol and n-heptane the trend is monotone and could easily be used to extend the temperature region in the

database. Overall trend of the curves follows the logical assumption that for higher temperatures the ignition becomes faster, increasing the forward reaction coefficient in the Arrhenius equation (2-1) and finally lowering the ignition delays, with an exception of the negative (or zero) temperature coefficient region for some fuels.

2.4 Pressure influence on autoignition

In the following figure (Figure 2-3) ignition delays of the selected fuels have been calculated with pressure variation. Pressure dependence is not usually investigated as temperature one, and there is also no special way to display it in the charts.

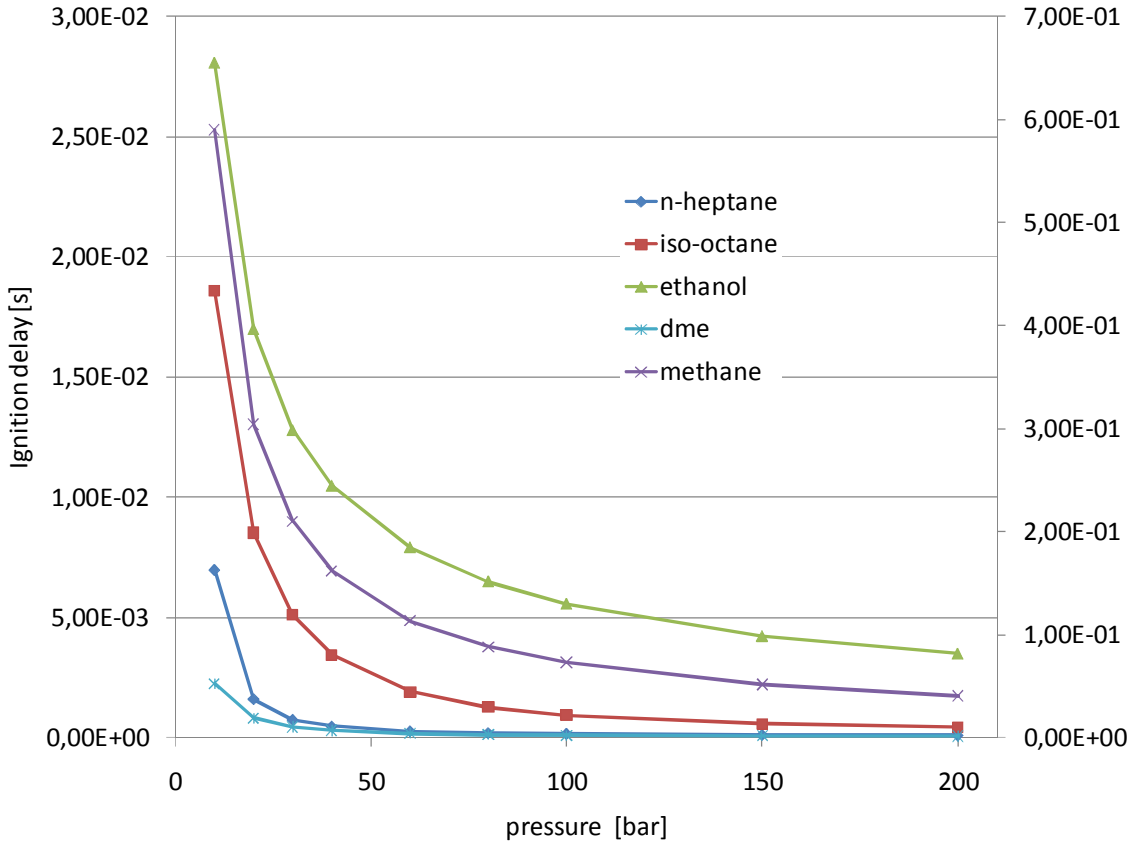

Figure 2-3 Pressure dependence of autoignition of selected fuels

On the above figure, methane curve was plotted using the alternative scale since the methane ignition in the selected conditions (temperature below 1000K) is considerably higher compared to other fuels.

As one could expect, the pressure increase also reduces the ignition delays (density is increased leading to the subsequent increase of the molar production rates), and the trend is evident with all fuels considered. There are also no local extrema in the curves, making pressure a valid candidate for database analysis and repair after the tabulation process.

2.5 Equivalence ratio influence on autoignition

In this chapter, dependence of ignition delay on the equivalence ratio is shortly investigated for selected fuels as shown in Figure 2-4.

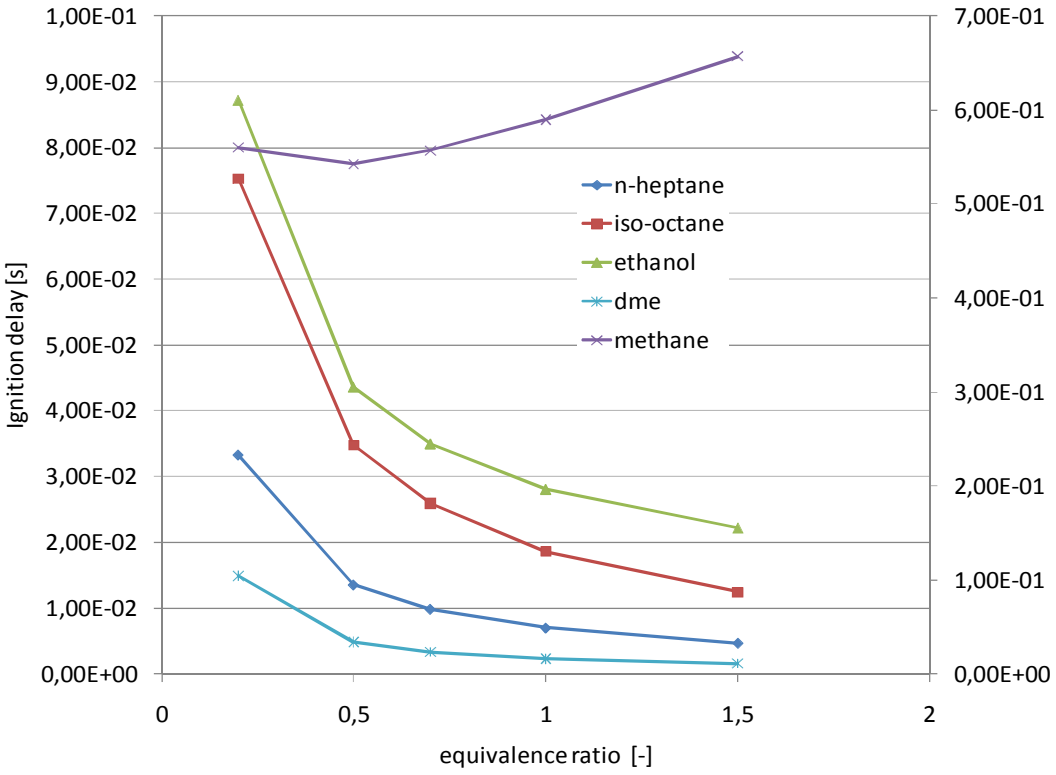

Figure 2-4 Equivalence ratio dependence of autoignition of selected fuels

In this image the methane ignition delays are also displayed on a secondary axis. For most of the fuels the equivalence ratio demonstrates the influence similar to the one observed from pressure variations and with similar conclusion on usability of this information for post-processing purposes. The methane curve, however, indicates the necessary caution one needs to address when applying the repair algorithms. In this case the behavior of methane ignition is completely different as for other fuels, indicating that for this specific fuel other criteria would be more suitable in the case of missing points correction (as seen in previous chapters, temperature criterion could easily be used for methane ignition data).

2.6 EGR influence on autoignition

Final parameter considered in this investigation is the residual gasses (EGR) mass fraction in the initial composition. Since the residual gasses, as explained more thoroughly in chapter 2.11.3 are mostly consisting of nitrogen, which is highly inert gas (on lower temperatures) and suppresses the main reaction branches for the fuel oxidation significantly increasing the ignition delay times as seen in Figure 2-5.

The ignition delay dependence is therefore also rather straightforward and is as such easily implemented in the repair algorithms (both for ignition delays and for laminar flame velocities). In the case displayed in the figure below, for instance, methane ignition for higher residual gasses values (which were, as displayed, not successfully calculated) could be easily extrapolated using second order differentials.

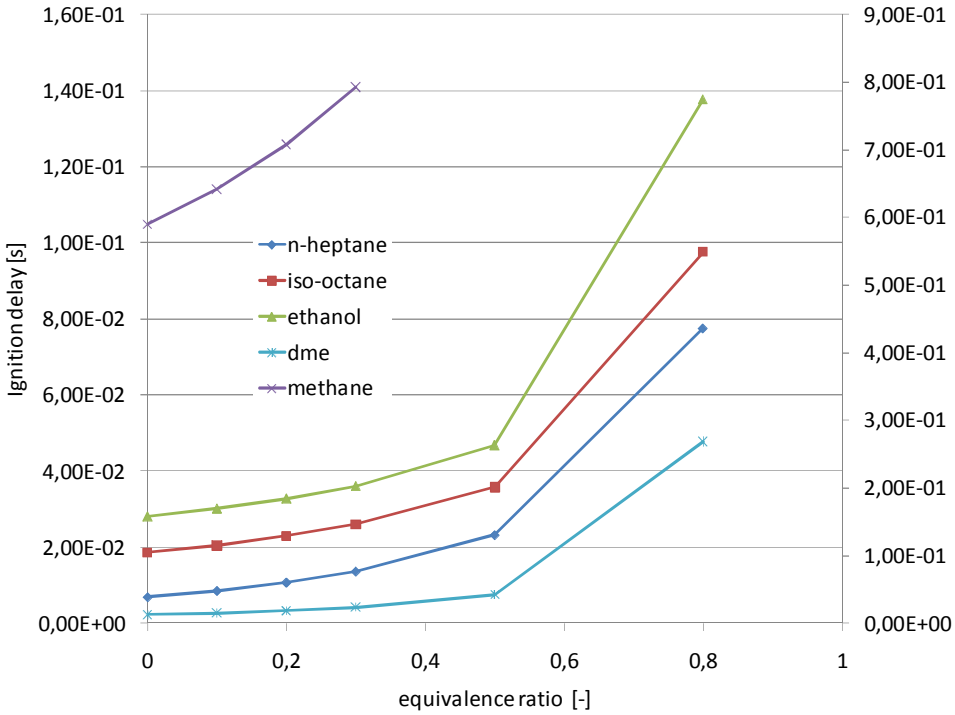

Figure 2-5 Residual gasses dependence of autoignition of selected fuels

2.7 Flame velocity

For calculation of laminar flame velocities, also needed by the CFD combustion model, another FORTRAN package based on the CHEMKIN library, the PREMIX solver, was used [72]. This package is capable of predicting temperature and species profiles in two laminar premixed flame configurations. The first, and the one most often used for analyzing species profiles in flame experiments, is the burner-stabilized flame with a known mass flow rate. The second flame configuration that is in fact used in this work is the freely propagating adiabatic flame. In the latter case, there are no heat losses (by definition) and thus the temperatures should be computed from the energy equation. Flame speed, partly, depends on the transport of heat, and predicting the temperature distribution is an integral part of the flame speed calculation. Since the PREMIX solver provides an

out-of-the box solution for calculating laminar flame speeds in the freely propagating flame calculations, and was not severely modified, only a short theoretical background will be presented here. Initially developed SL_SOLVER by [73], which acts as a shell around the PREMIX solver was used and slightly altered for wider tabulation applications (especially using numerically unstable reaction mechanisms).

PREMIX solver first reads detailed input from the user, which was the first step of the SL_SOLVER. It takes over the rather demanding calculation of the initial values for mixture, dependant on the defined equivalence ratio and EGR mass fraction from the supplied fuel and oxidizer species. Also, on top of the input from the user or the SL_SOLVER pre-processor, PREMIX solver depends on data and subroutines from the CHEMKIN and TRANSPORT packages. Therefore, to solve a flame problem the user must first execute two pre-processor programs that have access to thermodynamic and transport-property databases. Also in this case the SL_SOLVER steps in with the interpreter routines already implemented in the pre-processor requiring only the path to the desired reaction mechanism, thermodynamic and transport property documents.

PREMIX/SL_SOLVER is written as an application that is constituted out of a driver program calling several pre-processing subroutines that open all appropriate files, allocating the calculation memory work space, and calls the main flame program through its subroutine interface. PREMIX solver defines the governing equations, makes calls to the boundary value solver, and prints solutions for the flame problem.

The equations governing steady, isobaric, quasi-one-dimensional flame propagation consist of continuity, energy, species and equation of state where

$$\dot{M} = \rho u A \tag{2-15}$$

represents the continuity equation,

$$\dot{M}\frac{dT}{dx}-\frac{1}{c_p}\frac{d}{dx}\left(\lambda A\frac{dT}{dx}\right)+\frac{A}{c_p}\sum_{k=1}^{K}\rho Y_k V_k c_{pk}\frac{dT}{dx} + \frac{A}{c_p}\sum_{k=1}^{K}\dot{\omega}_k h_k W_k = 0 \tag{2-16}$$

represents the energy equation and species equation can be written as:

$$\dot{M}\frac{dY_k}{dx}+\frac{d}{dx}(\rho A Y_k V_k)-A\dot{\omega}_k h_k W_k = 0 \quad (k = 1..K). \tag{2-17}$$

Finally, equation of state is provided in the common form:

$$p = \frac{\rho\bar{W}}{\mathcal{R}T}. \tag{2-18}$$

In these above equations x denotes the spatial coordinate, $\dot{M}$ the mass flow rate (which is independent on x) and T is the temperature. The mass fraction of the k_{th} species among the total of K species is denoted by Y_k , p denotes the pressure, u the velocity of the fluid mixture, ρ its mass density and W_k the molecular weight of the k_{th} species. Furthermore, $\bar{W}$ is the mean molecular weight of the mixture, $\mathcal{R}$, as encountered in the earlier text, the universal gas constant, λ the thermal conductivity of the mixture, $c_p$the constant-pressure heat capacity of the mixture, c_{pk} the constant pressure heat capacity of the k_{th} species, $\dot{\omega}_k$ the molar rate of production by chemical reaction of the k_{th} species per unit volume; h_k the specific enthalpy of the k_{th} species, V_k the diffusion velocity of the k_{th} species and finally A denotes the cross-sectional area of the stream tube encompassing the flame. Molar net chemical production rate, denoted with $\dot{\omega}_k$ is calculated in the same manner as for the autoignition calculation as defined in the previous section in the equation

(2-3). The detailed description of the remaining terms in the above equations will not be the part of this work and could be found in the [72].

For freely propagating flames, used in this work for calculation of laminar flame velocity, $\dot{M}$ is an eigenvalue and must be determined as part of the solution. Therefore, an additional boundary condition is required, or alternatively one degree of freedom must be removed from the problem. The location of the flame is fixed by specifying the temperature at one point. This is sufficient for solving the flame speed eigenvalue $\dot{M}$. A point must be selected in a way to insure that the temperature and species gradients "nearly" vanish at the cold boundary. If this condition is not met, the resultant $\dot{M}$ will be too low because of some heat lost through the cold boundary.

Also, to start the calculation, the solver needs an initial estimate. It is presumed that the reaction zone exists changing the composition from the unburned mixture to the products. Estimates should, therefore, be provided for the location and thickness of the reaction zone and the product species (the burned mixture components). Since the tabulation procedures tries to encompass as little human intervention as possible, having the product species input required for each calculation would undermine the idea of making the database automatically. The pre-processor is used again here to calculate the product species for initial estimate using another of the supplied CHEMKIN package applications, the equilibrium solver, creating a sound estimate dependant on the values for each tabulation step initial parameter (EGR, equivalence ratio).

During the calculation the most severe nonlinearities in chemical kinetics come from the exponential dependence of the reaction rates on temperature. The PREMIX solver tries to step over this problem by eliminating the temperature from the iteration to make the flame problem considerably easier to solve. This is done, in general approach, in the same manner as discussed for the initial products composition. A viable initial estimate of the species distribution should also be provided. From many points of view this approach is really not feasible, as it was with the initial products composition. The problem with initialization of product

species was solved by running equilibrium calculations, and the initial distribution of species is initially solved by calculating the flame problem, using a predefined temperature (and also products defined earlier). The calculated species profile is then used in a second calculation as an initial guess, but this time with energy equation also solved.

The PREMIX uses the modular solver routine TWOPNT to solve the boundary value problem. After discretization on a given one-dimensional grid, TWOPNT attempts to solve a system of nonlinear algebraic equations by a damped Newton's method [72]. Newton's method determines a sequence of iterations or approximate solutions that approach the true solution. Details of the method will not be presented here, it can be found in the PREMIX and TWOPNT manuals and accompanying literature [72][74].

Principally, the final laminar flame velocity is calculated from the mass flow field at the inlet boundary having a stable flame front inside the defined domain.

2.8 CHEMKIN/SENKIN

One of the initial investigations during this work was the selection of the tool used as a basis for calculation of temporal distribution of mixture properties used for tracking ignition delay information. First tool investigated was a Fortran computer program, SENKIN, that computes the time evolution of a homogeneous reacting gas mixture in a closed system. The model accounts for finite-rate elementary chemical reactions, and performs kinetic sensitivity analysis with respect to the reaction rates. It is a standalone routine expecting several vectors of chemistry data interpreted from chemical mechanism and also a set of thermodynamic data. The calculation is performed using the low-level chemistry routines provided by CHEMKIN package. By default the SENKIN program uses DASAC numerical solver to solve both the nonlinear ordinary differential equations that describe the temperature and species mass fractions and the set of linear differential equations that describe the first-order sensitivity coefficients of temperature and species

composition with respect to the individual reaction rates, which makes the greatest impact on a computational performance compared to the alternative. The numerical method is based on the backwards differentiation formulas and is especially well suited for solving the stiff equations that are common in chemical kinetics applications [64]. The package is equipped with six types of predefined combustion systems (constant volume, constant pressure, volume as a specified function of time, constant pressure and temperature, constant volume and temperature and pressure and temperature as a temporal function). Since the ignition tabulation requires eventually only the two of the available systems (constant volume and constant pressure), from the scope of this work, many of the application's options remain unused.

As mentioned in the previous paragraph, SENKIN also performs, which is the most significant feature of the program, additional kinetic sensitivity analysis of the system, a powerful and systematic way to determine quantitatively the relationship between the solution to a model and the various parameters that appear in the model's definition. It is commonly used to determine the influence of the reactions on the selected mixture properties (species mass fractions, temperature, etc.). In the light of running consecutive tabulation calculations the sensitivity analysis also remains unused.

During this work, a driver program was created for calculation of initial condition information (initial composition based on equivalence ratio and EGR), and the SENKIN routine was modified, according to the discussion in previous chapters, implementing several criteria for monitoring ignition information and also for the calculation stopping (SENKIN by default requires fixed termination time step for finishing the calculation). Since DASAC solver uses variable, internally calculated time-step, it provides a relatively elegant way to obtain a stopping criterion for the calculation. A stopping time variable was introduced and after each DASAC computation, the predefined ΔT was compared against the one suggested by the solver. With several runs needed for an insight of selecting an

"optimal" value, finally the value of 1 [s] was defined, providing good performance over a range of different initial parameter cases.

SENKIN calculations proved to be rather robust and using described stopping criterion made no issue regarding the early calculation stopping or prolonged calculation. Only issue that was the calculation performance in terms of calculation times which made the more elaborate calculations of more comprehensive mechanism unfeasible on available computer power. The calculation speeds were found to be related to the used ODE solver which is in more detail discussed in the next chapter.

The second approach to ignition delay calculation was to disregard the SENKIN package, along with the solver it is using and the sensitivity analysis not needed in this work, and to create a driver application using the same low-level CHEMKIN routines calculating the chemical properties, which would include the setting-up the initial data for the calculation and also call the ODE solver and loop over the temporal discretization points. Also, as in the SENKIN program, two routines were created calculating the mixture properties for the characteristic cases of constant pressure and constant volume. Also, the ignition tracking and a different calculation stopping criteria has been implemented inside the loop. Since the DVODE solver does not change the predefined time-step size, the approach of tracking the temperature change in a larger time span, described earlier, was additionally used. This approach was also found to be appropriate since it did not generate excess calculation time nor stopping the calculations before any of the desired phenomena.

Calculation times, the main problem of the first approach, using the described CHEMKIN/DVODE combination have been significantly reduced. One would argue that the main influence on this reduction, having in mind that both applications use basically the same routines to calculate chemical properties, lies in using a different ODE solver. Also, in the latter approach, pre-processor used to interpret the chemical mechanism file and thermodynamic properties of species, is now ran separately, resulting in a binary file used by the driver application. When

using heavily reduced or skeletal mechanism, this separation does not make a huge difference regarding overall calculation time. However, using a more comprehensive mechanism, inside a tabulation loop when the interpreter should be called at the beginning of each calculation, this adds up to an amount worth considering. Since the data stored in the binary file is not dependant on the calculation properties, it is also rather practical since after the initial interpretation one has only one document with all necessary data. However, since the data is stored in a binary format, no additionally information, other than the name of the document, on the mechanism properties can be retrieved easily (the ASCII mechanisms are usually well commented with references to the mechanism itself and possibly a short description and references). Also, the problem could be the portability of such a binary representation, since it can only be used with applications that are custom written to read out the data stored in the exact manner.

2.9 ODE Solvers (DVODE, DDASAC)

As mentioned in the previous chapter, the choice between running the calculations and subsequent tabulations was made dependent on the time consumption of a single calculation. Finally, the difference of calculation speeds was attributed to using a different ODE solver. This section will give a brief description on each solver trying to elucidate their differences. The presentation of the solvers here will be brief, so one is encouraged to look for the details in some of the available literature sources [75][76].

First solver considered is the VODE solver, which is an upgrade to the older solvers EPISODE and EPISEODEB, and uses variable-coefficient multistep and backward differentiation methods with fully variable stepsize [76]. It is an initial value ODE solver for stiff an non-stiff systems. It was reported to enhance the older versions by incorporating the mentioned fully variable coefficients and stepsize and also the added algorithm for saving and reusing the Jacobian matrix, improving

the performance in some cases to over 30% (compared to older versions of ODEPACK). This solver is widely used and is still showing to outperform other algorithms.

In the second ODE solver tested, DDASAC, the derivatives are approximated by backward differentiation formulae (BDFs), and the resulting nonlinear system at each time-step is solved by Newton's method. The linear systems solving and error handling are accomplished using a separate subroutine packages (LINPACK and SLATEC, respectively). This code is reported to provide valid results for stiff ODEs and for differential algebraic equations of moderate size, where it is appropriate to treat the Jacobian matrix with dense or banded direct LU decomposition.

For this work DVODE solver used in the stand-alone homogeneous combustion case has been found easier to use than DASSL which was used as a part of SENKIN package, and was also proven to come to a solution of the system significantly faster than the DASSAC, which is in terms of similar comparisons provided by [77].

2.10 Chemical mechanisms

As mentioned earlier, one can specify several levels of chemical mechanism complexity. Most complex and detailed mechanisms are developed considering all aspects of a certain fuel (or more fuels) oxidation. This is usually done by thorough investigation of fuel decomposition branches, including all significant sub-mechanisms which consider a number of intermediate species making the mechanism reliable for a wide number of applications and desired property representation. Usually, however, for practical CFD application, one is concerned with only few combustion properties need to be accurately represented by the chemical mechanism (dependant on the specific application [78][79][80][81]). Therefore, reduced mechanisms are employed, providing satisfying accuracy for a desired property but also a reasonable computational demand [82].

Typically, numerical data are collected from simulations with detailed mechanisms performed for the targeted regimes of interest. With the numerical data, several methods can be used for developing skeletal mechanisms including rate analysis, sensitivity analysis, and Computer Singular Perturbation (CSP) [83][84]. In the following text, several fuels of interest will be presented, also compared side to side regarding the ignition delay calculations. In these calculations EGR will not be used as a varying parameter since most of the mechanisms have not been validated by their creators against the residual gases concentration.

2.10.1 Diesel fuels

Generally speaking, when discussing the possibilities of simulating combustion of a complex fuel such as a diesel fuel, usually a term "surrogate fuels" is mentioned. Literature defines a general diesel fuel as a complex blend of several hundreds of individual species. Chemical and physical properties of diesel fuel (European) are given in Table 2-1.

Table 2-1 Diesel fuel specifications

Property	Unit	Specification		Test
		Min	Max	
Cetane Number		52	54	ISO 5165
Density @15°C	kg/m3	833	837	ISO 3675
Distillation (vol. % recovered)	°C			ISO 3405
- 50% point		245	-	
- 95% point		345	350	
- final boiling point		-	370	
Flash point	°C	55	-	EN 22719
CFPP	°C	-	-5	EN 116
Viscosity @40°C	mm2/s	2.svi	3.svi	ISO 3104
Polycyclic aromatic hydrocarbons	% wt.	3.0	6.0	IP 391, EN 12916
Sulfur contenta	mg/kg	-	300*	ISO/DIS 14596

Copper corrosion		-	Class 1	ISO 2160
Conradson carbon residue (10% DR)	% wt.	-	0.2	ISO 10370
Ash content	% wt.	-	0.01	ISO 6245
Water content	% wt.	-	0.05	ISO 12937
Neutralization (strong acid) number	mg KOH/g	-	0.02	ASTM D974-95
Oxidation stability	mg/ml	-	0.025	ISO 12205

The above table, detailed as it may be, doesn't really represent the shear broadness of the term "diesel fuel". As mentioned in the text preceding the table, it is defining the European reference diesel fuel. The variations in diesel fuel properties go from international to regional and even local level, reflecting the nature of the crude and the process used to refine the fuel at each specific refinery. More detailed remarks on the distillation process, carbon number and the composition can be found in [4].

Surrogate fuels used to represent real-life diesel fuel are usually targeting a specific fuel property, behaviour or application. It could be either density (or C/H ratio, composition), autoignition delay, flame speed, emissions, combustion efficiency, etc... All of these properties or behaviours are measured in the laboratory experiments. Usually, matching the application targets (property or behaviour in an engine combustion experiment) is the goal of the research developing a suitable surrogate. Out of many suggested surrogates appropriate for CFD calculations (n-parrafins, iso-parrafins,cyclo-parrafins, aromatics) the one considered in more detail in this work is n-heptane.

Computational demand when incorporating the detailed (or comprehensive) mechanism in combustion simulation can be overwhelming. Therefore reduction of the mechanism is considered.

N-heptane, which is a straight-chained fuel, is assumed to lead to alkenyl decomposition products with alkyl radicals and olefins. Due to the comprehensive mechanism of n-heptane oxidation, n-heptane molecules undergo H-atom abstraction at high and low temperatures, leading to the formation of structurally distinct alkyl radicals. When alkane fuels have to stay partially or fully premixed in

an oxidizing atmosphere at elevated temperatures and pressures, ignition can occur in a multistage mode. The ignition process can follow completely different schemes of oxidation and is controlled by two different chain-branching reaction mechanisms: the low-temperature reaction path, where the fuel is oxidized by O2 in degenerated branched chains, and the high-temperature path, where the fuel is rapidly oxidized into C2 and C1 hydrocarbons and subsequently consumed. The low-temperature branch is quite complex and proceeds via different sub mechanisms, which are sensitively controlled by the temperature [16].

Cool flame phenomenon is especially important associated with knocking and homogeneous charge compression ignition (HCCI) combustion in internal combustion engines (ICE), and refers to the low-temperature (500-800 K) chemical activity partially oxidizing the hydrocarbon fuel without burning it completely (with no formation of soot precursors) [85]. Also, a characteristic negative temperature coefficient of reaction rate is associated with this phenomenon, due to the competition between chain-termination and chain branching reactions [86]. Special case is so called oscillatory cool flames, which are getting more attention recently [87]. Since they include specific interaction of thermal and chemical feedback they will not be studied futher in this work.

At high temperatures, reaction propagates via radical β-scission, the initial step in the chemistry of thermal cracking of hydrocarbons and the formation of free radicals. They are formed upon splitting the carbon-carbon bond. Free radicals are extremely reactive and short-lived. When a free radical undergoes a β-scission, it breaks two carbon atoms away from the charged carbon producing an olefin and a primary free radical, which has two carbon atoms less. At low and intermediate temperatures (600-900 K), peroxide chemistry becomes more important. The n-heptyl radical reacts with molecular oxygen, R + O2 = RO2, forming a heptylperoxy radical (C7H15OO). After the internal H-abstraction, the radical undergoes a second addition of O2 forming hydroperoxy-heptylperoxy radicals, which are very unstable and decompose easily. Its products are both chain propagating and degenerating branching agents [16].

When studying the complex chemical mechanism, it is possible to get a comprehensive insight of the chemical kinetics behind the phenomena of autoignition. Skeletal mechanisms (that include the main species and reactions) consist in general of 20-80 species with less than 250 reactions [11][88]. These can further be simplified to 4-40 steps, but this approach (done by mathematical transformations) can cause the loss of physical meaning of the individual species [89]. The complete detailed reaction mechanism for n-heptane oxidation includes 2450 elementary reactions with 550 chemical species and is intended to cover the entire range of conditions from low-temperature (600-900 K) pyrolysis and oxidation to high-temperature combustion. Several methods are used to reduce the chemical mechanisms to the size appropriate for reasonable computation (skeletal or reduced models), based on sensitivity analysis, and others (the Quasi-Steady-State Assumption (QSSA), the Intrinsic Low-Dimensional Manifold (ILDM) approach or the Computational Singular Perturbation method (CSP)) [90][84]. Also, one could base the survey on whether the mechanism simplification method is based on reduction of reactions [91] or reduction of species [92][93]. Principally, it can be stated that the full, complex models are validated with experimental data, while the reduction is made against the full mechanism calculation results of the interest (flame speed, auto-ignition) [94][95][96].

Recent studies show that, using auto-ignition delay as an optimization criterion, the above mentioned detailed mechanism could be reduced to 170-180 species [84], and some show improvement using even more reduced mechanisms (67 species and 265 reactions [97]). More useful information about this topic could be found in [3][4][15].

Several mechanisms of interest have been investigated in more detail in this work. Most comprehensive one, described in [iso-octane-paper], comprises out of 544 species and 2446 reactions. It was modelled and tested by its developers for certain scope of initial parameters: pressure (1-45 atm), temperature (500-1700K) and equivalence ratio (0.3-1.5). During the work in this thesis, some of the parameter ranges exceeded the above values, but the behaviour of the mechanism

seemed not to be compromised. Also the mechanism was developed additionally for combustion with nitrogen-argon dilution, but this option was not used during this work. Main point of interest for the developers of this mechanism was ignition and species composition data. Experimental studies on which the mechanism development was based were focused on shock tubes, rapid compression machines, engines, flow reactors, plug flow reactors and jet-stirred reactors. The mechanism was developed with two sub-mechanisms, low and high temperature regime, incorporating the negative temperature coefficient behaviour. More details on the mechanisms can be found in the paper [16].

Since, as stated before, such a mechanism is not suitable for the combustion simulation in real life applications (or for tabulation purposes if a cluster computing is not available), reductions of this mechanism have been proposed. One of them is from [98] who developed an intermediate (282 species and 1282 reversible reactions) and a "small" mechanism (160 species and 770 reversible reactions) [96]. The latter was used for a tabulation purposes in this work, and will be compared with the comprehensive one. Ignition delay times were used to effectively reduce the detailed mechanism, mainly for the case of steady, axisymmetric, laminar flow of two counterflowing prevaporized streams. However, for reduction purposes an ishoric homogeneous reactor configuration was used to calculate certain amount of calculations with predefined sets of initial conditions (wider range of temperatures, but it must be mentioned, relatively low pressures as reported – up to 13.5 bar), and the elementary reactions were submitted to an analysis which indicated the ones with higher influence on the overall ignition delay times.

Even smaller (skeletal) mechanism, showing relatively good ignition delay times has been developed and reported in [97]. It consists out of 43 species and 185 reactions making it very useful for quick investigations on trends and overall behaviour of main physical and chemical phenomena. This mechanism was developed to examine the effect of strain-rate on multistage n-heptane ignition in a

counter-flow case [99]. The document also provides a useful representation of the 18 global reaction steps in the case of n-heptane combustion as shown in Table 2-2.

Table 2-2 Global n-heptane reactions

No.	Reaction
I	$n\text{-}C_7H_{16} = C_3H_6 + 2C_2H_4 + H_2$
II	$n\text{-}C_7H_{16} + O_2 + OH = RO_2 + H_2O$
III	$RO_2 + O_2 = OR``O_2H + OH$
IV	$OR``O_2H = 2C_2H_4 + CH_2O + CH_3 + CO + OH$
V	$1\text{-}C_6H_{12} + + H_2O = C_3H_6 + C_3H_4 + H_2O$
VI	$1\text{-}C_4H_8 + + OH = C_2H_4 + CH_3 + CH_2O$
VII	$C_3H_6 + H_2O = C_2H_4 + CH_2O + H_2$
VIII	$C_3H_4 + H_2O = C_2H_4 + CO + H_2$
IX	$C_2H_4 = C_2H_2 + H_2$
X	$C_2H_2 + O_2 = 2CO + H_2$
XI	$CH_4 + H = CH_3 + H_2$
XII	$CH_3 + OH = CH_2O + H_2$
XIII	$CH_2O = CO + H_2$
XIV	$2H_2O = H_2O_2 + O_2$
XV	$H_2O_2 = 2OH$
XVI	$CO + H_2O = CO_2 + H_2$
XVII	$O_2 + H_2 = 2OH$
XVIII	$2H = H_2$

Reactions I and II are the initiation reactions for high- and low-temperature autoignition, respectively. The low-temperature initiation reaction II reveals the formation of heptylperoxy radicals (RO2). These react in global step III by internal isomerization reactions, a further O2 addition, and a first OH abstraction to ketoheptylperoxide OR″O2H. The decomposition of this component in reaction IV, which results in the formation of an OH radical, represents the chain branching in the low-temperature range. Reactions V–XIII describe the consumption of the intermediate component hexene, butene, propene, allene, ethene, acetylene, methane, the methyl radical, and formaldehyde, respectively. Steps XIV and XV lead to the formation of radicals in a very short, radical-poor initiation time, during which the H abstraction by O2 attack leads to a relatively high amount of

hydroperoxy radicals. These reactions also form radicals during ignition at high temperatures. The water gas shift reaction XVI represents the oxidation of CO to CO2, which occurs during thermal runaway and leads to strong heat release. Reaction XVII is the main radical producing step after ignition occurs, and finally, global reaction XVIII represents chain breaking by recombination reaction.

Furthermore, another compact mechanism has been derived by [96]. It is also based on the comprehensive mechanism mentioned first, and kept in smaller size by limiting the application of the low temperature oxidation pathways to the fuel molecule. The reaction paths have been simplified and reorganized by linear chemical lumping. Mechanism was validated against a wide range of initial parameters, low to high temperatures (550-2300 K), very lean to extremely rich mixtures (0.22-3) and low to medium pressures (1-42 bar).

Final mechanism of interest at this point is described in [100]. It is the most recent of all mentioned, and is in fact consisting of two mechanisms, each intended for a separate temperature range. It should also be mentioned that these mechanisms were developed and tested in the case of laminar burning velocities investigation and that ignition delay calculation results should be taken with the above fact in mind even the literature states that the mechanism was also validated for homogeneous combustion systems. The mechanism(s) were also derived from the comprehensive mechanism mentioned first. The reduction has been performed for a pressure range of 1-40 bar, equivalence ratio 0.5-2 and temperatures from 600-1500 K. Final mechanism(s) consist of 99 species and 699 reactions (high temperature) and 104 species and 403 reactions (low temperature module). Even if the reduction of the comprehensive mechanism was made with improving the laminar burning velocities in mind, much better agreement was observed in the case of ignition times. This fact only shows the problems regarding good calculation of burning velocity. The mechanism was also validated against the same chemical properties for several other fuels including propane, butane, iso-octane, PRF (primary reference fuel) making it a very useful mechanism in terms of

complexity (directly correlating to calculation times and usability in non-0D calculations).

Figure 2-6 shows the comparison of the mentioned mechanisms in a 0D homogeneous case with constant volume (also used in a series of calculations to perform a tabulation used in 3D CFD solvers).

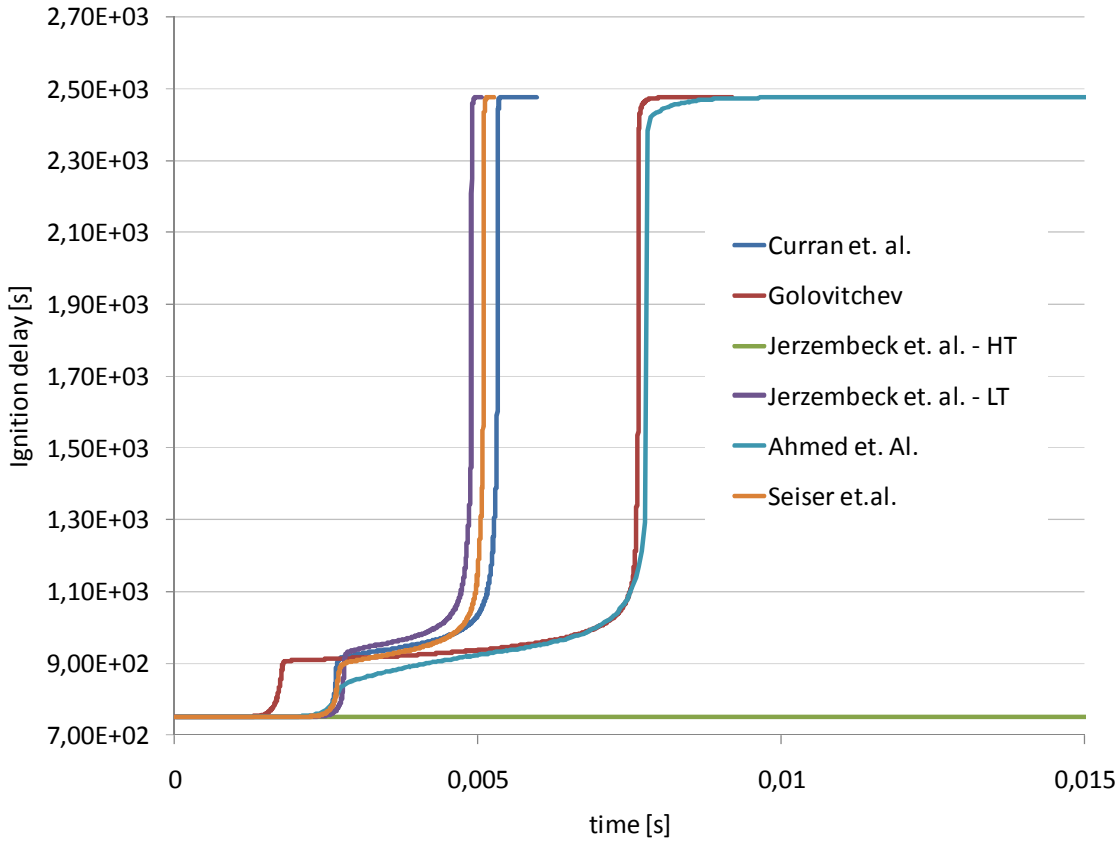

Figure 2-6 Comparison of several n-heptane mechanisms for a certain case

One can certainly observe a rather big discrepancy in the results making a future choice of mechanism used for tabulation purposes rather perplexed. One can assume that the most complex/comprehensive mechanism to be the one most accurate and true to the real chemical behaviour of the fuel in question, which was also the initial assumption made during this work.

On the Figure 2-7, above mechanisms have been compared against each other in terms of ignition delay dependence on temperature. Commonly the temperature dependence is displayed with ignition delay axis having a logarithmic scale, and the temperature being represented by 1000/T. Logarithmic scale is useful for displaying larger ranges of values, and is also advantageous in this case since it could be noticed that, for higher temperatures, all mechanisms provide results with very good agreement (except the Golovitchev mechanism[11], over predicting it by some margin). The discrepancies could be noticed at the NTC region, which would be expected since the behaviour of the mechanism in this area heavily depends on the level of detail. From the image below, one could be inclined to disregard the Jerzebeck at al. – HT mechanism, behaving poorly with lower temperatures, and use the LT mechanism which provides satisfactory results both at low and high temperatures (also with the pressure/equivalence ratio/EGR combination used in this case, it is the one providing the closest values to the ones obtained by using the comprehensive mechanism).

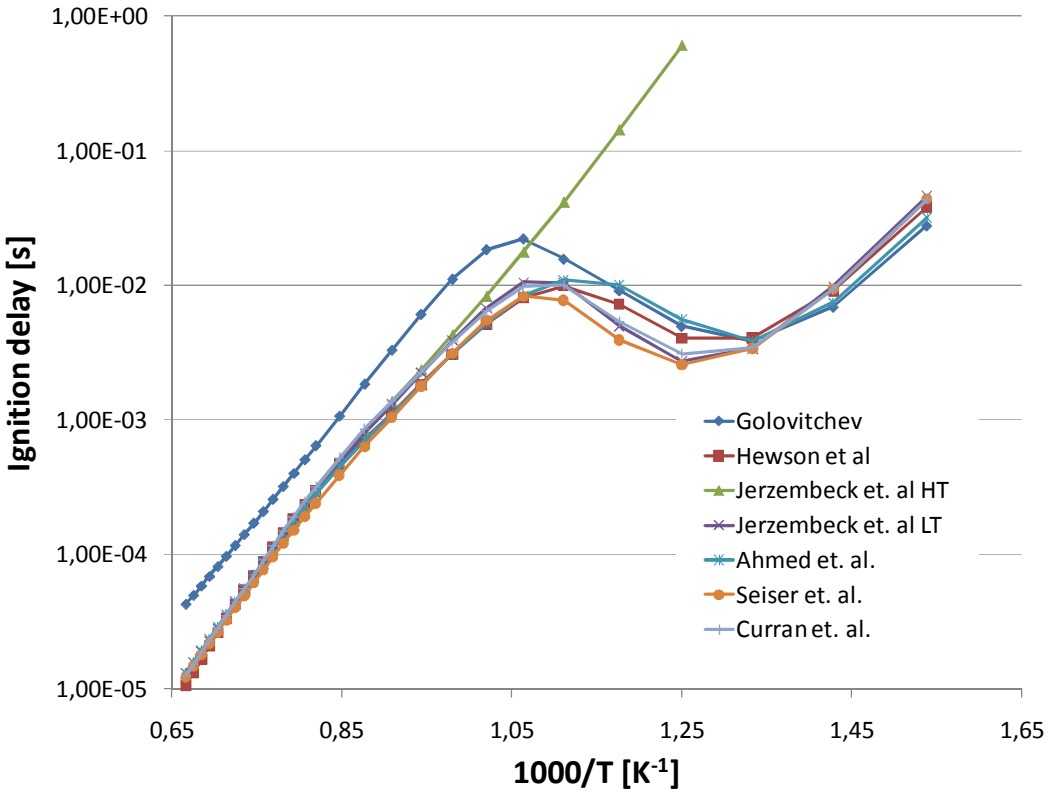

Figure 2-7 Comparison of mechanisms in a temperature dependant series (pressure at 10 bar, equivalence ratio of 0.9 and 0% EGR)

2.10.2 Other fuels

During this work a requirements for other fuel data has emerged. The tabulation procedure was aimed to create databases regardless of the fuel type, provided with a solid, working chemical reaction mechanism. Nowadays, interest in alternative fuels is constantly increasing, which made also the interest of the mechanism investigation broader. Since the n-heptane was the fuel of interest during the research, other fuels are represented with only few of the most widely used available mechanisms.

2.10.3 Iso-octane

First of the investigated fuels is not really an alternative, rather traditionally used as a surrogate for gasoline in the combustion simulation. Even if the auto-ignition is not a governing phenomenon in the combustion of iso-octane, a good prediction of it could lead to better understanding of an engine-knock conditions in internal combustion engines. Iso-octane is one of the primary reference fuels that determine octane numbers and knocking tendencies of gasoline mixtures under spark ignition operating conditions, and chemical kinetics of engine knock are very similar to kinetics of ignition under HCCI conditions.

Main detailed mechanism developed for this fuel has a strong correlation with the one mentioned before in the section dedicated to the n-heptane (in fact, iso-octane mechanism is based on the aforementioned one) since this mechanism encompasses the reaction chains for both fuels. Additionally, iso-octane dedicated complex mechanism developed consists of 857 species and 3606 reaction making it hardly usable in practical applications [2].

A skeletal iso-octane mechanisms, with two levels of complexity, based on the detailed one mentioned above have been developed as described in [83]. First one, with 258 species was developed for accurate predictions of ignition delays, and the second, the expanded version of the former, is aimed at accurate prediction of both ignition delays and unburned hydrocarbon emissions. Both mechanisms were validated against the operation regimes encountered in HCCI applications. Reduction of the mechanism was performed also as described earlier in the n-heptane section, by observing the importance of each species and reactions steps. These skeletal mechanisms were validated against the results obtained from the comprehensive mechanism (not an experiment, therefore, providing a good background for the earlier assumption on using the comprehensive mechanism as a reference) using three pressure points (10, 20, 40 bar), two equivalence ratios (0.3, 0.6), and as described in [83], for the higher temperature regimes the mechanisms provide almost identical ignition delay values as the reference

mechanism (since the mechanisms were developed for HCCI applications, this temperature regime was the critical one).

Also the reduced version of the Curran et al. mechanism [2], has been developed as described in [101]. It was developed by using automatic chemical lumping procedure, and in the final version used during this investigation consists of 84 species and 412 reactions. The method developed and used is called directed relation graph method with error propagation (DRGEP), and can be in more detail found as described in [93]. The mechanism created wasn't tested on a wider range of temperatures and pressures, with only three points used for temperature (between 750K and 1100 K) and one point for pressure (40 bar).

Finally, the largest mechanisms used in this work is developed by [15] and consists in total of 4961 reactions and 1121 species. It consists in detailed oxidation branches of isooctane, n-heptane, toluene, diisobutylene and ethanol fuels. Since the most of the above branches have been taken out of the mechanisms described earlier, it was decided to include this mechanism in the iso-octane investigation. Also important to this study, this mechanism incorporates some of the oxidation chains regarding the fuel blends (n-heptane/iso-octane, n-heptane/toluene) [102] which will be utilized in one of the following chapters. The literature source states the model predictions have been compared with shock tube autoignition delay time data over practical ranges of temperature and pressure with air as oxidizer ($690 < T < 1200$ K and at pressures of about 10, 30, 50 bar and equivalence ratio of 1). The mechanism was validated also for several fuel blends (as mentioned earlier).

Results comparing the comprehensive and reduced mechanisms are displayed in Figure 2-8 and Figure 2-9.

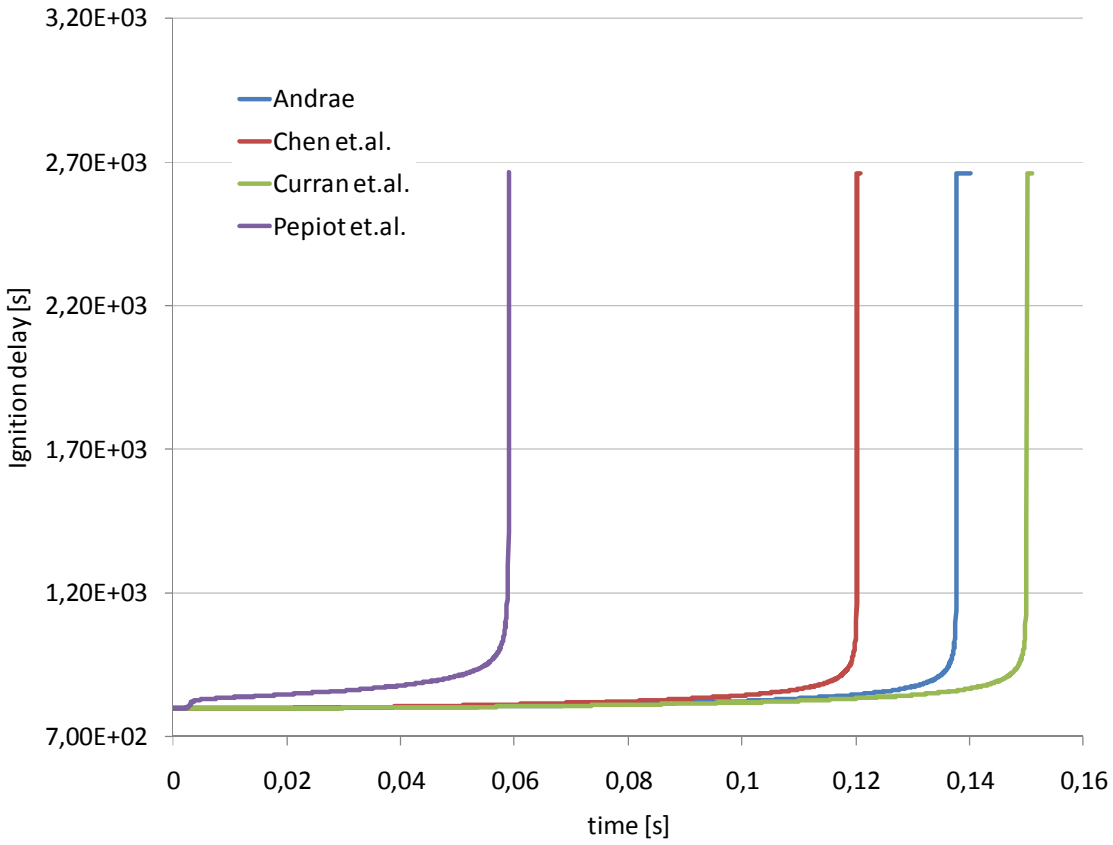

Figure 2-8 Comparison of the above iso-octane mechanisms for a certain case

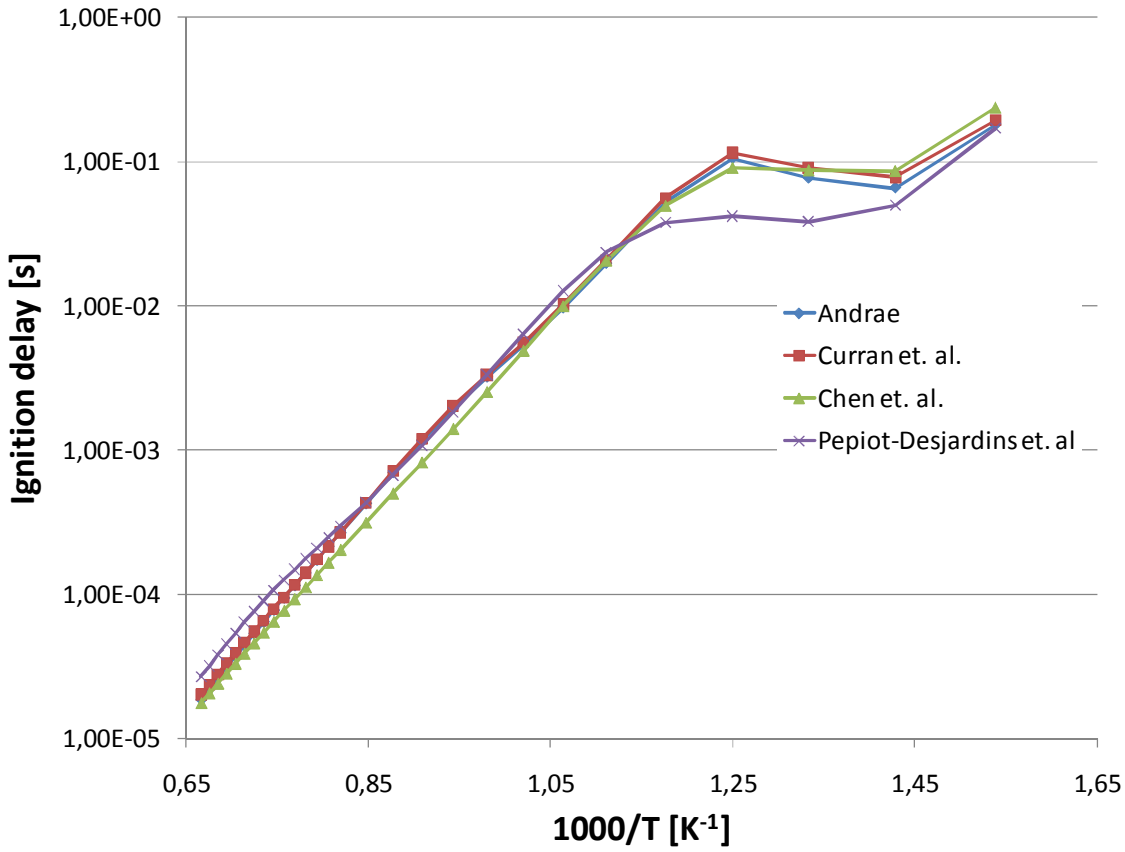

Figure 2-9 Comparison of mechanisms in a temperature dependant series (pressure at 10 bar, equivalence ratio of 0.9 and 0% EGR)

On the above figure, comparing the described mechanisms at the specified initial parameter combinations, one could also conclude that the heavily and automatically reduced mechanism by Pepiot et. al. provides valid results only at higher temperatures (>1000 K) and for the tabulation purposes, the Chen et al. mechanism would be sufficient compared to the detailed mechanisms from Curran et. al. and Andrae, displaying similar behaviour both at high temperatures and in the NTC region.

2.10.4 Ethanol

Considerable interests in ethanol as a fuel extender, octane enhancer, oxygenate, and a neat fuel has increased dramatically because of concerns associated with conventional transportation fuels. Therefore, the same amount of effort has been put into development of ethanol reaction mechanism. Several popular mechanisms are freely available, and will be mentioned in this chapter.

The most popular and widely used dedicated ethanol mechanism is the one developed within the same group as the detailed mechanisms for n-heptane and iso-octane, and is also a part of these mechanisms. As described in [6], the detailed chemical kinetic model was assembled using reaction sub-mechanisms developed previously by various authors for hydrogen, methane, ethylene, ethane, and propane oxidation. Final mechanism consists of 56 species and 351 reversible reactions. Finally, the mechanism was validated and subjected to sensitivity analysis compared to the experimental setup from [103] with ethanol-oxygen-argon mixture, temperature range of 1300-1700 K, pressure at 1 and 2 bar, and equivalence ratios of 0.5, 1 and 2. Also, an extended laminar burning velocity investigation of this mechanism was performed validating the results obtained using the mechanism against the experimental data at 1 bar, 298 K, and a equivalence ratio range of 0.6-1.4 providing good agreement in the low equivalence area, yet a slight under prediction with equivalence ratios between 1 and 1.5.

Since the presented mechanism, although a widely used, is rather dated, two newer have been also compared side by side on a small range of initial conditions. First one, also commonly cited in the literature, developed as described in [7], consists of 46 species and 235 reversible reactions. As reported in the literature this reaction mechanism is an augmentation of a mechanism developed for the combustion of hydrogen, carbon monoxide, methane, ethane, ethylene, acetylene, propane, propene, propyne, allene and methanol. It was compiled targeting the autoignition delays, laminar burning velocities and other chemical properties of

combustion systems at the temperatures above 1000 K, pressures below 100 bar and equivalence ratios under 3.

The last mechanism dedicated to ethanol, described in this section, will be the one developed by [104][105]. This mechanism, not like the other two mentioned earlier in the text is not dedicated to ethanol, but is rather a general purpose mechanism aimed for small hydrocarbon fuels combustion calculations. Also the intention of the development of this mechanism was also to provide a way to allow an accurate prediction of NO formation in lean and rich flames. Therefore, this mechanism is bigger than the other two in this section, with the total of 127 species and 1207 reactions.

Results of a homogeneous combustion case comparing the ignition delays of these mechanisms are presented in figures Figure 2-10 and Figure 2-11

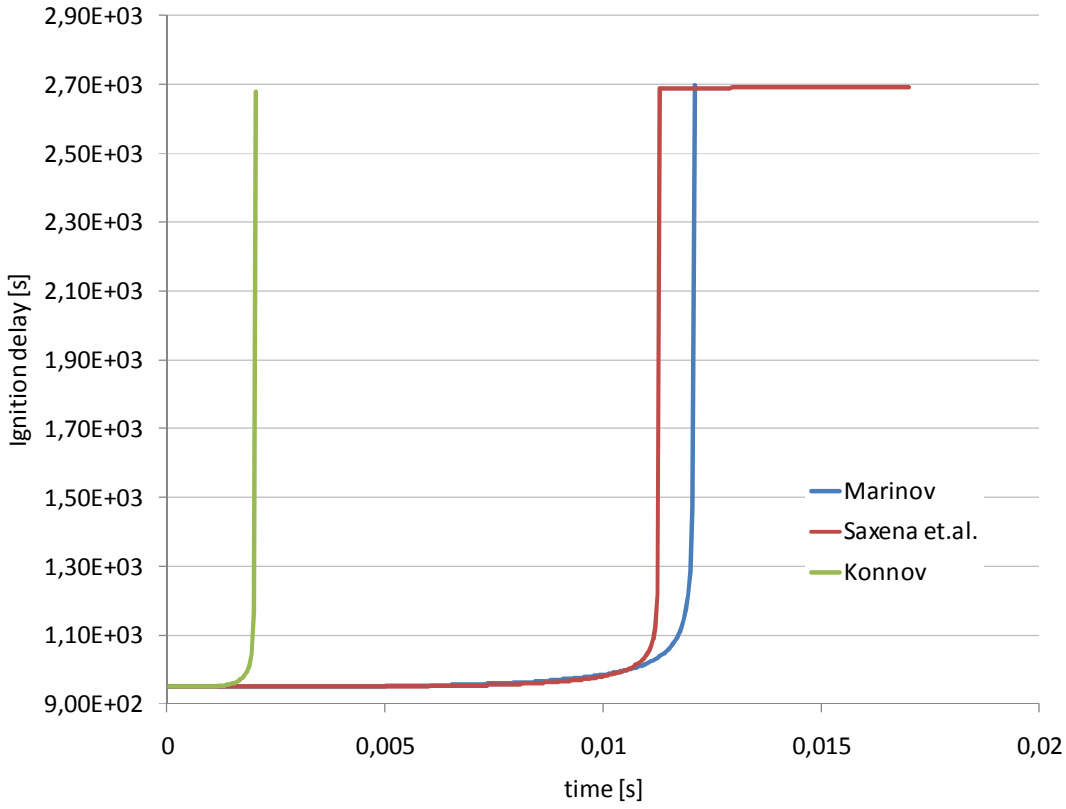

Figure 2-10 Comparison of the above ethanol mechanisms for a certain case

Figure 2-10 displays also significant deviation of the Konnov mechanism compared to the results of the Marinov and Saxena et. al. mechanisms. Marinov mechanism still being a standard one included in many other comprehensive mechanism for primary reference fuels, and also Saxena et al. developed separately providing very good agreement, with sufficient confidence, one could disregard the Konnov mechanism, which is also convenient from the computational and time-wise point of view for tabulation, since it is the biggest one of the three.

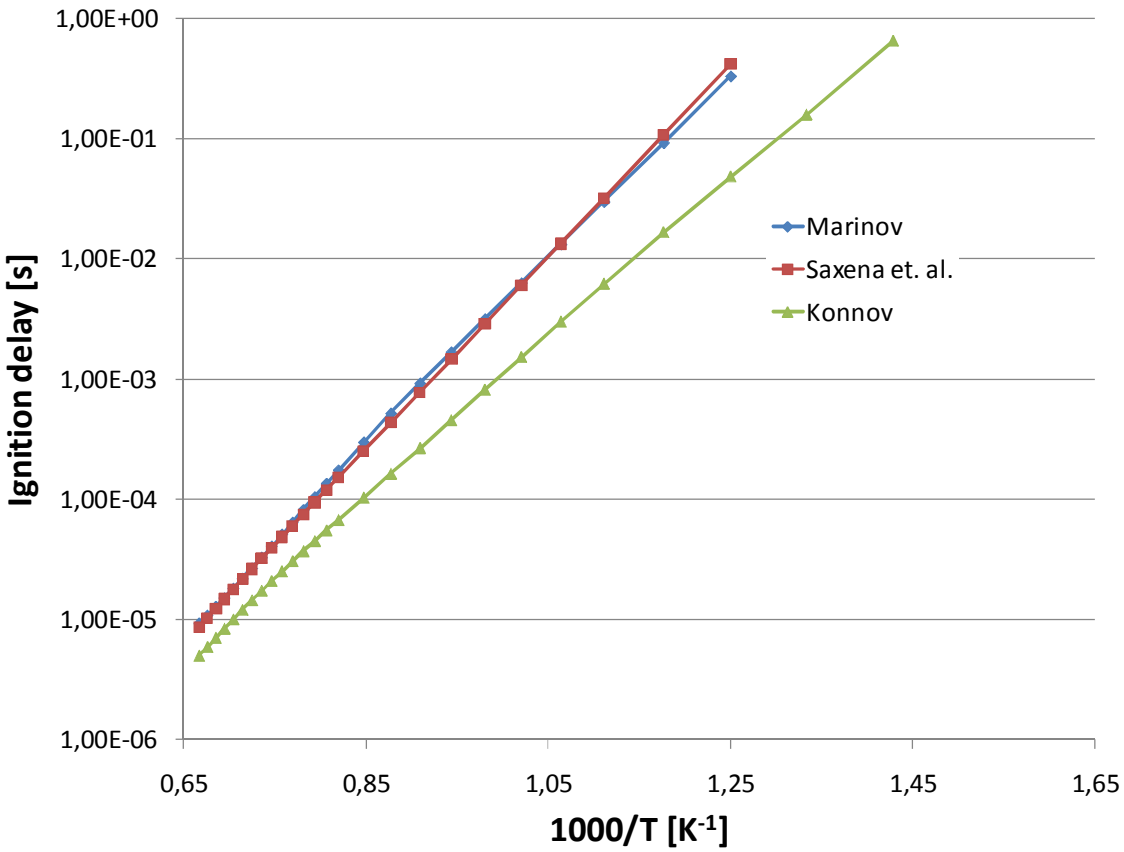

Figure 2-11 Comparison of mechanisms in a temperature dependant series (pressure at 10 bar, equivalence ratio of 0.9 and 0% EGR)

2.10.5 Methane

Methane as a fuel is found in many practical applications, it is important for electrical generation being burnt as a fuel in a gas turbine or steam boiler, or in the form of compressed natural gas used as a vehicle fuel claimed to be more environmentally friendly than other fossil fuels . Also, recent studies point to the methane as a potential rocket fuel (using his abundance in many parts of the solar system). There are many more reasons that make methane a fuel of particular interest not only to this study but also to many other studies trying to represent the combustion process of methane as accurate as possible.

Investigation calculations for methane have been made during this work. Since the GRI-Mech mechanism is probably the most used mechanism of all, and most of the other mechanisms are usually derived from this one, main point of ignition delay behaviour is focused on this mechanism. GRI-Mech is an optimized detailed chemical reaction mechanism capable of the best representation of natural gas (lower hydrocarbons) flames and ignition [5]. Being an optimized mechanism, meaning that, as several reduced mechanism mentioned earlier, it was created by analyzing a number of reactions for lower hydrocarbon oxidation and systematically discarded the ones proved to have lower influence on the final desired chemical/physical properties of the tested mixture (shock tube experiments, flame measurements, flame speeds, ignitions). As for many other investigations and mechanism reductions, sensitivity studies were the centre point of the process. Final mechanism comprises out of 53 species and 325 reactions (in the latest 3.0 version).

As mentioned in the previous section dedicated to ethanol mechanisms, the last reported mechanism, not being strictly ethanol based, but rather for an investigation of a small hydrocarbon combustion cases, it was originally reported for a case of methane combustion [105] where burning velocities of hydrogen enriched combustion of methane have been investigated, again in the light of achieving lower NOx emissions based on experimental data performed by the

mechanism authors. This mechanism has been validated with experimental data for oxidation, ignition, and flame structure of hydrogen, carbon monoxide, formaldehyde, methanol, methane, ethane, propane, and some of their mixtures as reported in the source [105].

Also, other methane mechanisms have been reported, i.e. Leeds methane mechanism [106], with 37 species and 351 irreversible reactions somewhat comparable to the GRI mechanism in terms of its size. As reported in the accompanying literature [106], this mechanism also accounts for the oxidation kinetics of hydrogen, carbon monoxide, ethane, and ethene in flames and homogeneous ignition systems in a wide concentration range and is reported to have been tested against a variety of experimental measurements of laminar flame velocities, laminar flame species profiles, and ignition delay times. The mechanism isn't, unlike many others not mentioned here, based on the GRI mechanism but was fully based on gas kinetics measurements. GRI mechanism as mentioned before was reduced automatically by a computer program with a rate parameters tuned to a bulk experimental data (maintained within predefined uncertainty limits). The Leeds mechanism was developed without any modification to the thermodynamic properties or rate coefficients, but only using sound and well documented values (for a better understanding of the mechanism one should refer to the Appendix of the [106] for a detailed description of main 44 reactions).

Final mechanism readily available is the one developed at the USC [107], and even though it is not very well documented by the developers, it is also used by others as a base for the development of more complex c1-c4 mechanisms. It should be noted that the mechanism is loosely based on the GRI mechanism, from which some of the reaction paths have been taken and modified (CO/CO2, CH2, CH3 and others). Final mechanism consists of 111 species and 784 reactions.

On the following figures (Figure 2-12 and Figure 2-13) comparison of the above mentioned mechanisms is presented.

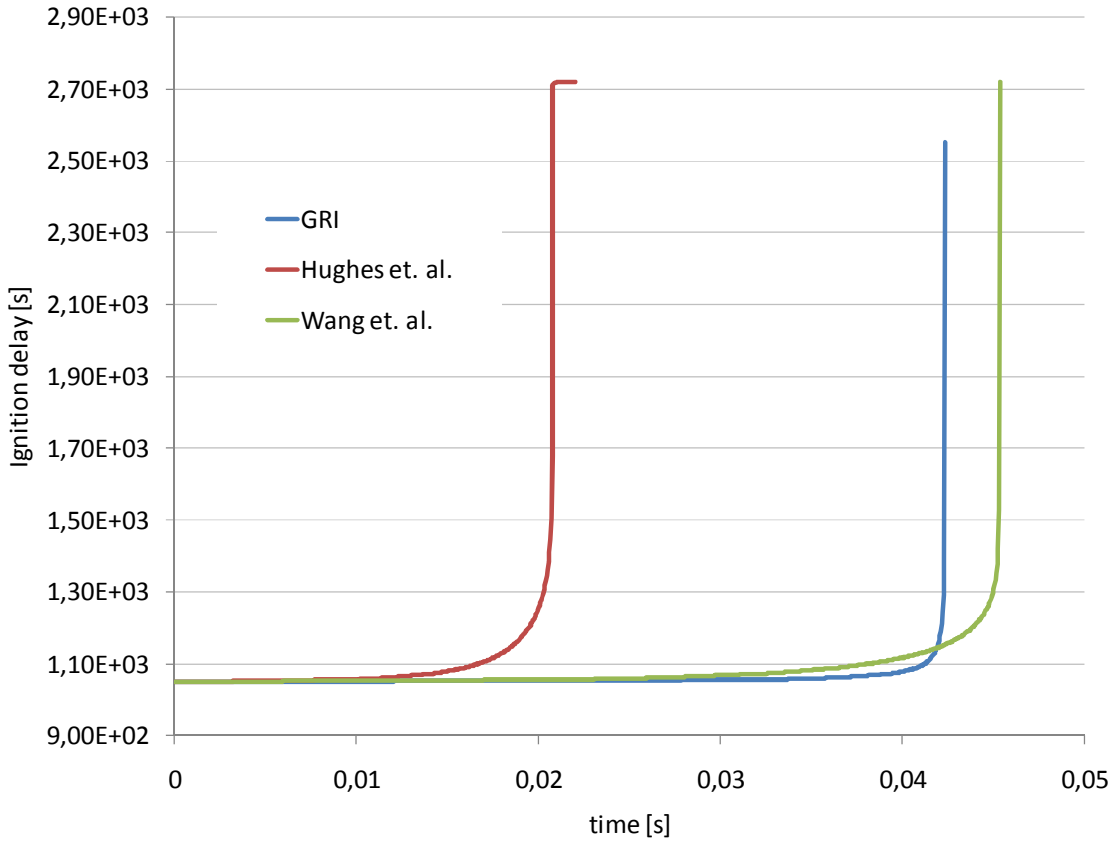

Figure 2-12 Comparison of the above methane mechanisms for a certain case

Figure 2-13 below compares, as for all the previous fuels, the behaviour of the investigated mechanism in terms of ignition-temperature dependence. In this case, the decision is not so clear. Wang et. al. mechanism is comparable to the GRI, and can get the values also for lower temperatures (comparing to GRI mechanism is disputable when observing the below image – extrapolating the values obtained by GRI one would get the value higher than 1s, which is not really usable anyway in terms of fast combustion applications). Also, it should be taken into consideration that the mechanism are validated against the high temperatures where both Wang et. al. and GRI provide similar values). Since the GRI is still widely accepted mechanism for lower hydrocarbon combustion, it was also used in this work for creating the autoignition tables.

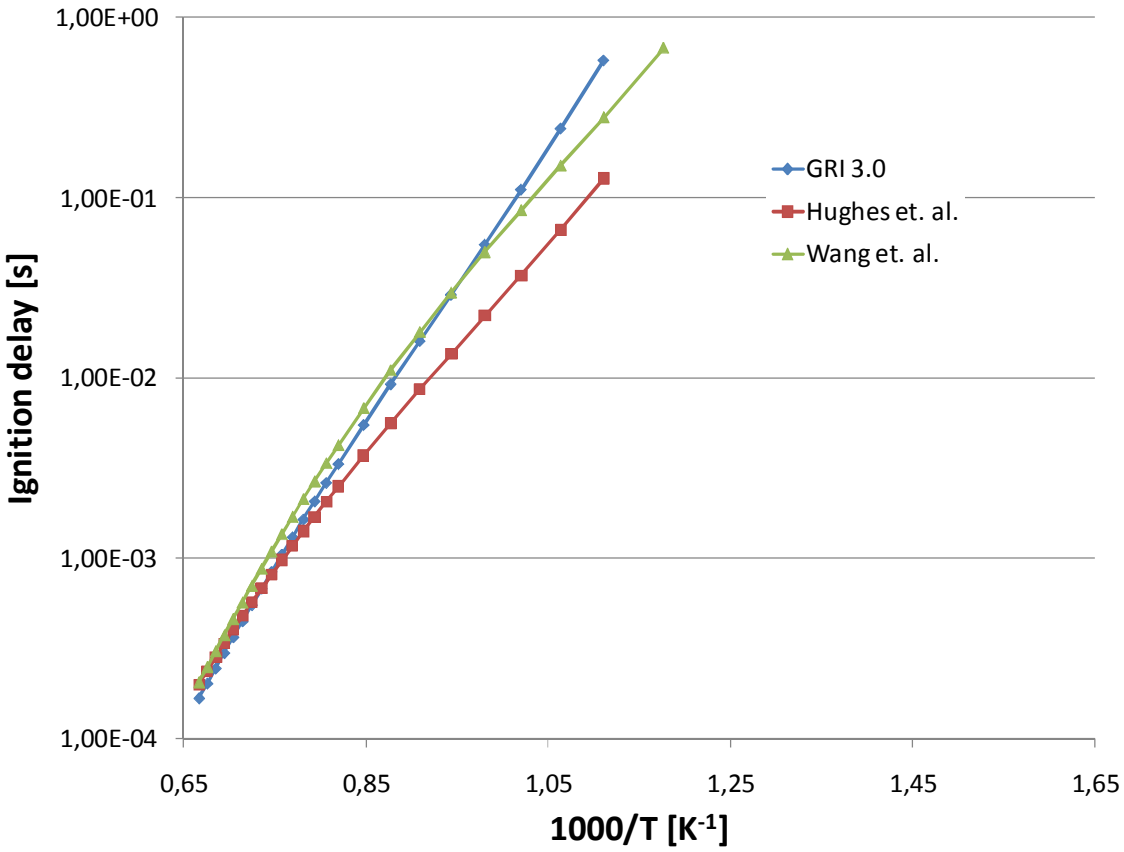

Figure 2-13 Comparison of mechanisms in a temperature dependant series (pressure at 10 bar, equivalence ratio of 0.9 and 0% EGR)

2.10.6 DME

Final fuel of interest is dimethyl-ether (DME) which is the simplest hydrocarbon molecule that exhibits typical two-stage autoignition. More and more recent publications present results from diesel internal combustion engines/vehicles running on pure DME making this fuel and this mechanism also rather interesting to this study. Even more so, if the mentioned results and experiments show that DME is a promising diesel fuel replacement with a high cetane rating providing low particulate emissions and keeping the NOx emissions similar to those from current regular disesel fuel under the same engine operating conditions [108].

The mechanism described here was developed by the same group behind the detailed mechanisms for n-heptane, iso-octane and ethanol. The mechanism was developed referencing measured data for lean and rich flat flames and validated under shock tube conditions at low temperatures and high pressures (a temperature range of 650 to 1300 K, pressures of 13 and 40 atm, and equivalence ratio of 1.0). Under shock tube conditions at high temperatures, the mechanism was validated over a temperature range of 1220 to 1600 K, a pressure of 3.5 bar, and equivalence ratios of 0.5, 1.0 and 2.0. The agreement between the calculations and the experiments is reported to be generally good (also compared in Figure 2-14). The mechanism itself is somewhat dated from the perspective of some of the already mentioned mechanisms, but it is still widely used in a number of applications and during this study it was difficult to obtain another DME mechanism for comparison. Most of the reported mechanisms are developed from this one and in most cases reduced and validated against the results obtained from the one used in this work but none is freely available.

Figure 2-14 displays the behaviour of the mechanism against the experimental data as reported in the literature [109].

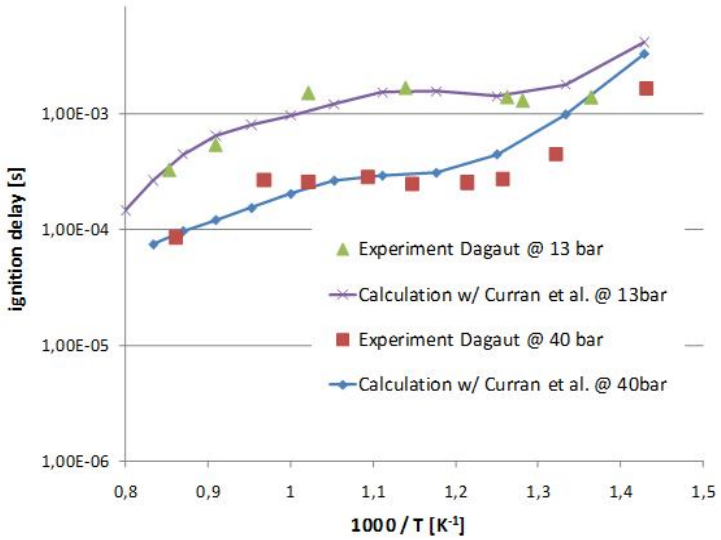

Figure 2-14 Comparison of the DME mechanism against experimental results

2.11 Tabulation

2.11.1 General Overview

As the main topic of this work, an efficient way to include detailed chemistry phenomena into a 3D computational fluid dynamics calculation code was investigated, especially regarding the low-temperature ignition paths. The CFD solver of choice already utilized the benefits of pre-tabulated data implementation, and the same approach was continued in this work [110]. Also, since the CFD solver was of a commercial type, the aspect of methodological usability was considered.

Tabulation procedure can be regarded as a three step process:

1. pre-processing
2. calculations
3. post-processing

Each of the mentioned steps will be shortly described in this chapter.

2.11.2 Pre-processing

The pre-processing stage usually includes the preparation for the calculations, in terms of determining the needed ranges for initial parameters, selection of appropriate mechanism, and setting up the calculation loop scripts. As shown in the previous chapter, one has to make sure that for the fuel of choice appropriate mechanisms are available, and to set up the initial parameters ranges according to ones specified in the mechanisms accompanying literature. If more mechanisms are available, as shown earlier for some fuels used more often, there will undoubtedly be a need for a compromise between the speed of the tabulation and the complexity (usually closely related to accuracy) of the mechanism. The calculation application used in the tabulation, equipped with a separately written

shell script, can also be used to calculate a single case with the temperature curve drawn in real-time to make the comparison and subsequently the decision straightforward.

In most cases, since the limited amount of experimental data is available to mechanism developers, the initial parameter range could be outside the one at which the validations have been performed. In this case, more calculations with the parameters outside the prescribed by the literature are needed. Usually, to find out if the needed range extension is valid, one needs to look for the stable trends continued from the valid parameter ranges. In some cases, however, the trend tracking is not so straightforward, which could be seen in the previous comparison of the mechanisms, but also later in the tabulation results, since the complex chemistry includes many intermediate phenomena that influences the behaviour of the results compared to the, e.g. initial temperature or equivalence ratio. In this work, a heavy assumption has been made regarding the influence of the EGR amount. With no reaction mechanism related literature making any comments on the behaviour depending on introduced product species into the initial mixture, it was taken that the species introduced as a part of the EGR provide reasonable results in terms of longer ignition times and lower flame speeds mostly due to inert species such as nitrogen.

2.11.3 Calculations

Tabulation itself, both for calculation of parameter dependant ignition delays and laminar burning velocity, uses applications described earlier written in programming language FORTRAN. Since such applications do not accept command-line arguments (and the number of arguments surpasses the already mentioned user oriented application) the initial data for applications is transferred by using an ASCII file interpreted by the application. Since the laminar burning velocity calculation application was written before the one intended for auto-

ignition tabulation, its format was used also in the latter case. The input document contains the parameters used as a initial and/or boundary values for one case:

- mixture pressure,
- mixture temperature,
- equivalence ratio,
- amount of residual gas mass fraction- EGR (defined as mass fractions of product species in the initial mixture)

Initial composition is calculated from equivalence ratio and EGR as shown in following equations. For simplicity, the content of the EGR gases is taken from a complete stoichiometric combustion case, and as such added to the fresh fuel and oxidizer mixture according to a defined rate. Definition of equivalence ratio and EGR comes from the basic general oxidation reaction:

$$F + n_{O_2} O_2 + n_{N_2} N_2 \rightarrow n_{H_2O} H_2O + n_{CO_2} CO_2 + n_{O_2} O_2 + n_{CO} CO + n_{N_2} N_2.$$

In the above reaction F denotes the fuel species (or blend of combusting species), which can be, in general form for hydrocarbon fuels, written as $C_xH_yO_z$. The quantities of reacting species and products are denoted by n_k (subscript k denoting the species). When regarding the combustion system defined as above, for easier calculation of the products few assumptions have been made:

- when the reacting mixture is lean, there is no consumption of excess oxygen;
- if the reaction mixture is rich, there is no oxygen among the product species, and the excess carbon appears as additional CO species, and therefore, no unburnt fuel appears in products.

If one assumes the reaction of 1 mole of fuel, the according amount of oxidizer, dependant on the equivalence ratio, can be calculated by the following equations:

$$O_{stoich} = x + \frac{y}{4} - \frac{z}{2}, \qquad (2\text{-}19)$$

$$n_{O_2} = O_{stoich}\frac{1}{\varphi}, \tag{2-20}$$

$$n_{N_2} = n_{O_2}\frac{0.71}{0.21}. \tag{2-21}$$

As discussed in the previous text, values x, y and z denote the number of atoms in the fuel species of carbon, hydrogen and oxygen respectively. Stoichiometric amount of oxygen neede for combustion of 1 mole of fuel is denoted above with O_{stoich}. The equivalence ratio is represented by the symbol φ defined as:

$$\varphi = \frac{actual\ air/fuel\ ration}{stoichiometric\ air/fuel\ ratio} = \frac{\frac{m_f}{m_{ox}}}{\left(\frac{m_f}{m_{ox}}\right)_{stoich}} = \frac{\frac{n_f}{n_{ox}}}{\left(\frac{n_f}{n_{ox}}\right)_{stoich}}. \tag{2-22}$$

The product mixture depends on the equivalence ratio and is calculated according to the assumptions provided earlier using the following equations:

$$n_{CO_2} = \begin{cases} x, & \varphi < 1 \\ 2n_{O_2}\big|_{react} - x - \frac{y}{2}, & \varphi \geq 1 \end{cases}, \tag{2-23}$$

$$n_{H_2O} = \frac{y}{2}, \tag{2-24}$$

$$n_{O_2} = \begin{cases} n_{O_2}\big|_{react} - n_{CO_2} - n_{H_2O}, & \varphi < 1 \\ 0, & \varphi \geq 1 \end{cases}, \tag{2-25}$$

$$n_{CO} = \begin{cases} 0, & \varphi < 1 \\ x - n_{CO_2}, & \varphi \geq 1 \end{cases}, \tag{2-26}$$

which, finally, provides the composition of the product species used to calculate initial composition of the mixture for the case of residual gasses, calculated as

$$EGR[-] = \frac{m_{products}}{m_{fuel} + m_{oxidizer} + m_{products}}. \tag{2-27}$$

The above equation is used to calculate the amount of species combined in the product mixture apposed to the EGR and the fuel+oxidizer by a simple algebraic manipulation of the equation (2-27)

$$m_{products} = \left(m_{fuel} + m_{oxidizer}\right) \frac{EGR}{1 - EGR}. \tag{2-28}$$

Finally, the calculated mass of recirculated products is then distributed among the constituting species which are augmented to the fuel and oxidizer species, thus finalizing the calculation of the initial composition of the reacting mixture. For the sake of easier tracking of the species the composition is normalized before the combustion calculation is initiated.

2.11.4 Technical Aspects

As an important part of this stage of the tabulation process, some technical aspects will be shortly presented here. Since the tabulation is performed as a looped series of calculations, rather than having entire loop ran from inside one executable application (such options also implemented), it was shown that more reliable, in terms of calculation monitoring and restarting, was the approach of creating the outside tabulation loop script to govern the calculation sequence. This approach

was first used for autoignition tabulation, which had few problems regarding stability but provided a simple way of tracking the progress of the tabulation and also a simple way to restart the tabulation process from within the loop script.

In the case of laminar flame velocity calculation which had, due to the more complex problem definition and differential equations needed to be solved, more difficulties getting to a converged solution, the calculation loop would be terminated if the solution of a certain case could not be obtained using the supplied parameters. This proved to be the main drawback of the hardcoded loop routine, and made the approach of using the outside looping script shell more appealing as a solution. This way, even if the calculation is terminated, the failure notice would be written in the result status file, but the loop would continue until all the cases are calculated (successfully or not), and the analysis as an early post-processing step could be performed to determine the best way to obtain the failed calculation results. During this work, three approaches were used to deal with the problem of missing data.

First approach would be a trivial one: if the calculations fail using one mechanism, one should try to rebuild the database with another. Of course, in this case, more elaborate investigation and comparison of the mechanisms should be performed, and when calculating the laminar flame velocities the investigation should be performed before the tabulation with the most stable mechanism selected. A good testing procedure would include calculations using a combination of lower temperature, lower pressure, and borderline equivalence ratios (extremely rich or lean mixtures).

Second approach can be used in the case of the laminar flame velocities tabulation failed calculation. Since the PREMIX calculation allows several parameters to be changed besides the ones needed for definition of thermodynamic and chemical properties, one could get a converged solution also trying to modify the parameters such as the geometrical information of the domain, number of discretization points, the initial position of the flame and several numerical parameters (absolute and relative tolerances for the termination of the Newton

iteration, number of iterations allowed in the steady state Newton method, etc.). The number of additional parameters to be tempered with indicates the necessity of ones experience dealing with the setting of these values and also a deeper insight on the technical aspects.

Final approach, also used and developed during this work, includes the mathematical analysis of the entire data and repairing the missing point using some of the methods described in the next chapter. This approach does not require additional computation, and can provide relatively acceptable results, conforming to the overall trends of the calculated values, in a reasonably short amount of time, giving also more detailed insight of the dependence of the calculated values on the initial parameters. The result of this stage was developing a several repair algorithms and correlation functions which can, along with repairing already created database, make further tabulation need less points of initial parameters.
Using the outer loop script in the current version also facilitates a looping strategy not only in sequential mode, but a more general form, making it appropriate to run additional repeated calculations with a scattered initial parameters data.

2.11.5 Repair Algorithms

In some cases, especially regarding laminar flame velocities tabulation, not all calculations of a tabulation procedure converges to a stable solution, providing in the end a result matrix missing some of the data. During this work, as explained in previous chapter, such cases have been dealt with in one of three approaches. This chapter will describe the methodologies used in the approach of using mathematical analysis of the existing data to fill the missing points without spending more time running repeated calculations varying the parameters of the numerical algorithms in the calculation application.
Repair algorithms discussed in this chapter usually follow the same principle, which is to ensure the correct representation of the trends observed by

investigating the result dependence on each of the varied initial parameters. Initially, several methods have been tried by using different third-party tools and applications, but finally the simple approach was found to provide the most satisfying results.

Two types of approaches were considered. First approach was to draw sound conclusions from the available calculated data and by using regression analysis try to represent observed behavioural rules with a relatively simple mathematical equation valid for as large parameter region as possible. Usually, it was a simple case of least square method to find the parameters of a polynomial or exponential function, or a simple mathematical assumption on the strict exponential behaviour of the values. For example, in the Figure 2-15, a set of results missing last few points is shown (case of missing laminar flame velocity data for ethanol).

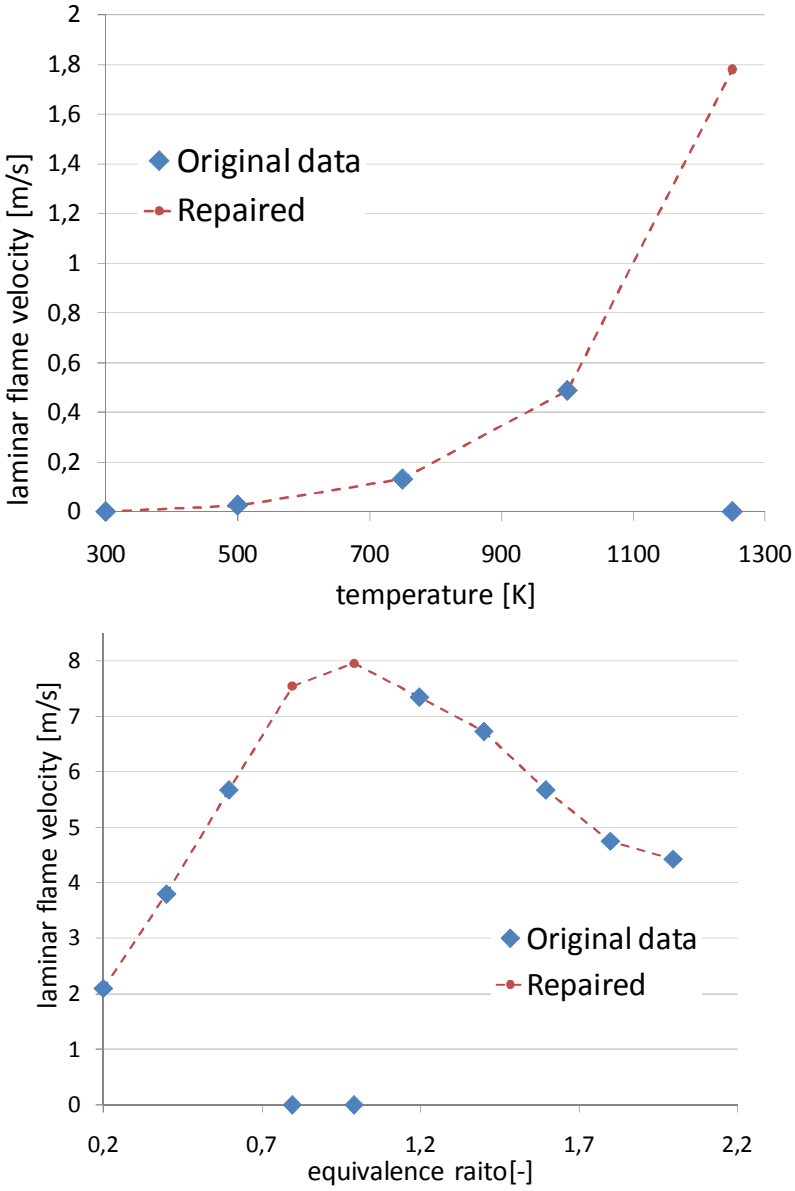

Figure 2-15 Sample set of results with missing data

An assumption, drawn from the sets which have all the points states that the dependence of the result on one of the parameters (in this case EGR) is exponential, in the form of:

$$y = Ae^{Bx}\,. \tag{2-29}$$

The parameters in the above functions are trivially calculated from two existing points:

$$A = y_o \quad \text{for } x_0 = 0, \tag{2-30}$$

$$B = \frac{ln\frac{y_1}{A}}{x_1}. \tag{2-31}$$

Usually, higher EGR points are more difficult to obtain so the 0% EGR value is available in most cases. If the 0% EGR point is not available the parameter values are again easily obtained as

$$B = \frac{ln\frac{y_1}{y_2}}{x_1 - x_2}, \tag{2-32}$$

$$A = y_1 e^{-Bx_1}. \tag{2-33}$$

If such regularity cannot be observed or would provide greater discrepancy of the results in terms of not following the trends when compared to the dependence on some other parameter, other approach could be used. This approach forces a predefined trend and does not try to use a single mathematical equation to describe the entire curve but simply to follow the behaviour set by the existing data points. The algorithm could be simply represented in following few steps (if we predefine an ascending trend):

1. start with the first available point and proceed to the next point in the prescribed direction;
2. search for not less than three available consecutive points conforming to the trend;

3. if a group of three points have been found, go in the prescribed direction and check each of the points against the demand of following the prescribed trend;
4. if the trend is not being followed, correct the point by calculating the new value from the three last "good" points using the second order extrapolation equation, or
5. search for the first point following the trend and use it to calculate the new values either by interpolation from the "good" points or the combination of the extrapolation from step 4 and interpolation combined as a mean value.

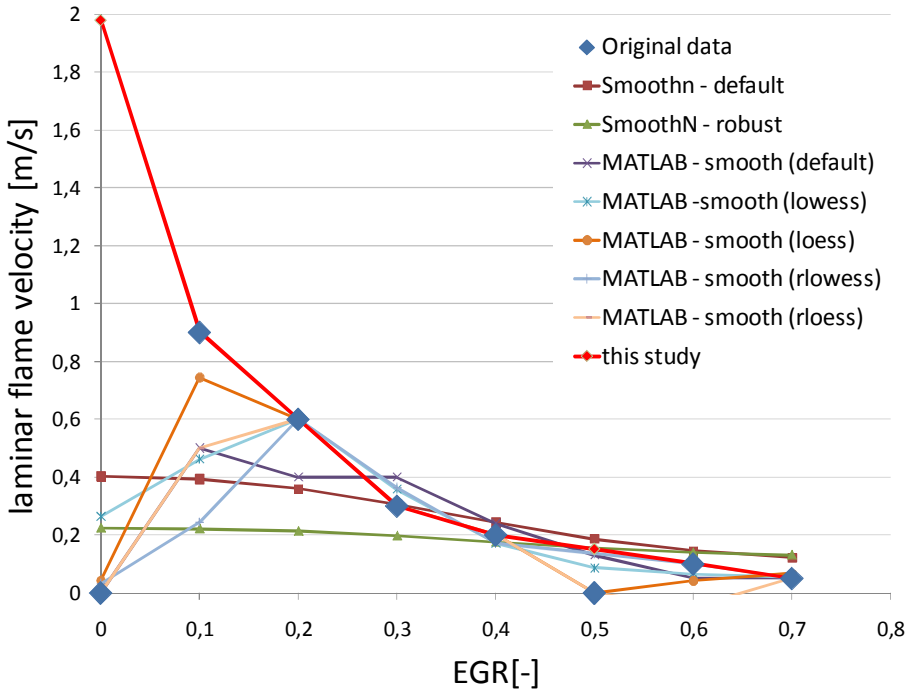

Figure 2-16 Comparison of several available smoothing routines

As shown in Figure 2-16, available smoothing routines were tested against a sample data with two missing points (e.g. dependence of laminar flame velocity on residual contents). In this case it was shown that using, for example, several degrees of implemented MATLAB® function "smooth"[111], which relies on using a moving average filter and as well a third-party MATLAB® routine "smoothn"

based on a penalized least squares method [112]. In general, used approaches have managed providing a smooth surface (in some cases), but lack at some point to maintain the curve trend. Also, inevitably, a valid data is also being tampered which is highly undesirable in this case. The proposed procedure has, in this types of cases, provided best results, simply altering the missing data and following prescribed trends. The methodology, however, is not general, but specific for the ignition tabulation where one has a fairly good idea on the behavior of data trends. In some cases number of "good" data is too scarce, but in the cases of autoignition and laminar flame velocity tabulation, there are four parameters at ones disposal and usually a good combination can be found to have enough "good" points for correcting the entire result matrix. Also, this type of database repair algorithm heavily depends on ones experience and a good insight on the final repaired database, since there will be cases of not so straightforward dependence of the resulting value on the parameter variations.

On the other hand, the above methodology allows also the option to combine the approaches. For example, as displayed in the Figure 2-17, the half of the data in specific case is missing. One usually has an overall idea of how should the shape of the curve look like, but in terms of repairing the entire database with more cases like the displayed one, it should be done in an automatic manner to require lesser human intervention. The approach to correct the data in this case was to combine the method of using a correlation function for another parameter and the second order extrapolation on the displayed data. The other parameter used in this case was temperature which was replaced in this case with an exponential function of the type described by (2-29).

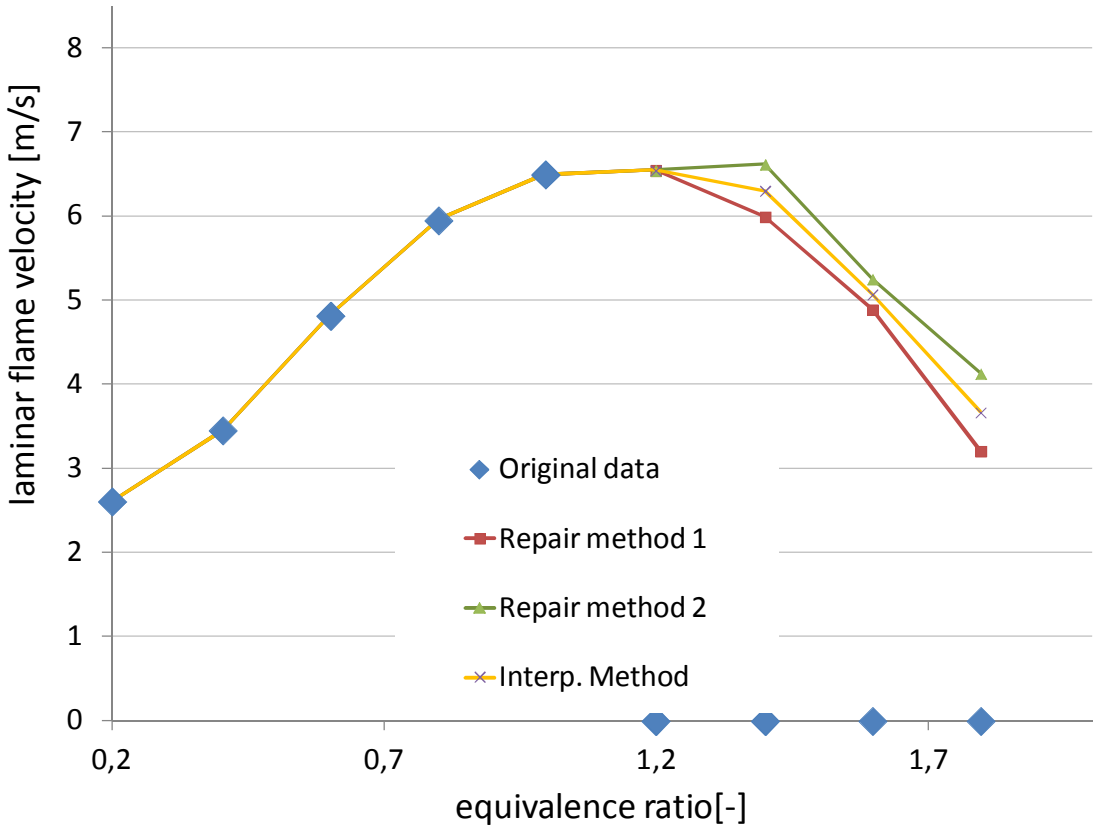

Figure 2-17 Sample set of results with missing more data
(also ethanol but the case with equivalence ratio)

The problem of using only one parameter for repairing of the database can now be observed. The correlation function provides reasonable augmentation of the data looking at the temperature curve, but the data calculated with this method, and mapped to a different parameter curve, in best case provide not so smooth result. However, since the temperature extrapolated points follow a general trend of the curve the data is not to be disregarded. On the other hand, using the second order extrapolation approach is valid if there is not more than one local maximum/minimum in the data. The reason for this is that the methodology follows only the trend provided by the existing points in a limited area. This will not cover all physically (nor chemically) influenced deviations in the curve (such as a NTC in the n-heptane combustion or, as in this case, flame velocity dependence

on equivalence ratio). The final approach of combining the two methodologies would be expected to ensure two significant subjects

1. respecting the expected trend,
2. respecting the quantities.

In the light of the presented case, one argues that the temperature correlation function provides the overall expected trend of the repaired curve (providing the minimum and maximum at the right places), but also overshoots the expected values of the data. On the other hand, second order extrapolation, as explained earlier, does not follow the trend entirely since it cannot predict the existence of the local minimum, but, since the values are calculated from the existing data, the overall quantities are satisfactory. The final solution to this matter would be to combine the two results by interpolating them to obtain the final points respecting both requirements of the two approaches. The interpolation can additionally be improved by using a weight coefficient to emphasise the significance of one of the approaches.

2.11.6 Correlation Functions

Basic use of the correlation functions has been already described in the previous chapter on data repairing techniques. However, in some cases correlation functions can be used to describe the behaviour of the data against a parameter even before the tabulation calculations start, thus removing the need of a certain parameter being looped through and, that way, significantly reducing the amount of calculations and time needed to create the entire database. Also if the data has already been calculated, the correlation functions can be used to check and repair the missing points.

In this work, two correlation descriptions have been investigated; one already known, but not valid for the entire scope of the parameter values, and the

other, potentially very useful for the tabulations of fuel blends. First one, introduced by [113] describes the behaviour of laminar burning velocities when changing the composition of the initial mixture. The data are calculated with a correlation functions (for iso-octane/air premixed combustion) varying equivalence ratio:

$$S_L = S_{L,0}\left(\frac{T}{T_0}\right)^{\alpha}\left(\frac{p}{p_0}\right)^{\beta}, \tag{2-34}$$

where S_L denotes the general laminar burning velocity, $S_{L,0}$ is the nominal burning velocity at standard pressure (p_0) and temperature (T_0) for a defined equivalence ratio described as:

$$S_{L,0} = 0{,}305m/s - 0{,}549m/s(\varphi - 1{,}21)^2, \tag{2-35}$$

and the parameters α and β also, as described in the literature, depend on equivalence ratio. Also, some authors extend the above equation to be used in some of the combustion models fit for internal combustion engines calculations by including the turbulence effects on flame development. Since this work is based on the tabulation of the data in the strict laminar flame combustion and the turbulence is handled by a CFD solver, this topic can be in more detail found in [114].

On the other hand the correlation equation for residual gasses is more interesting in terms of the investigations performed in this work. Initially suggested correlation function by [113] can be written as:

$$S_L = S_L^0(1 - 2{,}1y_{EGR}), \tag{2-36}$$

where the S_L remains the value of laminar burning velocity for a certain amount of introduced EGR (y_{EGR} as a mass fraction in the initial burning mixture

composition) and S_L^0 representing the laminar burning velocity of the same temperature, pressure and equivalence ratio values but with no EGR in the mixture. This correlation function is very useful to introduce the effects of residual gas recirculation in the problem without the need to additionally run a number of tabulation calculations where EGR proved to be disrupting factor in terms of calculation stability. The main drawback of the above equation is visible from the equation itself, having a fixed amount of y_{EGR} at which the calculated laminar burning velocity becomes zero ($y_{EGR} = 47{,}6\%$), and for higher values becomes negative. In this respect, an alternative correlation function is suggested. To overcome the issue of laminar burning velocity becoming negative, or zero for higher values than 50% EGR, an exponential function was selected and refined according to a set of existing data. Final correlation function is defined as:

$$S_L = S_L^0 e^{-Ay_{EGR}} \tag{2-37}$$

providing a sound estimate, compared to the data calculated by the PREMIX application, and also to other correlations found in literature [115] as shown in the Figure 2-18. It should be noted that the above correlation function was created to fit the data calculated for n-heptane and iso-octane flames. Other fuels have been tested to some extent and found to conform to the same type of the equation with slightly modified exponential constant *A*.

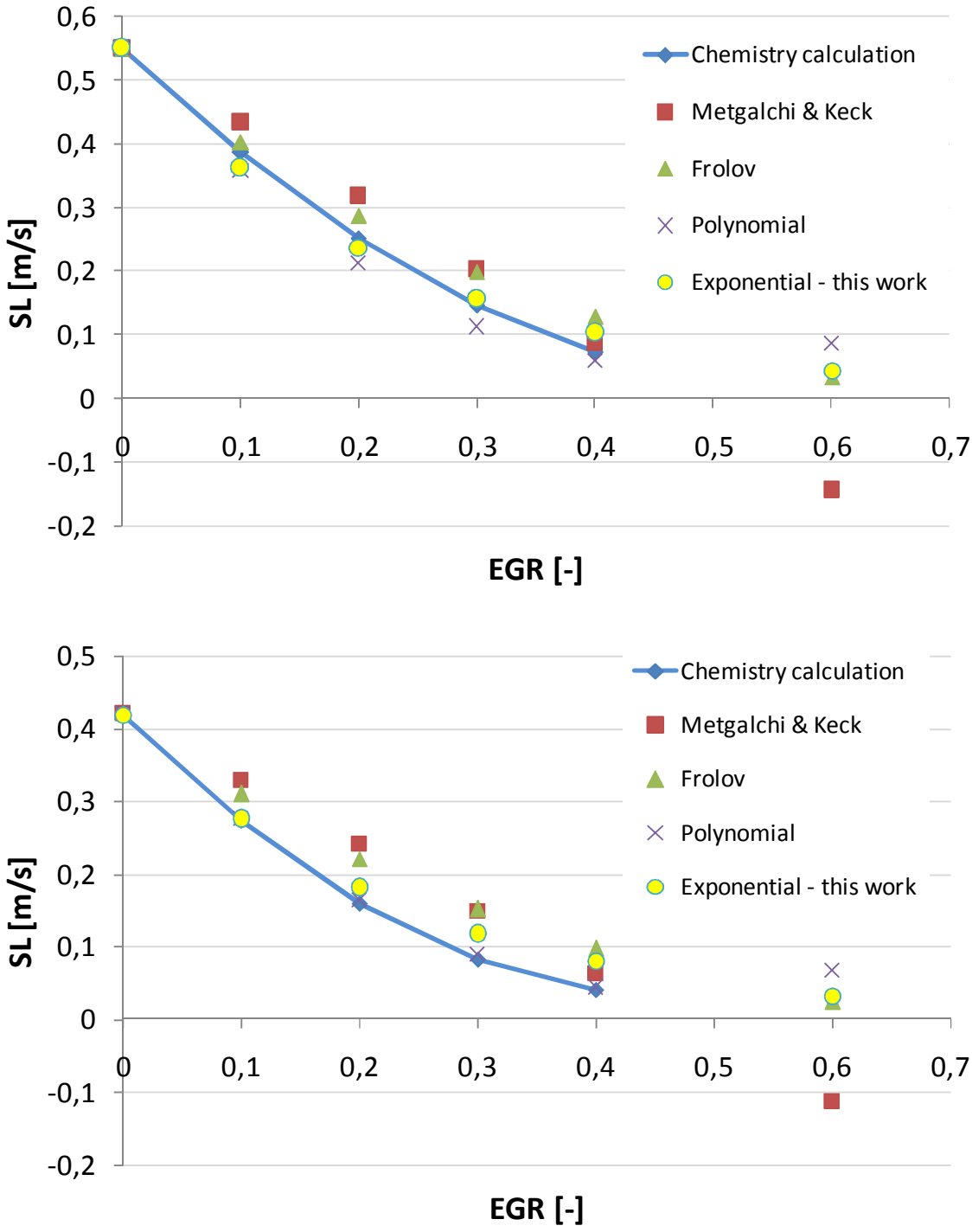

Figure 2-18 Comparison of several correlation functions

The parameter values for several lower hydrocarbon fuels can be found in Table 2-3.

Table 2-3 Exponential parameter *A* for correlation function (2-37) for fuels of interest

Ethanol	4.2
N-Heptane	3.2
Methane	4.3
Iso-octane	4.0

2.11.7 Fuel blends

In case the fuel is not a single component species, but a blend of more combusting species, another dimension is added to the tabulation database, also increasing the requirements for computation (at least doubling it). It would, in this case, be particularly useful to be able to, in case one considers blending the fuels for which there already exists a ignition database, calculate the ignition data using existing values.

Original idea behind this was to derive such a methodology for a specific n-heptane / ethanol blend, but at the moment of writing, to author's knowledge, a mechanism capable to calculate the desired fuel blend additionally validated at such task wasn't available. Therefore, for academic purposes, to test the assumption of developing a correlation function for a fuel blend, a readily available mechanism, also presented before, was used (Andrae et al. [15][102]). This mechanism was developed and also additionally validated to accommodate the simulation of iso-octane/n-heptane and toluene/n-heptane blends, with specific oxidation branches responsible for these cases. Having both iso-octane and n-heptane fuels considered in more detail during this work, and the realistic background behind the blend (n-heptane used to lower the Research Octane

Number (RON) of the fuel blend) of the two, make these suitable candidates for an attempt to create a dependence function for calculation of the ignition delay of the blend.

Several cases have been calculated varying few pressure, temperature and egr parameters, also with changing the composition of the fuel (from 100% iso-octane – RON=100 to 100% n-heptane – RON = 0). The results have then been investigated and a suitable mathematical representation of the ignition delay dependence on the fuel mixture has been found. The behaviour of the curves, as shown in Figure 2-19, was considered to be most likely represented by a simple power curve in a form:

$$AI = A\, nhept_{fr}{}^{B}. \qquad (2\text{-}38)$$

Including the influence of the both ignition delays in the above equation, after least square optimization of the coefficients, yields the final equation in the form:

$$AI = AI_{nhept}\left(nhept_{fr} + 1e^{-3}\right)^{-0.43\ln\left[\frac{AI_{ioct}}{AI_{nhept}}\left(1-3e^{-5}\frac{1}{AI_{nhept}}\right)\right]}. \qquad (2\text{-}39)$$

In above equations AI_{nhept}, AI_{ioct} and $nhept_{fr}$represent ignition delays of pure nhepane and iso-octane and nheptane mass fraction in the fuel blend (0-1), respectively.

Comparison of the values directly calculated using a constant volume homogeneous reactor (dots) and the ones calculated from 100% of each fuel and the equation (2-39) are also displayed in Figure 2-19 showing acceptable agreement. The nature of the equation, though, limits its usage near the pure iso-octane fuel and should be used for 95% iso-octane and lower (RON<95).

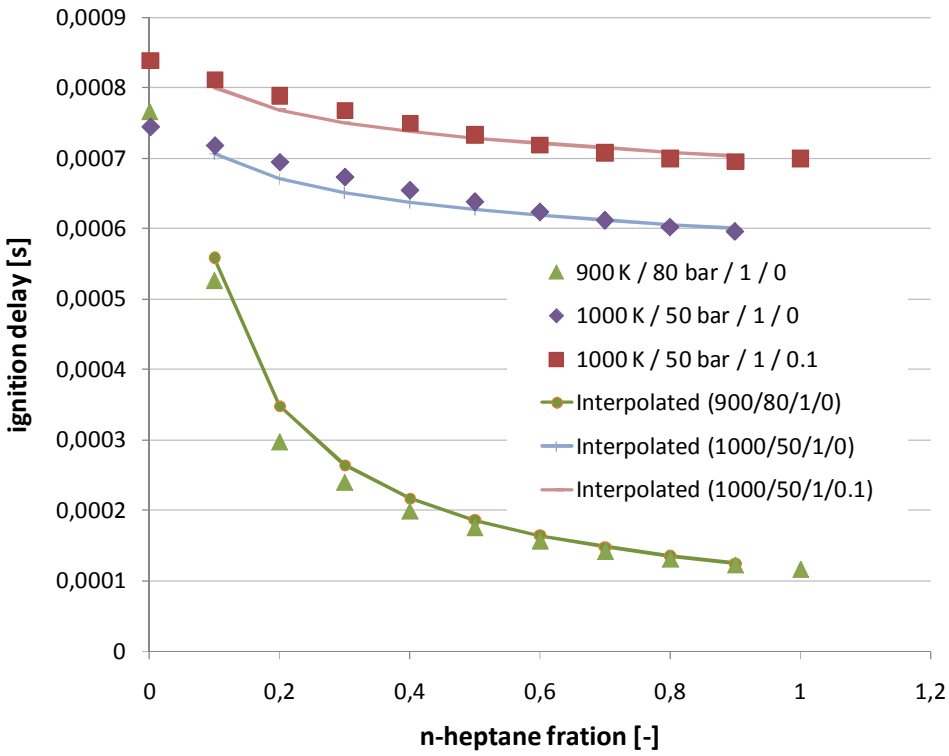

Figure 2-19 Fuel blend investigation cases with interpolated values

Looking at the above figure, one could also see larger difference at certain points (maximum at around 15% error). Having in mind the different results of the pure fuel species ignition using different mechanisms, a conclusion can be made that the error in this light is acceptable, since the trend of the curve is represented correctly.

If one would need to consider a case including a combustion of a nheptane/isooctane fuel blend of RON = 90, already having a databases for isooctane and nheptane, a final database could be created fast and with a reasonable accuracy. The calculation of the new database with included fuel blend coefficient would be advised only where a certain type of fuel blend is investigated in detail.

It should also be emphasized that the above formulation is only valid for the mentioned fuels. If another fuel blend is to be considered, even using one of the

species from this example, an investigation on the ignition delay behaviour must be performed, and the equation (2-39) modified.

2.12 CFD Modelling

Even if the vast majority of this work is based on 0D or 1D calculation, the final implementation of the tabulation results aims at a three dimensional CFD solver. This chapter briefly gives the fundamentals of modelling equations for heat and mass transfer. These equations are based on the conservation laws of:

- mass (overall and for chemical species);
- momentum;
- energy.

In previous chapters various forms of the mass and energy equations have been encountered; the governing energy and species mass conservation in the autoignition modelling and augmented with overall mass conservation equation in the laminar flame velocity calculations.

In terms of calculating the physical phenomena in the CFD, one regards the above mentioned laws through the prism of spatial discretization, dividing the flow into a finite number of control volumes and deriving the mathematical representation of the laws for each of them. Fluid being observed is regarded as a continuum, with averaged properties like density, pressure, velocity, turbulence, without having a deeper insight in the behaviour of the molecules from which it is made of.

Each property can be represented by a general equation for one of the control volumes:

$$(RATE\ OF\ CHANGE)_V + (OUT/INFLOW)_S = (SOURCE/SINK)_V$$

Where the subscript V denotes the fact that the term is derived over the control volume and the subscript S denotes the derivation over the surface of the control volume. More detailed representations of the above equation, written in various forms can be found in many standard textbooks such as [116][117][118]. This

chapter will only provide specific governing equations, derived for a case of a single phase fluid flow related to the topic of this work.

2.12.1 Mass Conservation Equation

The first of the fundamental equations is the mass conservation equation, already encountered in the chapter with a description of the equations used by the PREMIX solver. This equation basically states the fact that fluid mass cannot be created or destroyed inside a control volume, but it can change due to the difference of the inflow and the outflow through the control volume's boundaries, symbolically written in the integral form:

$$\int_S \rho u_j n_j dS = -\frac{\partial}{\partial t}\int_V \rho dV \,. \tag{2-40}$$

In the above equation the left side represents the rate of mass flux through the boundaries S and the term on the right side represents the rate of change of total mass in the control volume V. In a differential form, after submitting the above equation to Gauss divergence theorem, it can be written as:

$$\frac{\partial \rho}{\partial t} + \frac{\partial}{\partial x_j}\left(\rho u_j\right) = 0 \,. \tag{2-41}$$

and is commonly found in the standard literature.

2.12.2 Momentum Conservation Equation

The momentum conservation equation is the second of the fundamental laws in the mathematical description of the fluid flow, and is derived in similar manner as the mass conservation in the previous paragraph. Newton's second law defines the

time rate of change of momentum (of a fluid particle) as a sum of the acting volume and surface forces. The integral form of this statement can be written as:

$$\int_V \frac{\partial}{\partial t}(\rho u_i)dV + \int_S (\rho u_i)u_j n_j dS = \int_V \rho f_i dV + \int_S \sigma_{ji} n_j dS\,, \qquad (2\text{-}42)$$

where the first term on the left hand side represents the rate of change of the momentum, the second one is the net momentum flux through the volume boundary surfaces and the right hand side represents the sum of volume and surface forces acting on the fluid within the control volume.

Again, using the Gauss theorem transforming the boundary surface into the volume integral, and considering an arbitrary volume *V*, the above integral equation can be rewritten in a differential form:

$$\frac{\partial}{\partial t}(\rho u_i) + \frac{\partial}{\partial x_j}\left(\rho u_i u_j\right) = \rho f_i + \frac{\partial \sigma_{ji}}{\partial x_j}. \qquad (2\text{-}43)$$

The right hand side of the differential representation of this law can be transformed by decomposing the surface forces (the second term, the first one represents the volume forces) into pressure and viscous stress forces as:

$$\sigma_{ij} = -p\delta_{ij} + \tau_{ij}\,, \qquad (2\text{-}44)$$

where δ_{ij} denotes the Kronecker tensor (equal to 1 if i=j, 0 otherwise) and τ_{ij} represents the rate of the strain tensor (the symmetric part of the deformation tensor) [119] defined as:

$$\tau_{ij} = \mu\left(\frac{\partial u_i}{\partial x_j} + \frac{\partial u_j}{\partial x_i}\right) - \frac{2}{3}\mu\frac{\partial u_k}{\partial x_k}\delta_{ij}\,. \qquad (2\text{-}45)$$

In the above equation μ is the dynamic viscosity coefficient. Finally the differential form of the momentum conservation law can be written substituting the Newton's law of viscosity resulting in the set of equations in the following form:

$$\frac{\partial}{\partial t}(\rho u_i) + \frac{\partial}{\partial x_j}(\rho u_i u_j) = -\frac{\partial p}{\partial x_i} + \frac{\partial}{\partial x_j}\left[\mu\left(\frac{\partial u_i}{\partial x_j} + \frac{\partial u_j}{\partial x_i}\right) - \frac{2}{3}\mu\frac{\partial u_k}{\partial x_k}\delta_{ij}\right] + \rho f_i. \quad (2\text{-}46)$$

This set of equations is known as the Navier-Stokes equations where the first term on the right hand side represents the pressure gradient forces acting on the control volume, the second one the normal and shear stress actions on the control volume surface, and the last one represents the volume forces acting on the control volume.

2.12.3 Energy Conservation Equation

One form of the energy conservation equation has been encountered when discussing the basic equations behind the homogeneous reactor and 1D freely propagating flame calculations. The principle behind the derivation of the energy conservation equation follows the physical principle that the energy in the system remains constant as it neither gets created nor destroyed. The first law of thermodynamics states that the rate of energy change is equal to the sum of the rate of heat addition and the rate of work done (on a fluid particle). Considering the total energy as the sum of kinetic and internal energy:

$$e = \frac{1}{2}u_i u_i + i\,.$$

The integral form of the energy conservation equation for a control volume can be written as:

$$\int_V \frac{\partial}{\partial t}(\rho e)dV + \int_S (\rho e)u_j n_j dS = \int_V \rho f_i u_i dV + \int_V S dV + \int_S \sigma_{ji} n_j u_i dS - \int_S q_j n_j dS \,, \tag{2-47}$$

with the first term on the left hand side representing the rate of change of total energy, second term represents total loss of the energy through the control volume boundaries. The terms on the right hand side represent specific power by the volume forces then distributed internal heat source due to radiation, chemical reactions or any other volumetric heat source, surface sources as the time rate of work done by the pressure and viscous stresses on the fluid element and finally the heat flux vector commonly written in the form of Fourier's law of heat conduction:

$$q_j = -k\frac{\partial T}{\partial x_j}, \tag{2-48}$$

which linearly relates the temperature to the heat flux with the thermal conductivity coefficient k. As with the previous fundamental laws, the energy conservation equation can be submitted to the Gauss theorem and finally transformed into a differential form as:

$$\frac{\partial}{\partial t}(\rho e) + \frac{\partial}{\partial x_j}(\rho e u_j) = \frac{\partial}{\partial x_j}(\sigma_{ji} u_i + q_j) + S + \rho f_i u_i. \tag{2-49}$$

The above differential form can also be written as a specific enthalpy conservation equation having $\rho h = \rho i + p$:

$$\frac{\partial}{\partial t}(\rho h) + \frac{\partial}{\partial x_j}(\rho h u_j) = \frac{\partial p}{\partial t} + \frac{\partial}{\partial x_j}(p u_j) + \frac{\partial}{\partial x_j}(\sigma_{ji} u_i + q_j) + S\,. \tag{2-50}$$

2.12.4 General Transport Equations

Following all the above representations, a general form of the conservation equation for any dependent variable can be derived. Denoting such a variable with φ (not to be confused with the equivalence ratio from previous chapters) and obeying the generalized conservation principle an integral form of a conservation equation of a scalar property φ can be written in the case of a fixed control volume as:

$$\int_V \frac{\partial}{\partial t}(\rho\varphi)dV + + \int_S (\rho\varphi)u_j n_j dS = \int_V S_\varphi dV + \int_S \left(\Gamma_\varphi \frac{\partial \varphi}{\partial x_j}\right) n_j dS\,. \tag{2-51}$$

In the above equation, the first term on the left side is the unsteady term, the second term represents the convection, and on the right hand side, the first term is the source or the sink and the second one represents the diffusion. Across the control volume boundaries, one can distinguish two types of transport mechanisms – convection as the transport of the property due to the movement of the fluid, and diffusion as the transport due to the differences in concentration (concentration gradient).

Again, to transform the integral representation of the general transport equation into the differential form, Gauss divergence theorem is used, and subsequently we can write:

$$\frac{\partial}{\partial t}(\rho\varphi) + \frac{\partial}{\partial x_j}(\rho\varphi u_j) = \frac{\partial}{\partial x_j}\left(\Gamma_\varphi \frac{\partial \varphi}{\partial x_j}\right) + S_\varphi \,. \tag{2-52}$$

In case of a time dependent problem, the integral form of the general transport equation must also include a temporal integration over a small interval Δt in the following form:

$$\int_{\Delta t} \frac{\partial}{\partial t}\left(\int_V (\rho\varphi) dV\right) dt + + \int_{\Delta t}\int_S (\rho\varphi) u_j n_j dS\, dt = \int_{\Delta t}\int_V S_\varphi dV\, dt + \int_{\Delta t}\int_S \left(\Gamma_\varphi \frac{\partial \varphi}{\partial x_j}\right) n_j dS\, dt \,. \tag{2-53}$$

The above final representation of the general transport equation plays a significant role in the computational fluid dynamics in the finite volume approach.

2.12.5 Turbulent Flows

Modelling turbulence phenomena in the computational fluid dynamics is also important in correct reproduction of all physical properties of the fluid inside the system being simulated. All the fundamental laws' equations derived in previous chapters are to be applied to the laminar fluid flow, but in most practical cases the turbulence is not to be disregarded. Sometimes, if the spatial discretization is sufficiently fine to resolve the smallest eddies, the equations can be applied unchanged (via direct numerical simulation – DNS [120][121][122]). The size of these smallest eddies are proportional to the Kolmogorov length scale, becoming

smaller with an increasing Reynolds number. Realistic geometries are rarely small in size or simple enough to enable reasonable computational times with an adequate number of control volumes for DNS [123]. Therefore, a numerically efficient mathematical modelling representing the turbulence influence on the fluid flow has to be used in such cases.

An approach using the averaged governing equations, with instantaneous values of flow quantities replaced by an average and fluctuating value is then used. This approach is known as Reynolds Averaged Navier-Stokes equations (RANS), and results in the equations having a form similar to the original Navier-Stokes conservation equations with a difference in two additional terms, Reynolds stresses and turbulent heat fluxes, due to averaging process. The turbulence model is used for modelling the two to close the system of equations. Averaging of the equations can be found in most CFD handbooks and will not be discussed here in detail [124]. This approach, representing heavy approximations compared to DNS modelling, in terms of accuracy can be superseded by the compromise from the both sides as Large Eddy Simulation methodology (LES) [125][126][127]. It also requires, unlike RANS, a finer control volume mesh to resolve large scale eddies directly. Smaller scale eddies are additionally modelled with simpler turbulence models [128]. However, since this approach also requires fine spatial discretization, it is still considered computationally too demanding for a large number of practical applications [129][130]. Also in this work, the RANS approach has been used and is briefly described in the following text.

As explained earlier, to close the averaged system of conservation equations, one needs to model the Reynolds stresses and turbulent heat fluxes. In many cases, this is done by exploiting the concept of turbulent viscosity or turbulent diffusivity based on the Boussinesq hypothesis which assumes that the turbulent Reynolds stress tensor can be modelled in the same way as the viscous stress tensor (with turbulent viscosity replacing the molecular viscosity). This principle, also applied to the turbulence heat flux equations, finally results in the time averaged conservation equations having the same form as in the laminar case, with the

laminar exchange coefficient (viscosity, diffusivity and conductivity) replaced by effective turbulent exchange values. Number of transport equations to be solved in the model differentiates the turbulence models into zero-, one- and two-equation models. First of them calculates turbulent exchange coefficients by empirical relations, in the second one an additional transport equation for turbulent kinetic energy k is solved, and in the last one additional transport equations for turbulent kinetic energy k and dissipation ε are solved. There are also second order closure models, such as Reynolds stress models which solve additional six partial differential conversion equations making this approach gaining in accuracy but lacking in computational demands [125].

In this work, as turbulence model of choice two of the popular ones were considered. Two-equation $k-\varepsilon$ model, with its own serious disadvantages, such as limited applicability to flows with strong streamlines curvature or strong rotation, this is the model of choice for wide number of applications due to its strong sides – the simplicity, numerical stability and has been proven to work well in a number of applications (for this work most important are heat transfer and combustion) [131][132][133]. Since this model also has pronounced problems regarding the wall treatment functions, in terms of using damping which introduces additional non-linearity and often numerical stiffness, the focus was turned to the other recent approach as described in [134], the ζ-f model. The model is best suited when one opts for the compromise between the model simplicity and performance [135].

This model is a variant of Durbin elliptic relaxation model [135], but with eddy viscosity defined as:

$$\nu_t = C_\mu^\zeta \zeta \frac{k^2}{\varepsilon}, \tag{2-54}$$

where

$$\zeta = \frac{\overline{\overline{v^2}}}{k}, \tag{2-55}$$

Represents the velocity scales ratio, which can be interpreted as the ratio of wall normal and general turbulence time scales $\tau_v = \overline{v^2}/\varepsilon$ and $\tau = k/\varepsilon$.

The transport equations of the model are defined as follows:

$$\frac{D\zeta}{Dt} = f - \frac{\zeta}{k}\wp + \frac{\partial}{\partial x_k}\left[\left(\nu + \frac{\nu_t}{\sigma_\zeta}\right)\frac{\partial \zeta}{\partial x_k}\right], \tag{2-56}$$

$$\frac{Dk}{Dt} = \wp - \varepsilon + \frac{\partial}{\partial x_j}\left[\left(\nu + \frac{\nu_t}{\sigma_k}\right)\frac{\partial k}{\partial x_j}\right], \tag{2-57}$$

$$\frac{D\varepsilon}{Dt} = \frac{C_{\varepsilon 1}\wp - C_{\varepsilon 2}\varepsilon}{\tau} + \frac{\partial}{\partial x_j}\left[\left(\nu + \frac{\nu_t}{\sigma_\varepsilon}\right)\frac{\partial \varepsilon}{\partial x_j}\right], \tag{2-58}$$

$$L^2\nabla^2 f - f = \frac{1}{\tau}\left(C_1 - 1 + C_2'\frac{\wp}{\varepsilon}\right)\left(\zeta - \frac{2}{3}\right). \tag{2-59}$$

In the above equations the time and length scale are limited with the Kolmogorov scales as the lower, and Durbin's realisability constraints as the upper bounds in the following form:

$$\tau = max\left[\min\left(\frac{k}{\varepsilon}, \frac{a}{\sqrt{6}C_\mu^\zeta |S|\zeta}\right), C_\tau\left(\frac{\nu^3}{\varepsilon}\right)^{1/2}\right], \tag{2-60}$$

$$L = C_L max\left[\min\left(\frac{k^{3/2}}{\varepsilon}, \frac{k^{1/2}}{\sqrt{6}C_\mu^\zeta |S|\zeta}\right), C_\eta\left(\frac{\nu^3}{\varepsilon}\right)^{1/4}\right]. \tag{2-61}$$

The model coefficients are by default, set for a generic flow and listed below as:

$$C_\mu^\zeta = 0.22, C_{\varepsilon 1} = 1.4\left(1 + \frac{0.012}{\zeta}\right), C_{\varepsilon 2} = 1.9, C_1 = 1.4, C_2 = 0.65,\ \sigma_k = 1,\ \sigma_\varepsilon = 1.3,$$
$$\sigma_\zeta = 1.2, C_\tau = 6.0, C_L = 0.36, C_\eta = 85.$$

2.13 Combustion modelling

2.13.1 General Approach

In respect to the topic of this work, the need to represent the effects of detailed chemistry in the 3D CFD application as accurately as possible is considered. Using the general gas phase modelling including chemistry mechanism would provide the most accurate data, but using the mechanisms other than the basic one- or two step ones would yield computational times which are not practically usable, even in the simplest of computational domains. This work relies on the tabulation approach to pre-calculate the distinctive properties of a homogeneous combustion in a constant volume case, and then use this data efficiently in the combustion model as a part of the CFD solver.

The combustion model of choice for this work is the Extended Coherent Model with Three Zones (ECFM-3Z) explained in more details in the further text. This combustion model uses tabulated data for ignition tracking, but does not provide such a good agreement with the CHEMKIN calculations until additional properties are tabulated. An attempt was made in this work to utilize the approach of tabulating the basic properties and to obtain viable results comparable to the 0D homogeneous calculations.

Coherent flame models (CFM) are combustion models particularly suited to the simulation of combustion in the premixed regime, thus being adopted mostly for the simulation of the spark ignition engines. The extension of the basic CFM, the ECFM model, also accounts for the case of unmixed combustion. This model is based on a flame surface density equation taking into account the wrinkling of the

flame front surface by turbulent eddies and a conditioning averaging technique for the precise reconstruction of local properties in fresh and burned gasses [136][137]. The unmixed combustion needed a description of the mixing state which is represented by three mixing zones (hence the 3Z in the model acronym) as displayed inFigure 2-20 [32][33][138].

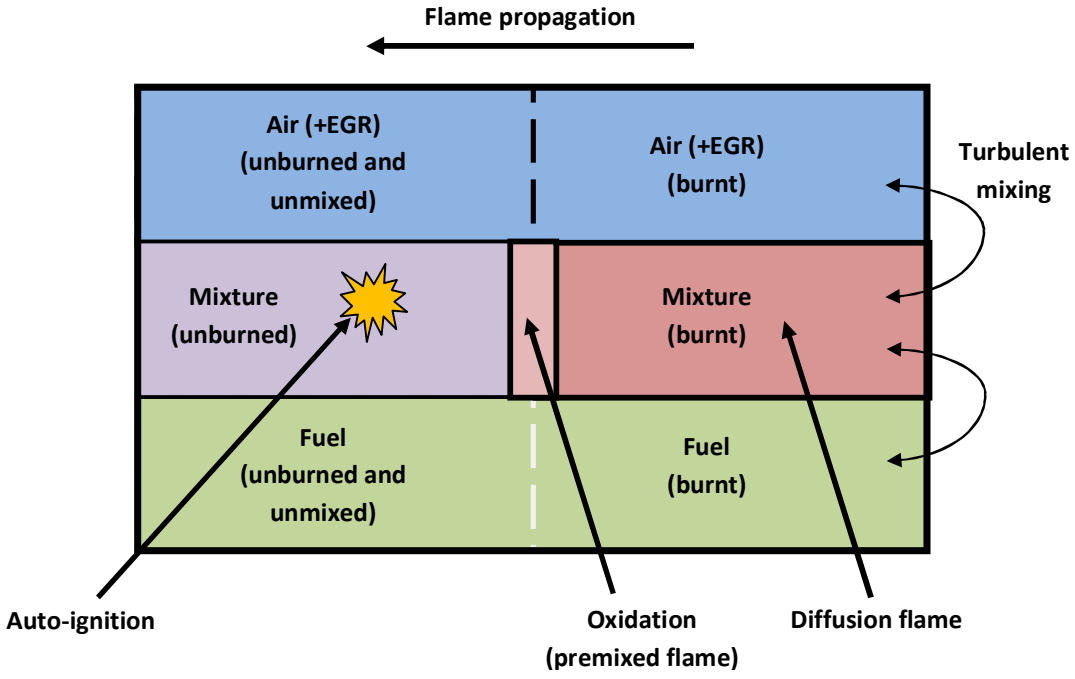

Figure 2-20 ECFM-3Z model description of mixing zones [32]

As seen on the above image the state of gases mixture is defined in the two dimensional space with mixture fraction variable Z (vertically) and a progress variable c (horizontally). The general approach splits each computational cell (control volume) into three zones:

- the unmixed fuel zone;
- the mixed zone, which contains fuel, air and EGR (if any);

- the unmixed air plus EGR (if any).

The zones as defined above are not set fixed in time, but they evolve influenced by the overall state in the computational cell. For instance, in the case of fuel being injected into the system, observing the development in a certain representative computational cell, it is initially constituted only out of unburned and unmixed air. When a fuel is introduced, after evaporation (if needed) it occupies a finite amount of cell space, initially remaining unmixed with existing air therefore creating two zones at that moment (unmixed and unburned air and unmixed and unburned fuel). Next, the fuel and air start to mix in the zone between the two, creating the third, mixed and unburned zone. The mixed zone is at this point ready for tracking the ignition criterion. When the ignition criterion has been met, the combustion starts propagating through the mixed zone dividing it into two sub-zones, the burnt and unburned mixed zone. As the literature states, the same basic principle can be applied also to a system with forced ignition (e.g. via the spark plug in the ICE) with the combustion model accounting for the evolution of the flame surface density that consumes the unburned gases, again forming the two subzones.

This combustion model also accounts for diffusion flame combustion, in the case when there are gases contained in the fuel and air region of the burned subzone. These mix with in the burned mixed zone with product gases and are consumed by post-flame kinetics in this region (mixing controlled combustion). The literature states that the fuel and air subzones (burned and unburned) retain the same composition and the same temperature with different presumed position. All the combustion modes described show that this combustion model is well suited for description of wide variety of combustion types, therefore making it a good choice regardless whether the premixed or non-premixed case is being considered.

Basic transport equations in the ECFM3Z model are governed by the fact that the state of gases is represented by two properties, the progress variable c and the mixture fraction Z. Twelve additional transport equation of the species are solved,

which include O_2, N_2, NO, CO_2, CO, H_2, H_2O, O, H, N, OH and soot. General form of these transport equations is (Favre averaged for species k):

$$\frac{\partial(\bar{\rho}\widetilde{Y_k})}{\partial t} + \frac{\partial(\bar{\rho}\widetilde{Y_k}\tilde{u}_j)}{\partial x_j} = \frac{\partial}{\partial x_j}\left[\left(\frac{\mu}{Sc} + \frac{\mu_t}{Sc_t}\right)\frac{\partial \widetilde{Y_k}}{\partial x_j}\right] + \overline{\dot{\omega}_k}. \tag{2-62}$$

As in the chapter dedicated to turbulence modelling, μ and μ_t denote the laminar and turbulence viscosities respectively, $\overline{\dot{\omega}_k}$ is the Reynolds averaged combustion source term of the species k, and $\widetilde{Y_k}$ is the Favre averaged mass fraction of species k defined for a constant volume as:

$$\widetilde{Y_k} = \frac{\overline{m}_k}{\overline{m}} = \frac{\bar{\rho}_k}{\bar{\rho}}, \tag{2-63}$$

with Reynolds averaged values for mass and density denoted by $\overline{m}$ and $\bar{\rho}$ respectively. Laminar and turbulent Schmidt numbers in the equation(2-62), Sc and Sc_t, by the definition represent the dimensionless numbers defined as the ratio of the viscosity (momentum diffusivity) and mass diffusivity which can be represented as:

$$Sc = \frac{\nu}{D} = \frac{\mu}{\rho D}, \tag{2-64}$$

where D denotes the molecular or mass diffusion rate. Turbulent Schmidt number is defined in the same manner, taking into consideration the turbulent transfer of momentum (eddy viscosity) and the turbulent mass transfer.

The general transport equation defined previously is divided, referring to the burned and unburned subzones of the computational cell when considering the fuel species:

$$\frac{\partial\left(\bar{\rho}\widetilde{Y_F^u}\right)}{\partial t}+\frac{\partial\left(\bar{\rho}\widetilde{Y_F^u}\tilde{u}_j\right)}{\partial x_j} = \frac{\partial}{\partial x_j}\left[\left(\frac{\mu}{Sc}+\frac{\mu_t}{Sc_t}\right)\frac{\partial\widetilde{Y_F^u}}{\partial x_j}\right]+\bar{\rho}\tilde{\dot{S}}_F^u+\bar{\dot{\omega}}_F^u-\bar{\dot{\omega}}_F^{u\to b}, \tag{2-65}$$

$$\frac{\partial\left(\bar{\rho}\widetilde{Y_F^b}\right)}{\partial t}+\frac{\partial\left(\bar{\rho}\widetilde{Y_F^b}\tilde{u}_j\right)}{\partial x_j} = \frac{\partial}{\partial x_j}\left[\left(\frac{\mu}{Sc}+\frac{\mu_t}{Sc_t}\right)\frac{\partial\widetilde{Y_F^b}}{\partial x_j}\right]+\bar{\rho}\tilde{\dot{S}}_F^b+\bar{\dot{\omega}}_F^b+\bar{\dot{\omega}}_F^{u\to b}. \tag{2-66}$$

This division of the fuel species into the unburned (represented by Y_F^u) and burned (represented by Y_F^b) is necessary to accommodate for the simulation of both propagating and diffusion flames. In the case of propagating flame, the unburned fuel is consumed by the rate represented by $\overline{\dot{\omega}_F^u}$, and on the other side the reaction rate $\bar{\dot{\omega}}_F^b$ represents the oxidation of burned fuel by diffusion flame. These consumption rates are dependent on the local flame surface density and laminar flame velocity and are calculated as described in the following text. If the local equivalence ratio is rich, there will not be enough oxygen in the unburned sub-zone to consume all of the unburned fuel. Therefore, some of the unburned fuel is going to be transferred in to the burned sub-zone by the source term (from the burned sub-zone perspective) $\bar{\dot{\omega}}_F^{u\to b}$. Rate of the production of gaseous fuel due to, for example, evaporation of liquid fuel droplets, is denoted by $\tilde{\dot{S}}_F$ and is distributed between the burned and unburned sub-zones according to the progress variable $\tilde{c}$ in the following manner:

$$\tilde{\dot{S}}_F^u=\tilde{\dot{S}}_F\,\tilde{c}\,, \tag{2-67}$$

$$\tilde{\dot{S}}_F^b=\tilde{\dot{S}}_F\,(1-\tilde{c}). \tag{2-68}$$

Progress variable definition relies on the CFM assumption of the flame being infinitely thin interface separating the fresh and burned gases. If it is defined that each species in the unburned gases is consumed by propagating flame proportionally to its mass fraction in this sub-zone, it allows also the simple definition of the local progress variable (or burned mass fraction) to be proportional to the fuel mass fraction oxidized since the start of combustion:

$$\tilde{c} = 1 - \frac{\overline{m}^u}{\overline{m}} = 1 - \frac{\widetilde{Y_F^u}}{\tilde{Y}_{TFu}}, \tag{2-69}$$

where $\tilde{Y}_{TFu}$ is the mass fraction of fuel before the onset of combustion. From the first part of the above formulation, one can see that the value of the local progress variable varies from the value of zero when the fuel is not being consumed up to the value of 1 when there is no fuel species in the computational cell.

This combustion model uses species tracers to describe the behaviour of the species transport in more detail. By the definition set in the literature [32] the species tracer is subject to convection and diffusion in the same manner as the species but is not being consumed during the combustion nor it is used in the thermodynamic balances. Basically, following the definition the temporal evolution of this pseudo-species is also described by an equation derived from the equation (2-62):

$$\frac{\partial\left(\bar{\rho}\widetilde{Y_{Tk}}\right)}{\partial t} + \frac{\partial\left(\bar{\rho}\widetilde{Y_{Tk}}\tilde{u}_j\right)}{\partial x_j} = \frac{\partial}{\partial x_j}\left[\left(\frac{\mu}{Sc} + \frac{\mu_t}{Sc_t}\right)\frac{\partial\widetilde{Y_{Tk}}}{\partial x_j}\right] + \bar{\rho}\tilde{\dot{S}}_k . \tag{2-70}$$

The basis of all coherent flame modelling approach is the formulation of the rate of fuel consumption per volume unit by the product of the flame surface density and the local velocity at which the fuel/oxidizer mixture is consumed. Denoting the flame surface density with Σ one yields its transport equation according to [32][33]:

$$\frac{\partial \Sigma \bar{\rho}}{\partial t} + \frac{\partial \left(\Sigma \bar{\rho} \tilde{u}_j\right)}{\partial x_j} = \frac{\partial}{\partial x_j}\left[\left(\frac{\mu}{Sc} + \frac{\mu_t}{Sc_t}\right)\frac{\partial \tilde{Y}_k}{\partial x_j}\right] + (P_1 + P_2 + P_3)\Sigma - \mathrm{D} + P_k. \tag{2-71}$$

In the above equation, besides already defined convection, diffusion and unsteady terms, on the right hand side several other source/sink terms are introduced which are described by the equations that follow.

$$P_1 = \alpha K_t. \tag{2-72}$$

This property is flame surface production by turbulent stretch with K_t being intermittent turbulence net flame stretch [139] and α is the model constant (equal to $\alpha = 1.6$). The second of the sink terms, P_2, represents the flame surface production by mean flow dilatation and is modelled as:

$$P_2 = \frac{2}{3}\frac{\partial \tilde{u}_j}{\partial x_j}. \tag{2-73}$$

The last term in the section appearing next to the flame surface density, P_3, denotes the effects of the flame expansion and curvature in the following manner:

$$P_3 = \frac{2}{3}\bar{S}_L \frac{1-\tilde{c}}{\tilde{c}}\Sigma. \tag{2-74}$$

Sink term in the equation (2-71), D, is the destruction term due to fresh gas consumption defined by the equation:

$$D = \beta \bar{S}_L \frac{\Sigma^2}{1-\bar{c}}, \tag{2-75}$$

where β represents the model constant usually set to $\beta = 1$. Additional source term, P_k, is introduced for ICE application and as is applied during the ignition period in the case of spark plug ignition [33].

Finally, consumption rate found in equation (2-65) is calculated according to the flame surface density and the laminar flame velocityS_L:

$$\overline{\dot{\omega}_F^u} = \bar{\rho}^u|_u \widetilde{Y_F^u}\Big|_u S_L \Sigma\,. \tag{2-76}$$

In the above equation the values for density and fuel fraction have been conditionally averaged according to the sub-zone in which the calculation is performed. According to equation (2-63) for the unburned zone one can write the following:

$$\widetilde{Y_k^u}\Big|_u = \frac{\overline{m}_k^u}{\overline{m}^u}, \tag{2-77}$$

$$\widetilde{Y_k^b}\Big|_b = \frac{\overline{m}_k^b}{\overline{m}^b}. \tag{2-78}$$

These relate to the averaged mass fraction in the computational cell according to the progress variable in the following manner:

$$\tilde{Y}_k = \tilde{c}\,\widetilde{Y_k^b}\Big|_b + (1-\tilde{c})\widetilde{Y_k^u}\Big|_u\,. \tag{2-79}$$

The difference of the quantities $\widetilde{Y_k^u}\big|_u$ and $\widetilde{Y_k^u}$ (or $\widetilde{Y_k^b}\big|_b$ and $\widetilde{Y_k^b}$) is that the $\widetilde{Y_k^u}$ represents the mass fraction of the species *k*, contained in the fresh/unburned gases in the entire cell (compared against the total cell mass), and $\widetilde{Y_k^u}\big|_u$ defines the average mass fraction of the species *k* in the fresh gases.

2.13.2 Ignition Modelling

Autoignition occurs usually away from stoichiometry at a "most reactive mixture fraction", usually approximately determined from homogeneous or laminar flow autoignition calculations, and at locations in the turbulent flow with low scalar dissipation [140].

In the ECFM-3Z combustion model, a simple ignition tracking methodology is used (based on the methodology commonly used for prediction of knocking in the gasoline engines) with introduction of a tracking, non-reacting intermediate species ***I***. This species is purely fictious and is simply used to track the correct time to commence the ignition. Initially, it was used to track only the main ignition, but according to [62] the principle can be extended also to low temperature ignition, thus accounting for the cool flame phenomenon in the combustion simulation [141].

In the combustion model itself the intermediate species are temporally evolved according to the equation:

$$\frac{\partial \bar{Y}_I^M}{\partial t} = \bar{Y}_{TF}^M|_M F(\tau_d)\,. \tag{2-80}$$

In the above equation *M* denotes the mixture zone and the definitions of the mass fractions apply according to the explanations related to equation . The ignition delay is denoted by τ_d and represents the value extracted from the database tabulated according to chapter 2.11. The function of the ignition delay is defined according to [62] as:

$$F(\tau_d) = \frac{\sqrt{B^2\tau_d^2 + 4(1 - B\tau_d)\frac{\bar{Y}_I^M|_M}{\bar{Y}_{TFu}^M|_M}}}{\tau_d}\,. \tag{2-81}$$

In the equation (2-81) B denotes the model constant, and in this case is set to $B = 1[s]$. The same approach can be applied to the modelling of the low temperature ignition delay, simply adding additional intermediate species tracers [138]. The temporal change of this tracer is calculated also according to the above equation simply using a tabulated value for low temperature ignition delay. The intermediate species tracers change their values from zero to local fuel tracer value. When the low temperature ignition tracer's value reaches the maximum, the certain amount of fuel is allowed to be consumed, and is defined by the previously tabulated values for released heats during both the low and high temperature delays according to the relation:

$$m_i = \frac{\Delta H_{HT} + \Delta H_{LT}}{\Delta H_{LT}}. \tag{2-82}$$

If there is no low temperature delay, the above equation is, naturally, not taken into consideration. By the model's formulation the entire amount of the fuel in the fresh gases is consumed almost instantaneously according to the equation:

$$\frac{\partial \bar{\rho} \tilde{Y}_F}{\partial t} = -\bar{\rho} \frac{\tilde{Y}_F}{\tau_{ign}}. \tag{2-83}$$

Temporal evolution of the ignition tracers compared to calculated temperature can be seed as displayed in the Figure 2-21 clearly depicting the theoretical basics described in this section. The fuel used for testing this hypothesis was n-heptane, which has the largest number of available reaction mechanisms with various degrees of complexity, and clearly distinguishable low and high temperature ignition steps, but it was also shown used with other fuels (without low temperature ignition, and some changes applied [142])

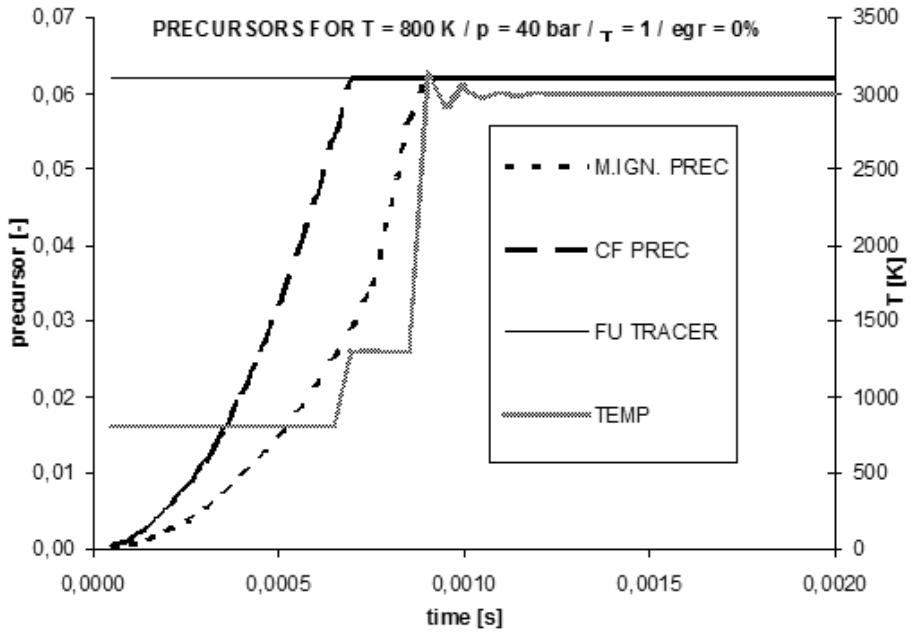

Figure 2-21 Temporal evolution of intermediate species tracers and temperature

Interpolation of the ignition delays is performed at each calculation time step from the 5D matrix. The matrix is composed of the result vector and four parameter vectors as defined in earlier chapters when discussing the tabulation setup. Interpolation of the results is linear, which proved to provide the resulting values of satisfying accuracy, and is also taken into consideration when defining the values for calculation parameters. The first database created during this work was post-processed in the MATLAB® software package and was also checked by the MATLAB's several interpolation functions (linear, quadratic, spline...). These were all compared against each other not showing significant deviations when compared to the linear interpolation used in CFD implementation. Also, this software package was intensively used for data processing, both for data manipulation presented in the chapter 2.11.5 and also for implementation validation.

The initial parameters should have been selected in the way that accommodates the linear interpolation with as smaller error as possible. This is simply done by a limited number of initial runs, or a quick literature survey on the mechanism (or the fuel, generally) behaviour against certain parameter.

3 Numerical Simulations and Results

This chapter will present the results of calculations performed for the pre-processing tabulation stage, with a short discussion on the behaviour of the mechanisms and the eventual issues that might have arisen which could be used as a reference to any future calculations being performed.

After presenting the tabulation results, accompanied by the information of the mechanisms used alongside the initial parameter values, the results of implemented tabulation results (database) in the CFD software will be compared against the calculations with the CHEMKIN application used for the tabulation itself, having the same initial parameters, in several benchmark cases:

- a case with the initial parameters as they are used in the tabulation; this test case would validate the implementation of the database results and the low temperature ignition delay definition in the ECFM-3Z model;
- a case with one parameter between the tabulated parameters; if the first benchmark case provided good agreement the second one would be used to test the 4D interpolation routine – since it is trivial to calculate the exact interpolated values on the side and compare it to the results provided by the implemented interpolation routine, any deviations would indicate a critical error in the routine; this step should also be performed for all parameters to test the behaviour of the entire interpolation routine – this makes any necessary debugging straightforward since each deviation would point to the exact part of the code;
- a case with all parameters with the values not equal to the ones used in the tabulation procedure; if the previous routine would provide the correct value for all the parameters, the final check of the interpolation would include all parameters being used in the interpolation routine; the results could be checked against the values obtained by third-party interpolation routines (e.g. MATLAB's *interpn* function).

3.1 Tabulation Results

In this chapter the results of the tabulation procedure for the several fuels will be presented, both in the case of ignition delays and laminar flame velocities (for some fuels). Each fuel will be accompanied by the selected chemical mechanism and sets of initial parameter values. Since the resulting database is a 5D matrix, there is no simple graphic manner to represent it graphically, so a sampled set of parameters is used for 3D interpretation (two selected parameters held constant, and two varied through their respective range).

3.1.1 N-Heptane

The first fuel of choice was, as it was in the earlier chapters, n-heptane, interesting since it is often used to represent a diesel fuel whose combustion is governed by the self ignition. After the comparison made according to the chapter 2.10.1, initially the Golovitchev mechanism [11], successfully reproducing the combustion phenomena (cool flame ignition) and correct trends for initial data variations, was used to point to the specific areas of initial parameters that could be used with comprehensive mechanisms to reduce the necessary number of calculation points. This tabulation (with initial data as shown in Table 3-1) enabled the pressure and temperature discretization to be altered. The reduced number of calculation points was used with more detailed mechanism selected as described in [96], and used with the sets of initial data as presented in Table 3-1. Finally, a detailed n-heptane mechanism (described in [16]) was used with slightly altered initial data set (higher pressure values were needed in this case).

Table 3-1 Initial parameters data for n-heptane autoignition tabulation

using LLNL reduced mechanism [96]	
Temperature [K]	650-750 K (20 K step), 790-1110 K (40 K) and 1500 K
Pressure [bar]	10 20 30 60 80

Equivalence rat. [-]	0.3 0.5 0.7 1 1.5 3
EGR [%]	0 0.3 0.6 0.8
using LLNL mechanism [16]	
Temperature [K]	600-760 K (20 K step), 800-1440 K (40 K) and 1500 K
Pressure [bar]	1 5 10 20 30 40 50 80 110 140 170 200
Equivalence rat. [-]	0.3 0.4 0.5 0.7 1 1.5 3
EGR [%]	0 0.15 0.3 0.45 0.6 0.8
using Golovitchev mechanism [11]	
Temperature [K]	600 - 1500 (20K step)
Pressure [bar]	10 15 20 25 30 40 60 80
Equivalence rat. [-]	0.3 0.5 0.7 1 1.5 3
EGR [%]	0 0.3 0.6 0.8

Resulting database is presented in the following figures.

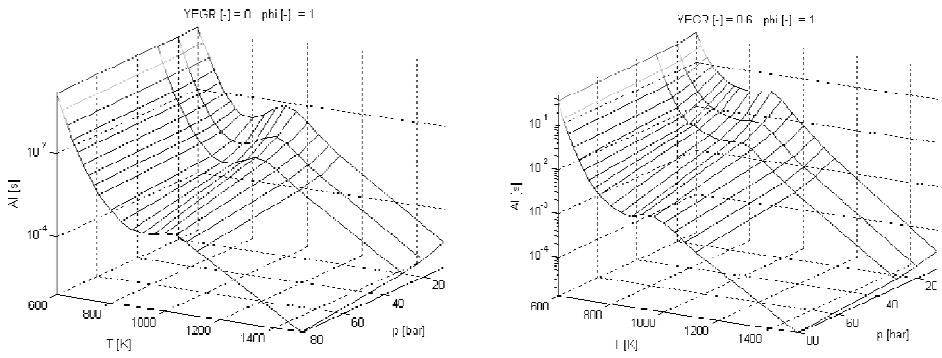

Figure 3-1 n-heptane table for phi = 1, and EGR = 0 (left) and EGR = 0.6 right using Ahmed et al. mechanism

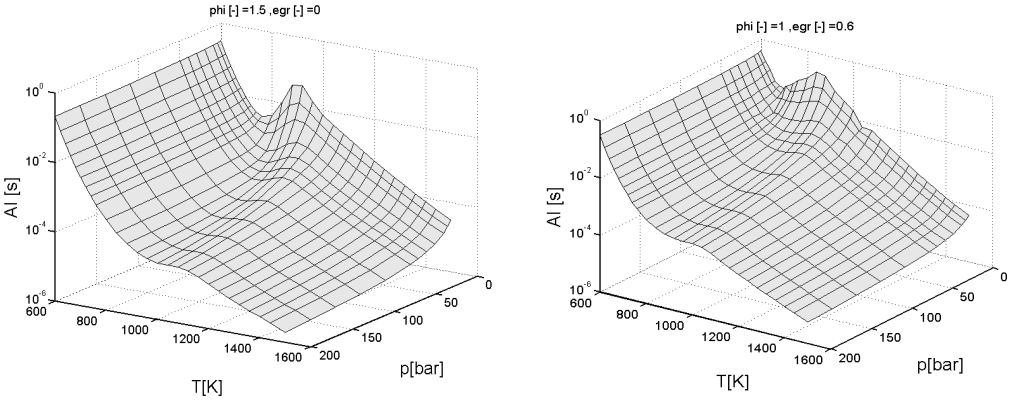

Figure 3-2 n-heptane table for phi = 1.5, and EGR = 0 (left) and EGR = 0.6 right using Curran et al. mechanism

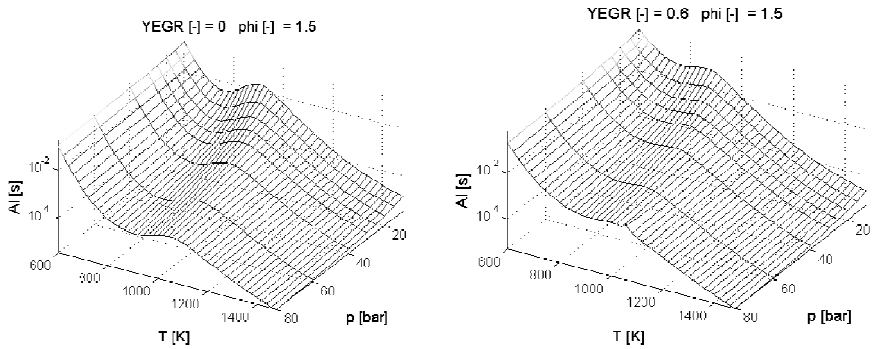

Figure 3-3 n-heptane table for phi = 1.5, and EGR = 0 (left) and EGR = 0.6 right using Golovitchev mechanism

The figures above show the NTC regions represented correctly for all mechanisms used, and compared to each other, also an influence of residual gas mass fraction. Comparing different mechanisms used, an increase in the ignition delay values with more complex mechanisms can be seen, which follows the expectations.

3.1.2 Ethanol

In the case of ethanol fuel, only one mechanism was used to calculate the autoignition table, as described in [6]. This mechanism being widely used, was a

good reference for comparing other mechanisms, and with its size suitable for calculating the database with even more points than the ones as shown in table Table 3-2 (especially compared to the mechanisms used for n-heptane tabulation described in previous section). Total number of needed calculations was 17280.

Table 3-2 Initial parameters used for ethanol autoignition tabulation

using Marinov mechanism [6]	
Temperature [K]	600 - 1500 (20K step)
Pressure [bar]	10 15 20 25 30 40 60 80
Equivalence rat. [-]	0.3 0.5 0.7 1 1.5 3
EGR [%]	0 0.3 0.4 0.5 0.6 0.7 0.8 0.9

As shown in Figure 3-4 below, the procedure provides a smooth data with low temperature data missing, which is expected since the mechanism isn't suited for low temperature combustion.

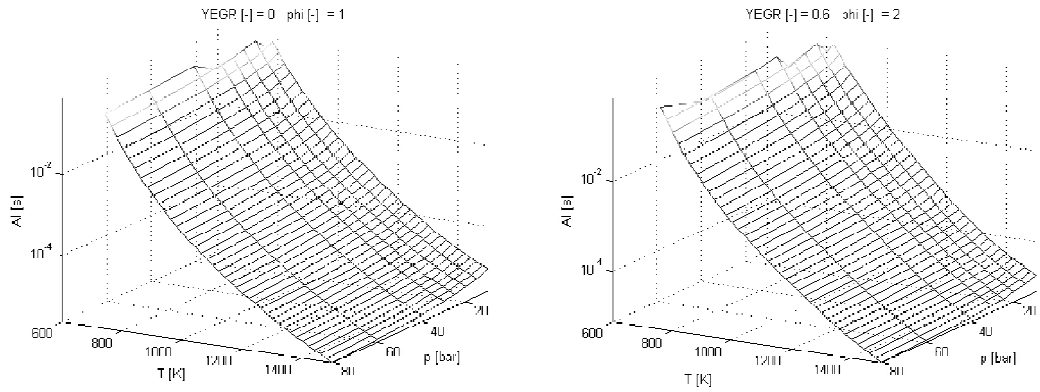

Figure 3-4 Ethanol autoignition table with EGR = 0 and phi = 1 (left) and EGR = 0.6 and phi = 2 (right)

3.1.3 DME

Having only one available mechanism for dymethil-ether oxidation the database was created using the Curran et al. [108] mechanism. As one can see in the

following images, dymethil-ether also exhibits a negative temperature coefficient region. The data used for the tabulation was as defined in Table 3-3. Total number of calculation points is the same as the case of ethanol (with the same initial data range) 17280.

Table 3-3 Initial parameters used for dimethyl-ether autoignition tabulation

using LLNL mechanism [108]	
Temperature [K]	600 - 1500 (20K step)
Pressure [bar]	10 15 20 25 30 40 60 80
Equivalence rat. [-]	0.3 0.5 0.7 1 1.5 3
EGR [%]	0 0.3 0.4 0.5 0.6 0.7 0.8 0.9

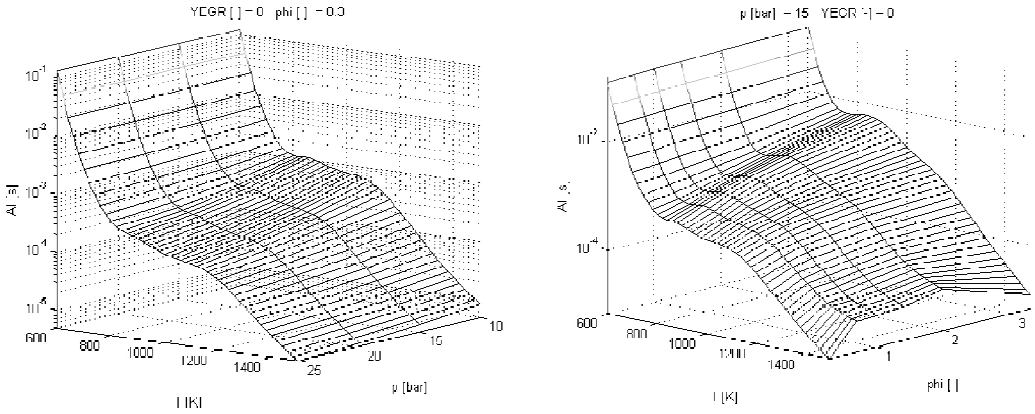

Figure 3-5 DME autoignition table with variable temperature and pressure for EGR = 0 and phi = 0.9 (left) and variable temperature and equivalence ratio with p = 15 bar and EGR = 0 (right)

3.1.4 Methane

For tabulation of methane autoignition, the most frequently used mechanism was utilized [5]. This mechanism also provided a smooth table for high temperature

regions, but in low temperature cases some of the calculations did not provide valid data (see Figure 3-6). Since the rest of the table provide clear temperature trend without any NTC regions, the missing points have been successfully extrapolated. Instabilities of the methane ignition in low temperatures have been also considered when defining the initial data, as displayed in Table 3-4. Importance of higher temperature behaviour it therefore observed with denser temperature distribution in the above 1220 K region. Total number of calculations was 4176.

Table 3-4 Initial parameters used for methane autoignition tabulation

methane	
Temperature [K]	800 850 900-1220 (40K step) 1220-1600 (20K step)
Pressure [bar]	10 20 30 60 80 85
Equivalence rat. [-]	0.3 0.6 0.8 1 2 3
EGR [%]	0 0.3 0.6 0.8

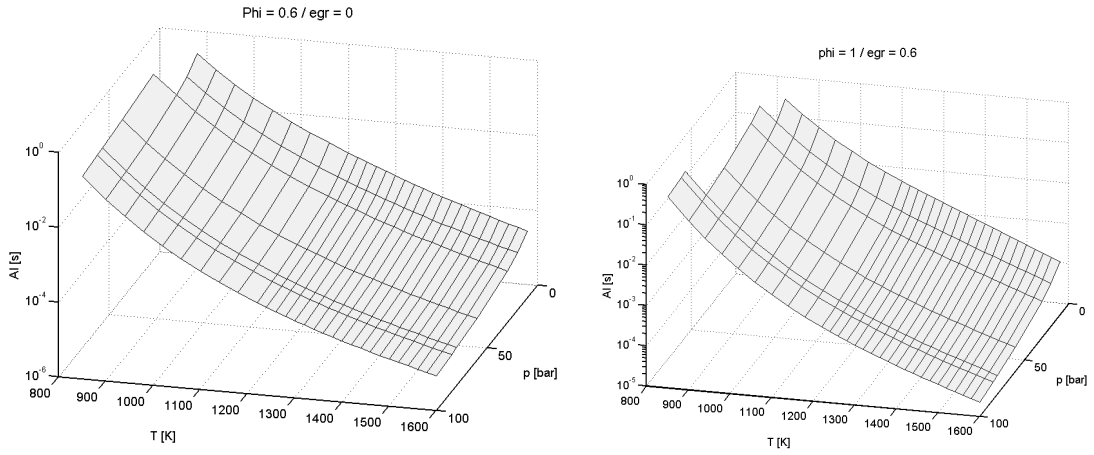

Figure 3-6 Methane autoignition tables with variable pressure and temperature and with phi = 0.6 and egr = 0 (left), and with phi = 1 and egr = 0.6 (right)

3.1.5 Iso-octane

Iso-octane was the last fuel intended for tabulation during this work, considering that the smallest available mechanism (usable for the tabulation) was made of 258 species [83], and the limited computer power, a somewhat sparse initial data table (displayed in Table 3-5) used for tabulation was formulated with the total of 2160 points. This table, however, also provided usable database, which at certain points needed to be smoothed out (as seen on the right in the Figure 3-7).

Table 3-5 Initial parameters used for iso-octane autoignition tabulation

using Chen et al mechanism	
Temperature [K]	600-1500 (100K step)
Pressure [bar]	10 20 30 60 80
Equivalence rat. [-]	0.3 0.5 0.7 1 1.5 3
EGR [%]	0 0.3 0.4 0.5 0.6 0.7 0.8 0.9

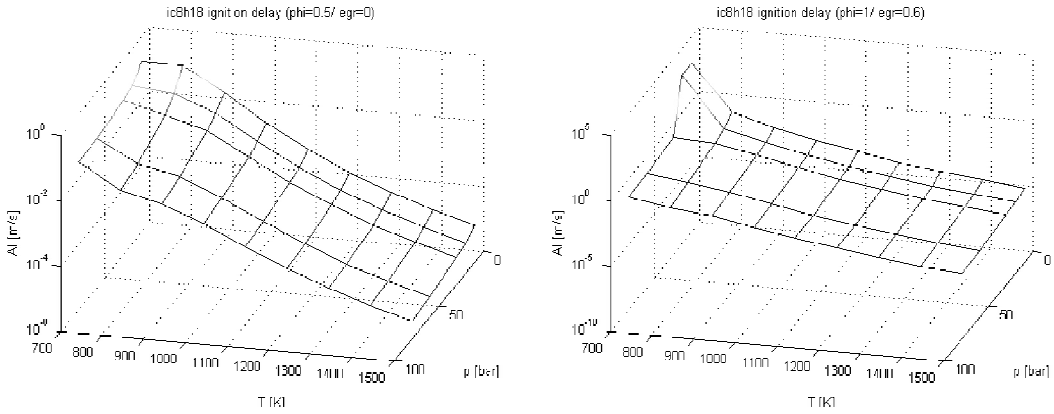

Figure 3-7 Iso-octane autoignition tables with variable pressure and temperature and with phi = 0.5 and egr = 0 (left), and with phi = 1 and egr = 0.6 (right)

The above data, combined with the database done for n-heptane also provides a base point for calculating several other fuel blends with research octane numbers in range of 0-100.

3.2 0D CHEMKIN against 3D FIRE

To obtain a good representation of the comparable results, a simple computational cell grid was used, with ignition being the main combustion driving phenomenon. The computational grid was created with parameters as shown in Table 3-6.

Table 3-6 Computational grid parameters

Width [m]	1
Height [m]	1
Cell width [m]	0.1
Cell height [m]	0.1
Total number of cells	100

Final simple grid is displayed in Figure 3-8.

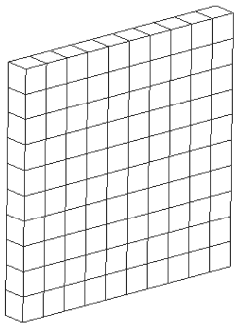

Figure 3-8 Computational cell used in ignition simulation

Initial results, following the work plan as explained at the beginning of this chapter, are shown in the Figure 3-9 comparing the CHEMKIN 0D calculation against the FIRE solver using the ECFM-3Z model with modified ignition model. The 4D interpolation routines were initially implemented using a user-function approach available by the solver [143]. This was also used to modify the original ignition model.

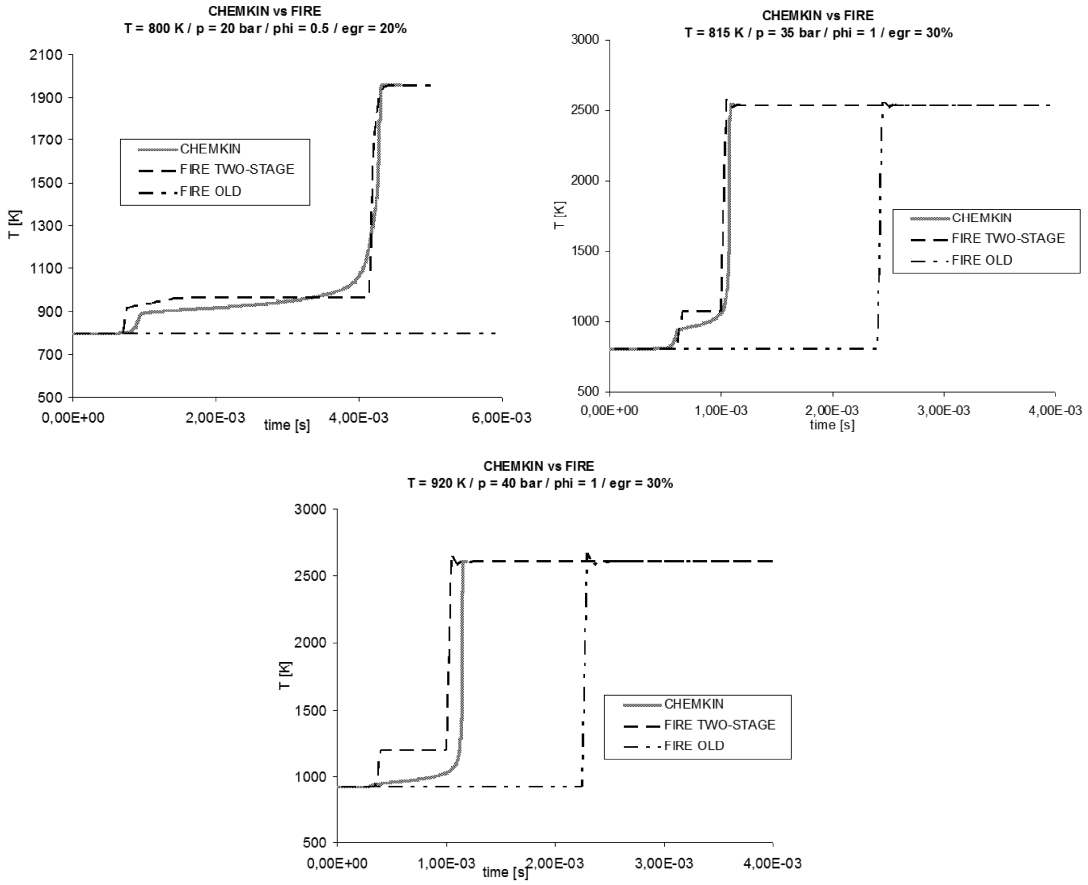

Figure 3-9 CHEMKIN vs FIRE ECFM-3z

This image points out to two facts that need to be briefly annotated. First issue is the combustion model starting with the fuel consumption as soon as the low/high temperature intermediate species tracer reaches the value governed by the ignition delay taken from the table. If the criterion for ignition delay during the tabulation is set only to the temperature curve inflexion, it would suggest that the combustion has started half way through the actual ignition. Therefore, this criterion was changed to a temperature increment leading to earlier combustion in the ignition model and finally produced a better agreement. If a table has already been made using only inflexion criterion for the ignition tracking, as was the case in the early stages of this work, to avoid recalculation of the entire table the

following function to alter the cool flame ignition delay is proposed based on few assumptions:

$$\tau'_{LT} = \tau_{LT}\left(1 - 0.035\left(1 + \frac{\tau_{HT} - \tau_{LT}}{\tau_{HT}}\right)\right). \quad (3\text{-}1)$$

The above equation modifies the low temperature ignition delay on the assumption that the temperature has a steeper temporal gradient when the low and high ignition delays are closer to each other. This usually happens when there is low amount of residual gases or at higher temperature or pressure values. Initial value to decrease the low temperature delay was, after short investigation, set to 3.5% which would cover wide range of tabulated values. This value is additionally increased if there is a larger difference between the low and high temperature delays, indicating the lower gradient in the temperature curve and therefore the inflexion point being more distant from the actual ignition start as presumed by the ECFM-3z combustion model.

Other issue for discussion is the high temperature ignition delay interpretation in the lights of the implementation in the transient 3D CFD calculation. The values extracted from the database are interpolated against the current state in each computational cell. In the cases calculated during this stage, there is no diffusion and convection, with fuel autoignition being the governing mechanism of the combustion process. Therefore, in this case, after the combustion starts, and certain amount of fuel is consumed as described in previous sections, the instantaneous values of parameters used for the interpolation are also altered. Comparing the CFD combustion model to 0D chemical calculation, one would theoretically expect to obtain the similar curve using the same ignition delays in the combustion model's calculation of intermediate species. In such case, after the intermediate species tracer reaches the low temperature ignition and consumes part of the fuel, the high temperature ignition delay would change by the rate calculated before the first ignition occurred resulting in the tracers reaching

the delay as tabulated for this specific set of initial parameters. On the other hand, this theory is not really met, mainly because the model has to encompass all the phenomena encountered in the general calculation case (diffusion, convection, etc…). With low temperature combustion taking place during an infinitesimal amount of time, already in the next step of temporal discretization, the state of the computational cell changes drastically, having increased pressure, temperature and different composition. This new state is from this point forward used to interpolate the values from the database to calculate the high temperature ignition tracer which rate is at this point expected to be significantly different from the one prior to the low temperature ignition. One would, therefore, expect a heavy under prediction of the high temperature ignition. This, however, is not encountered when observing the results of the CFD calculation compared to the CHEMKIN results.

Even if the temperature and pressure used for tabulations after the low temperature ignition are higher, thus indicating the reduction in the high temperature ignition times, they are also compensated by the change of the composition inside a computational cell. The new composition at this point also consists of a certain amount of product species which would finally lead to increasing the ignition delay extracted from the database.

3.3 3D Real Life Model

As the last validation of the ignition model, but also the overall behaviour of the combustion model, calculations using a research internal combustion engine design has been performed [144]. This engine is equipped with electro hydraulic valve actuation (EHVA) and three intake points with swirl flaps. As specified in [144] the ω shaped piston was used (piston schematic is shown inFigure 3-10)

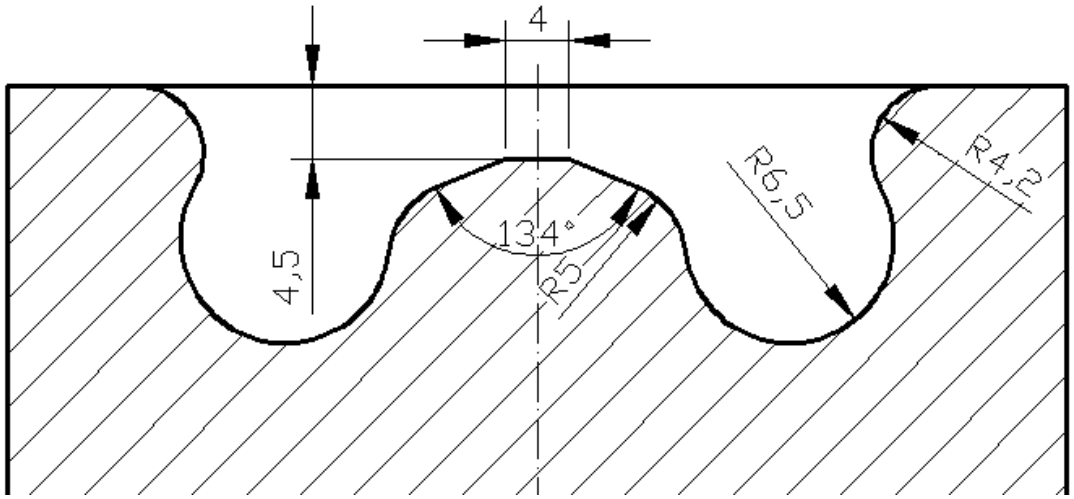

Figure 3-10 Piston geometry used for simulation

Additional engine technical specifications needed for the definition of the simulation are displayed in Table 3-7.

Table 3-7 Test engine specifications

bore	85mm
stroke	94mm
displacement	0.533dm³
compression ratio	16
nozzle	8-hole/1000 bar/ 704.5 mm³

The simulation was performed targeting the compression and expansion stroke of the engine cycle, starting at the moment of valve closure, at 115 crank angle degrees before top dead centre (TDC), and finishing at 138 degrees after TDC. Since there are, as displayed in the above specification table, eight nozzle holes per cylinder, with assuming radial symmetry, one eight of the cylinder was used as a computational domain (with the nozzle hole positioned at the centre) as shown in Figure 3-11.

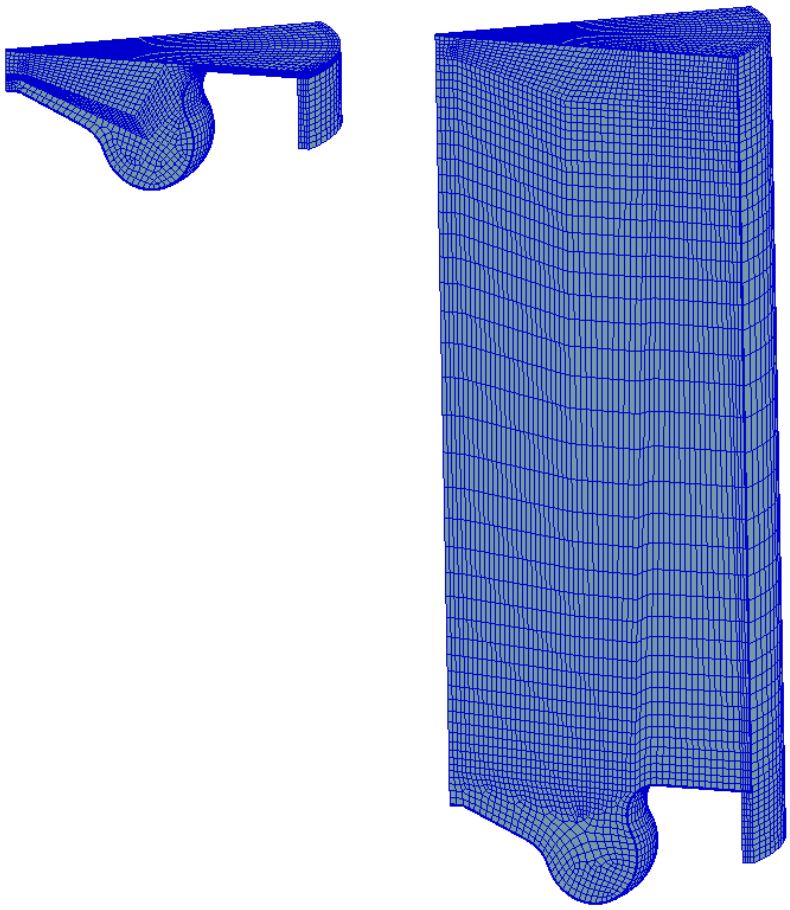

Figure 3-11 Computational domain (at bottom piston position and TDC)

Both compression and expansion strokes being simulated, implying the constant modification of the computational grid (which could also be perceived in the above figure). This is achieved by using the solver's moving mesh capability (this was used as is and will not be explained here, details can be found in[110]). Therefore, combustion domain had variant number of computation cells ranging from 67558 at bottom piston position to 23834 at the TDC.

Initial conditions for the calculations, pressure, temperature and residual gas mass fraction, were taken from [144] where the 1D code (BOOST) was used to obtain these values.

The results of the calculation are presented in following images.

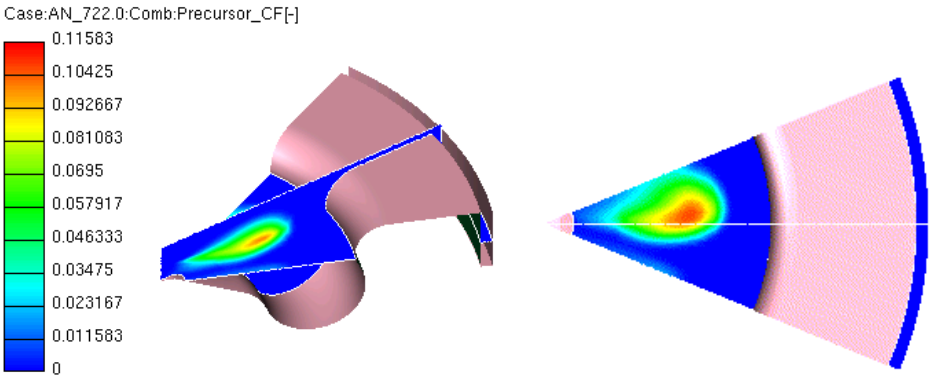

Figure 3-12 Precursor variable in two selected cuts

On the above figure (Figure 3-12) a low temperature ignition precursor variable has been displayed. The image was taken at the 722° CA (crank angle degrees). One can also observe the impact of the swirl, driving the combustion region to one side of the calculation domain.

Temperatures obtained during the simulations are compared to the validation data in the Figure 3-13 showing very good agreement between the two. Some difference can be seen in the expansion part of the cycle, which is due to the limitations of the combustion model encompassing the post-flame kinetics.

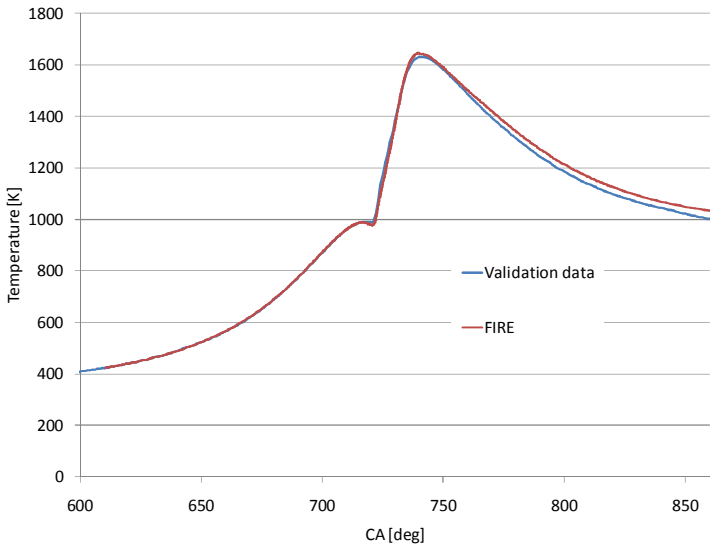

Figure 3-13Validation data and calculated temperature profile

Finally, also showing good agreement, the comparison of the calculated and validation pressure in the cylinder is shown in the Figure 3-14.

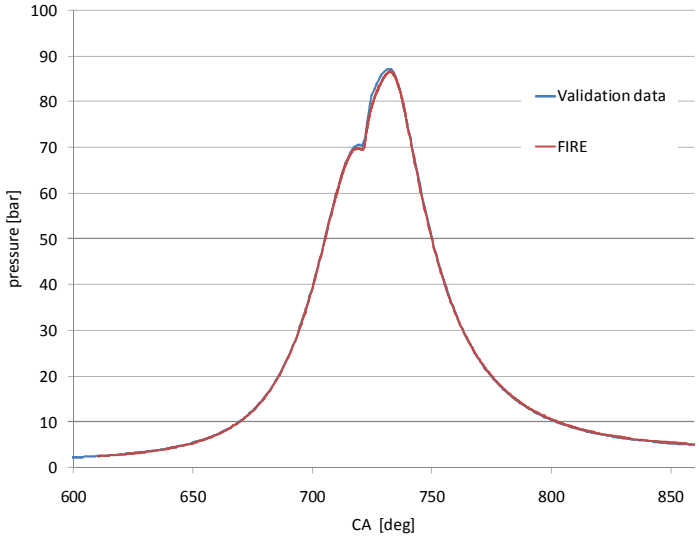

Figure 3-14 Validation data and calculated pressure profile

Overall, considering all the aspects of the methodology implementation and the results comparison, it could be concluded that the entire workflow, from the mechanism selection to 3d CFD calculation provides a straightforward process fit for practical usage on wider application scale.

4 Conclusion

To accurately simulate the combustion of the fuel, one of the key components is the correct prediction of the fuel ignition. To do this, one could use the computationally demanding full chemistry calculation in a form of general gas phase reactions, or inaccurate correlation functions which simply cannot encompass all influences on ignition, especially when considering the simulation of different fuels. Therefore, the pre-tabulated ignition data approach was investigated during this work.

An effort has been made to enable an efficient and accurate prediction of fuel auto-ignition within the commercial CFD code. Since a wider use of the procedure was also considered, a general tool enabling an accessible auto-ignition database creation for future use was developed. This includes several individual components. First, the assistance is provided in pre-processing by enabling an optimal reaction mechanism selection Next, the tabulation procedure itself with an interface providing a flexible calculation settings with parallel tabulation loops joined in the last part of the tabulation, the post-processing stage. This stage enables the inspection of tabulated data, correcting the data either by inserting the missing points or applying one of the smoothing techniques. It also prepares the data putting it into a specific format required by the CFD software, which is then easily implemented and ready to be used in the full combustion calculation case.

The first stage of this work included the thorough inspection of available chemical mechanisms for different fuels, comparing them and presenting a clear visualization, possibly helping the decision of mechanism selection. The tabulation routine would have three major properties needed to be weighed before starting the calculations; the mechanism accuracy, its complexity and stability. Mechanism accuracy, as shown in chapter 2.10 is a starting point always open to discussion. Even if the ignition definition is straight forward, the experimental setups vary providing mechanisms that can differ in simple 0D calculation results by some margins. Therefore, each mechanism is presented along with a literature reference

which would have to be studied in this stage. Mechanism complexity is a topic blending into the previous discussion, influencing the computational demand and time of the tabulation procedure. One needs to investigate all mechanism available to test if the reduced or even skeletal mechanism conforms to the demand. As a rule of thumb, a more complex mechanism usually equals a more accurate mechanism, but several comparison calculations are always welcome. The last issue, the mechanism's stability is unfortunately the one that usually arises after the tabulation is done, and due to the numerical problems, some points are missing or do not conform to expected trends in respect to certain parameter variations. For these cases post-processing tools have been developed to avoid repeating the missing calculation and to use mathematical algorithms to fix the troublesome data. Also in the case of blending two fuels a combination of iso-octane and n-heptane was considered, developing an acceptable accurate correlation equation to be used in determining the ignition delay of the mixture, dependent on the ignition delays for combustion of pure fuels and the blending factor.

The implementation of tabulated data has been described in chapter 2.13.2. The approach of utilizing a previously developed combustion model has been considered with applying a simplified ignition model, showing that even without adding additional tabulation data (such as the progress variable), one can acquire decent results. The implementation was tested in several test case set-ups, using a simple computational grid. The results were compared to the zero-dimensional chemistry calculation using the CHEMKIN library, showing good agreement. The influence of the low temperature ignition was shown when compared to the results obtained by using the previous implementation (with only high temperature ignition tabulated).

Finally, a real life case with more complex geometry was used to test and display the capabilities of the ignition model in a practical application. The results in this case also showed a good agreement to the data used for validation.

Overall, this work has provided a set of pre-tabulated databases for several fuels of interest, a ready tabulation workflow for any additional fuel with a working

chemical mechanism and accompanying thermodynamic data which can be used in a 3D CFD environment for simulation of any kind of combustion case.

5 References

[1] H. J. Curran, W. J. Pitz, C. K. Westbrook, C. V. Callahan, and F. L. Dryer, "Oxidation of Automotive Primary Reference Fuels at Elevated Pressures," *Proceedings of the Combustion Institute*, vol. 27, pp. 379-387, 1998.

[2] H.J. Curran, P. Gaffuri, W.J. Pitz, and C.K. Westbrook, "A Comprehensive Modeling Study of iso-Octane Oxidation," *Combustion and Flame*, vol. 129, pp. 253-280, 2002.

[3] W. J. Pitz et al., "Development of an Experimental Database and Chemical Kinetic Models for Surrogate Gasoline Fuels," in *SAE 2007-01-0175*, 2007.

[4] J.T. Farrell et al., "Development of an Experimental Database and Kinetic Models for Surrogate Diesel Fuels," in *SAE 2007-01-0201*, 2007.

[5] G.P. Smith et al. GRI 3.0. [Online]. http://www.me.berkeley.edu/gri_mech

[6] N. M Marinov, "A Detailed Chemical Kinetic Model for High Temperature Ethanol Oxidation," *International Journal of Chemistry Kinetics*, vol. 31, pp. 183-220, 1999.

[7] P. Saxena and F.A. Williams, "Numerical and experimental studies of ethanol flames," *Proceedings of the Combustion Institute*, vol. 31, pp. 1149–1156, 2007.

[8] D.I. Kolaitis and M.A. Founti, "A tabulated chemistry approach for numerical modeling of diesel spray evaporation in a “stabilized cool flame” environment," *Combustion and Flame*, vol. 145, no. 1-2, pp. 259-271 , 2006.

[9] P.G. Lignola and E. Reverchon, "Cool flames," *Progress in Energy and Combustion Science*, vol. 13, no. 1, pp. 75–96, 1987.

[10] S.R. Hoffman and J. Abraham, "A comparative study of n-heptane, methyl decanoate, and dimethyl ether combustion characteristics under homogeneous-charge compression–ignition engine conditions," *Fuel*, vol. 88, no. 6, pp. 1099-1108 , 2009.

[11] T. Rente, V. I. Golovitchev, and I. Denbratt, "Numerical Study of n-Heptane Spray Auto-Ignition at Different Levels of Pre-Ignition Turbulence," in *Thermo- and Fluid Dynamics, COMODIA 2001*, 2001.

[12] A. Donkerbroek, "Combustion in an optical diesel engine studied by light-based diagnostics," Radboud University Nijmegen, PhD Thesis 2010.

[13] M.J. Murphy, J.D. Taylor, and R.L. McCormick, "Compendium of Experimental Cetane Number Data," National Renewable Energy Laboratory, Subcontractor report 2004.

[14] J.M. Simmie, "Detailed chemical kinetic models for the combustion of hydrocarbon fuels," *Progress in Energy and Combustion Science*, vol. 29, no. 6, pp. 599-634 , 2003.

[15] J.C.G. Andrae, "Development of a detailed kinetic model for gasoline surrogate fuels," *Fuel*, vol. 87, no. 10-11, pp. 2013-2022, 2007.

[16] H.J. Curran, P. Gaffuri, W.J. Pitz, and C.K. Westbrook, "A Comprehensive Modeling Study of n-Heptane Oxidation," *Combustion and Flame*, vol. 114, no. 1/2, pp. 149-177, 1998.

[17] J. F. Griffiths, "Reduced kinetic models and their application to practical combustion systems ," *Progress in Energy and Combustion Science*, vol. 21, no. 1, pp. 25-107 , 1995.

[18] S. Jay and O. Colin, "A variable volume approach of tabulated detailed chemistry and its applications to multidimensional engine simulations," *Proceedings of the Combustion Institute*, vol. 33, no. 2, pp. 3065-3072 , 2011.

[19] M. Baburić, "Numerically efficient modelling of turbulent non-premixed flames," Department of Energy, Power Engineering and Environment, University of Zagreb, Zagreb, PhD Thesis 2005.

[20] M. Baburić et al., "Steady laminar flamelet concept and hybrid turbulence modelling strategy applied on numerical simulation of a turbulent piloted jet

diffusion flame," in *Proceedings 2nd International Workshop on trends in numerical and physical modelling of turbulent processes in gas turbine combustors*, Germany, 2004, pp. 45-51.

[21] A. W. Cook, J. J. Riley, and G. Kosaly, "A Laminar Flamelet Approach to Subyrid-Scale Chemistry in Turbulent Flows," *Combustion and Flame*, vol. 109, pp. 332-341, 1997.

[22] C. Chen, M. Bardsley, and R. Johns, "Two-Zone Flamelet Combustion Model," SAE Paper 2000-01-2810 2000.

[23] S. Singh, R. D. Reitz, and M. P. B. Musculus, "Comparison of the characteristic time (CTC), representative interactive flamelet (RIF), and direct integration with detailed chemistry models against optical diagnostic data for multi-mode combustion in a heavy-duty DI diesel engine," SAE paper 2006-01-0055 2006.

[24] H. Pitsch, H. Barths, and N. Peters, "Three-Dimensional Modeling of NOx and Soot Formation in DI-Diesel Engines Using Detailed Chemistry Based on the Interactive Flamelet Approach," SAE Paper 962057 1996.

[25] J.C. Ferreira, R. Bender, and H. Forkel, "A presumed PDF-ILDM model for the CFD-analysis of turbulent combustion," *Progress in Computational Fluid Dynamics*, vol. 5, no. 6, pp. 327 - 333, 2005.

[26] G. Ribert, O. Gicquel, N. Darabiha, and D. Veynante, "Tabulation of complex chemistry based on self-similar behavior of laminar premixed flames," *Combustion and Flame*, vol. 146, no. 4, pp. 649-664, 2006.

[27] F. Contino, H. Jeanmart, T. Lucchini, and G. D'Errico, "Coupling of in situ adaptive tabulationnext term and dynamic previous termadaptivenext term chemistry: An effective method for solving combustion in engine simulations," *Proceedings of the Combustion Institute*, vol. 33, no. 2, pp. 3057-3064, 2011.

[28] V. Bykov and U. Maas, "Extension of the ILDM method to the domain of slow chemistry," *Proceedings of the Combustion Institute*, vol. 31, no. 1, pp.

465-472, 2007.

[29] B. Fiorina et al., "Modelling non-adiabatic partially premixed flames using flame-prolongation of ILDM," *Combustion Theory and Modelling*, vol. 7, no. 3, pp. 449-470 , 2003.

[30] C. Bekdemir, L.M.T. Somers, and L.P.H. de Goey, "Modeling diesel engine combustion using pressure dependent Flamelet Generated Manifolds," *Proceedings of the Combustion Institute*, vol. 33, no. 2, pp. 2887-2894, 2011.

[31] O. Colin, A. Pires da Cruz, and S, Jay, "Detailed chemistry-based auto-ignition model including low temperature phenomena applied to 3-D engine calculations," *Proceedings of the Combustion Institute*, vol. 30, no. 2, pp. 2649-2656, 2005.

[32] O. Colin and A. Benkenida, "The 3-Zones Extended Coherent Flame Model (ECFM3Z) for Computing Premixed/Diffusion Combustion," *Oil & Gas Science and Technology - Rev. IFP*, vol. 59, no. 6, pp. 593-609, 2004.

[33] O. Colin, A. Benkenida, and C. Angelberger, "3D Modeling of Mixing, Ignition and Combustion Phenomena in Highly Stratified Gasoline Engines," *Oil & Gas Science and Technology - Rev. IFP*, vol. 58, no. 1, pp. 47-62, 2003.

[34] M. Zellat, D. Abouri, and T. Conte, "Advanced modeling of GDI and DI Diesel Engines: Investigations on Combustion and High EGR level," in *15th International Multidimensional Engine User's Meeting at the SAE Congress*, Detroit, 2005.

[35] C. Pera, O. Colin, and S. Jay, "Development of a FPI Detailed Chemistry Tabulation Methodology for Internal Combustion Engines," *Oil & Gas Science and Technology - Rev. IFP* , vol. 64, no. 3, pp. 243 - 258, 2009.

[36] W. W. Kim, S. Menon, and H. Mongia, "Numerical Simulations of Reacting Flows in a Gas Turbine Combustor," *Combustion Science and Technology*, vol. 143, pp. 25-62, 1999.

[37] B. S. Brewster, S. M. Cannon, J. R. Farmer, and F. Meng, "Modeling of lean

premixed combustion in stationary gas turbines," *Progress in Energy and Combustion Science*, vol. 25, no. 4, pp. 353-385 , 1999.

[38] J. Warnatz, U. Maas, and R.W. Dibble, *Combustion: Physical and Chemical Fundamentals, Modeling and Simulation, Experiments, Pollutant Formation.*: Springer, 2006.

[39] P.G. Aleiferis, A.G. Charalambides, Y. Hardalupas, A.M.K.P. Taylor, and Y. Urata, "Axial fuel stratification of a homogeneous charge compression ignition (HCCI) engine," *International Journal of Vehicle Design*, vol. 44, no. 1-2, pp. 41-61, 2007.

[40] N. Docquier, "Experimental Investigations in an Optical HCCI Diesel Engine," in *19th International Colloquium on the Dynamics of Explosions and Reactive Systems*, 2003.

[41] J. Abraham, F.V. Bracco, and R. D. Reitz, "Comparison of Computed and Measured Premixed Charge Engine Combustion," *Combustion and Flame*, vol. 60, pp. 309-322, 1985.

[42] U.B. Azimov, K.S. Kim, D. S. Jeong, and Y. G. Lee, "Evaluation of low-temperature diesel combustion regimes with n-Heptane fuel in a constant-volume chamber," *International Journal of Automotive Technology*, vol. 10, no. 3, pp. 265-276, 2009.

[43] N. Peters, "Laminar Flamelet Concepts in Turbulent Combustion," in *Proceedings of the 21st Symposium (International) on Combustion*, Pittsburgh, 1986.

[44] N. Peters, *Turbulent Combustion*. Cambridge, UK: Cambridge University Press, 2000.

[45] H. Pitsch and N. Peters, "A consistent flamelet formulation for non-premixed combustion considering differential diffusion effects," *Combustion and Flame*, vol. 114, pp. 26-40, 1998.

[46] H. Pitsch, M Chen, and N. Peters, "Unsteady Flamelet Modeling of Turbulent

Hydrogen-Air Diffusion Flames," in *Proceedings of the 27th Symposium (International) on Combustion*, Pittsburgh, 1998.

[47] C. Hasse, G. Bikas, and N. Peters, "Modeling DI Diesel Combustion using the Eulerian Particle Flamelet Model," SAE Paper 2000-01-2934 2000.

[48] S.K. Kim and Y. Kim., "Assessment of the Eulerian particle flamelet model for nonpremixed turbulent jet flames," *Combustion and Flame*, vol. 154, no. 1-2, pp. 232-247 , 2008.

[49] A.Y. Klimenko, "Multicomponent Diffusion of Various Admixtures in Turbulent Flow," *Fluid Dynamics*, vol. 25, no. 3, pp. 327-334, 1990.

[50] R.W. Bilger, "Conditional Moment Closure for Turbulent Reacting Flow," *Physics of Fluids*, vol. 5, no. 2, pp. 436-444, 1993.

[51] A.Y. Klimenko and R.W. Bilger, "Conditional moment closure of turbulent combustion," *Progress in Energy and Combustion Science*, vol. 25, pp. 595–687, 1999.

[52] S. B. Pope, "Computations of turbulent combustion: Progress and challenges," *Proceedings of the Combustion Institute*, vol. 23, pp. 591–612, 1990.

[53] Y.Z. Zhang, E.H. Kung, and D.C. Haworth, "A PDF method for multidimensional modeling of HCCI engine combustion: effects of turbulence/chemistry interactions on ignition timing and emissions ," *Proceedings of the Combustion Institute*, vol. 30, no. 2, pp. 2763-2771 , 2005.

[54] P.K. Jha and C. P. T. Grothy, "Parallel Adaptive Mesh Refinment Scheme with Presumed Conditional Moment and FPI Tabulated Chemistry for Turbulent Non-Premixed Combustion," AIAA Paper 2011-0206 2011.

[55] F. Marble and J. Broadwell, "The coherent flame model of non-premixed turbulent combustion," Purdue University, Project Squid TRW-9-PU 1977.

[56] A. S. Wu and K. N. C. Bray, "A coherent flame model of premixed turbulent

combustion in a counterflow geometry," *Combustion and Flame*, vol. 109, no. 1-2, pp. 43-64 , 1997.

[57] E. Van Kalmthout and D. Veynante, "Direct numerical simulations analysis of flame surface density models for nonpremixed turbulent combustion ," *Physics of Fluids*, vol. 10, pp. 2347 -2369, 1998.

[58] F.A. Tap, R. Hilbert, D. Thévenin, and D. Veynante, "A Generalized Flame Surface Density Modelling Approach for the Auto-Ignition of a Turbulent Non-Premixed System," *Combustion Theory and Modelling*, vol. 8, no. 1, pp. 163-193, 2004.

[59] L. Vervisch, R. Hauguel, P. Domingo, and M. Rullaud, "Three facets of turbulent combustion modelling: DNS of premixed V-flame, LES of lifted nonpremixed flame and RANS of jet-flame," *Journal of Turbulence*, vol. 4, pp. 1-36, 2004.

[60] P. Domingo, L. Vervisch, and R. H. Sandra Payet, "DNS of a premixed turbulent V-flame and LES of a ducted flame using a FSD-PDF subgrid scale closure with FPI-tabulated chemistry," *Combustion and Flame*, vol. 134, no. 4, pp. 566-586, 2005.

[61] O. Gicquel, N. Darabiha, and D. Thévenin, "Laminar premixed hydrogen/air counterflow flame simulations using flame prolongation of ILDM with differential diffusion," *Proceedings of the Combustion Institute*, vol. 28, no. 2, pp. 1901-1908 , 2000.

[62] A. Pires da Cruz, "Three-dimensional Modeling Of Self-Ignition in HCCI and Conventional Diesel Engines," *Combustion Science and Technology*, vol. 176, no. 5-6, pp. 867-887, 2004.

[63] R. J. Kee, F. M. Rupley, and J. A. Miller, "Chemkin-II: A Fortran chemical kinetics package for the analysis of gas-phase chemical kinetics," Sandia National Laboratory, Report No. SAND89-8009.UC401, 1989.

[64] A.E. Lutz, R.J. Kee, and J.A. Miller, "SENKIN: A Fortran Program for Predicting Homogeneous Gas Phase Chemical Kinetics with Sensitivity

Analysis," Sandia National Laboratory, Report No. SAND87-8248.UC-4, 1987.

[65] N. Duić, "Contribution to the Mathematical Modelling of Gaseous Fuel Combustion in a Steam Generator Furnace," Department of Energy, Power Engineering and Environment, University of Zagreb, Zagreb, PhD thesis (in Croatian) 1998.

[66] C.K. Law, "Heat and mass transfer in combustion, Fundamental concepts and analytical techniques," *Progress in Energy and Combustion Science*, vol. 10, pp. 295-318, 1984.

[67] Z. Gomzi, *Kemijski reaktori*, 2nd ed. Zagreb, Croatia: Hinus, 2009.

[68] "Chemkin-PRO Software, Tutorials Manual," Reaction Design, CK-TUT-15082-0809-UG-1 2008.

[69] C. N. Markides. (2004) Advanced Autoignition Theory / Introduction. [Online]. http://www2.eng.cam.ac.uk/~cnm24/autoignition.htm

[70] M. Ban and N. Duić, "Adaptation of N-heptane Autoignition Tabulation for Complex Chemistry Mechan," *Thermal Science*, vol. 15, no. 1, pp. 137-146, 2011.

[71] J.R. Yang and S.C. Wong, "On the suppression of negative temperature coefficient (NTC) in autoignition of n-heptane droplets," *Combustion and Flame*, vol. 132, no. 3, pp. 475-491 , 2003.

[72] "PREMIX: A Program for Modeling Steady, Laminar, One-dimensional Premixed Flames," Reaction Design, PRE-036-1 2000.

[73] M. Baburić. (2003) CSC Solver. [Online]. http://powerlab.fsb.hr/mbaburic/CSC.htm

[74] J. F. Grcar, "The Twopnt Program for Boundary Value Problems," Sandia National Laboratories, Report 1992.

[75] W.E. Stewart, M. Caracotsios, and J.P. Sorensen, "DDASAC Software Package Documentation," University of Wisconsin, Madison, 1995.

[76] P.N. Brown, G.D. Byrne, and A.C. Hindmarsh, "VODE, a Varible-Coefficient ODE Solver," Lawrence Livermore National Laboratory, Livermore, 1988.

[77] S.B. Pope, "Predictive Turbulent Combustion Models for 21st Century Transportation Fuels," in *Abstract book of First Annual Conference of the Combustion Energy Frontier Research Center*, Princeton, 2010, pp. 89-93.

[78] G. Blanquart, P. Pepiot-Desjardins, and H. Pitsch, "Chemical mechanism for high temperature combustion of engine relevant fuels with emphasis on soot precursors," *Combustion and Flame*, vol. 156, pp. 588–607, 2009.

[79] D. R. Schneider, "Investigation of the possibility of the SO3 reduction during heavy-oil fuel combustion," Department of Energy, Power Engineering and Environment, University of Zagreb, Zagreb, PhD thesis (in Croatian) 2002.

[80] Ž. Bogdan, N. Duić, and D. R. Schneider, "Three-dimensional simulation of the performance of an oil-fired combustion chamber," in *Proceedings of the 2nd European Thermal Sciences & 14th UIT National Heat Transfer Conference*, Rome, 1996.

[81] M Vujanovic, N Duić, and R Tatschl, "Validation of reduced mechanisms for nitrogen chemistry in numerical simulation of a turbulent non-premixed flame," *Reaction Kinetics and Catalysis Letters*, vol. 96, no. 1, pp. 125-138, 2009.

[82] K. Kuo, *Principles of Combustion*.: John Wiley and Sons, 1986.

[83] Y.H. Chen and J.Y. Chen, "Development of Isooctane Skeletal Mechanisms for Fast and Accurate Predictions of SOC and," in *Fall Meeting Western States Combustion Institute*, Stanford, 2005.

[84] H.N Najm, A. G. Dimitris, F. Donato, F. Creta, and M. Valorani, "A CSP-Based Skeletal Mechanisma Generation Procedure: Auto-Ignition and Premixed Lemaninar Flame in n_Heptane/Air Mixtures," in *Proceedings of ECCOMAS CFD 2006*, 2006.

[85] D.I. Kolaitis and M.A. Founti, "A 3D CFD Modelling Study of a Diesel Oil

Evaporation Device Operating in the “Stabilized Cool Flame” regime," in *Seventh International Conference on CFD in the Minerals and Process Industries Proceedings*, 2009.

[86] A.A. Pekalski. et al., "The relation of cool flames and auto-ignition phenomena to process safety at elevated pressure and temperature," *Journal of Hazardous Materials*, vol. 93, pp. 93-105, 2002.

[87] H. Pearlman, "Multiple cool flames in static, unstirred reactors under reduced-gravity and terrestrial conditions," *Combustion and Flame*, vol. 148, pp. 280-284, 2007.

[88] S. Tanaka, F. Ayala, and J. C. Keck, "A reduced chemical kinetic model for HCCI combustion of primary reference fuel in a rapid compressio machine," *Combustion and Flame*, vol. 133, pp. 467-481, 2003.

[89] N. Peters, G. Paczko, R. Seiser, and K. Seshadri, "Temperature Cross-Over and Non-Thermal Runaway at Two-Stage Ignition of NHeptane," *Combustion and Flame*, vol. 128, no. 1-2, pp. 38-59 , 2002.

[90] M. Valorani, F. Creta, F. Donato, H. N. Najm, and D. A. Goussis, "Skeletal mechanism generation and analysis for n-heptane with CSP," *Proceedings of the Combustion Institute*, vol. 31, no. 1, pp. 483-490, 2007.

[91] B. Bhattacharjee, D. Schwer, P. Barton, and W. Green, "Optimally-reduced kinetic models: reaction elimination in large-scale kinetic mechanisms," *Combustion and Flame* , vol. 135, no. 3, pp. 191-208, 2003.

[92] T. Lu and C. Law, "A directed relation graph method for mechanism reduction," *Proceedings of the Combustion Institute*, vol. 30, no. 1, pp. 1333-1341, 2005.

[93] P. Pepiot and H. Pitsch, "Systematic reduction of large chemical mechanism," in *Proceedings of the 4th Joint Meeting of the US Sections of the Combustion Institute*, 2005.

[94] M. Hamdi, H. Benticha, and M. Sassi, "Evaluation of Reduced Chemical

Kinetic Mechanisms Used for Modelling Mild Combustion for Natural Gas," *Thermal Science* , vol. 13, no. 3, pp. 131-137, 2009.

[95] R. Ennetta, M. Hamdi, and R. Said, "Comparison of Different Chemical Kinetic Mechanisms of Methane Combustion in an Internal Combustion Engine Configuration," *Thermal Science* , vol. 12, no. 1, pp. 43-51, 2008.

[96] S.S. Ahmed, F. Mauss, G. Moréac, and T. Zeuch, "A comprehensive and compact n-heptane oxidation model derived using chemical lumping," *Physical Chemistry Chemical Physics*, vol. 9, pp. 1107-1126, 2007.

[97] J. C. Hewson. (1997) Pollutant Emissions from Nonpremixed Hydrocarbon Flames. Doctoral dissertation.

[98] H. Seiser, Pitsch H., Seshadri K., Pitz W.J., and Curran H.J., "Extinction and Autoignition of n-Heptane in Counterflow Configuration," *Proceedings of the Combustion Institute*, vol. 28, pp. 2029-2037, 2000.

[99] S. Liu, J.C. Hewson, J. H. Chen, and H. Pitsch, "Effects on Strain Rate on High-Pressure Nonpremixed N-Heptane Autoignition in Counterflow," *Combustion and Flame*, vol. 137, pp. 320-339, 2004.

[100] S. Jerzembeck, N. Peters, P. Pepiot-Desjardins, and H. Pitsch, "Laminar Burning Velocities at High Pressure for Primary Reference Fuels and Gasoline: Experimental and Numerical Investigation," *Combustion and Flame*, vol. 156, no. 2, pp. 292-301, 2009.

[101] P. Pepiot-Desjardins and H. Pitsch, "An automatic chemical lumping method for the reduction of large chemical kinetic mechanisms," *Combustion Theory And Modelling*, vol. 12, no. 6, pp. 1089-1108, 2008.

[102] J. Andrae, D. Johansson, P. Björnbom, P. Risberg, and G. Kalghatgi, "Co-oxidation in the auto-ignition of primary reference fuels and n-heptane/toluene blends," *Combustion and Flame*, vol. 140, no. 4, pp. 267-286 , 2005.

[103] K. Natarajan and KA. Bhaskaran, "An experimental and analytical

investigation of high temperature ignition of ethanol," in *Proceedings of the 13th International Symposium on Shock Tubes and Waves*, 1981, pp. 834-842.

[104] A.A. Konnov, "Development and validation of a detailed reaction mechanism for the combustion of small hydrocarbons," in *Proceedings of the 28-th International Symposium on Combustion*, Edinburgh, 2000, p. 317.

[105] A.A. Konnov, "Implementation of the NCN pathway of prompt-NO formation in the detailed reaction mechanism," *Combustion and Flame*, vol. 156, pp. 2093–2105, 2009.

[106] K.J. Hughes, T. Turanyi, A.R. Clague, and M.J. Pilling, "Development and Testing of a Comprehensive Chemical Mechanism for the Oxidation of Methane," *International Journal of Chemical Kinetics*, vol. 33, no. 9, pp. 513–538, 2001.

[107] H. Wang et al. (2007) USC Mech Version II. High-Temperature Combustion Reaction Model of H2/CO/C1-C4 Compounds. [Online]. http://ignis.usc.edu/USC_Mech_II.htm

[108] H.J. Curran et al., "Experimental and Modeling Study of Premixed Atmospheric-pressure Dimethyl Ether-Air Flames".

[109] P. Dagaut, C. Daly, J.M. Simmie, and M. Cathonnet, "The oxidation and ignition of dimethylether from low to high temperature (500–1600 K): Experiments and kinetic modeling," in *Twenty-Seventh Sysposium (International) on Combustion Volume One* , 1998, pp. Pages 361-369.

[110] "AVL FIRE(TM), CFD solver v8.4," AVL LIST GmbH, Graz, 2005.

[111] "MATLAB - Manual and help documentation," version 7.5.0 2007.

[112] D. Garcia, "Robust smoothing of gridded data in one and higher dimensions with missing values," *Computational Statistics and Data Analysis*, vol. 54, pp. 1167-1178, 2010.

[113] M. Metgalchi and J.C. Keck., "Burning velocities of mixtures of air with

methanol, iso-octane, and idolene at high pressure and temperature," *Combustion and Flame*, vol. 48, pp. 191-210, 1982.

[114] B.T. Shaw, "Modelling and Control of Automotive Coldstart Hydrocarbon Emissions," University of California, Berkley, PhD Thesis 2002.

[115] S.M. Frolov, "Flame tracking method for modeling turbulent combustion and pollutant formation," N. N. Semenov Institute of Chemical Physics, Moscow, Final Internal Report 2010.

[116] J.C. Tannehill, D.A. Anderson, and R.H. Pletcher, *Computational fluid mechanics and heat transfer*.: Taylor & Francis, 1997.

[117] T. Cebeci, J. P. Shao, F. Kafyeke, and E. Laurendeau, *Computational Fluid Dynamics for Engineers*.: Springer, 2005.

[118] S.V. Patankar, *Numerical Heat Transfer and Fluid Flow*. New York: Hemisphere, 1980.

[119] I. Alfirević, *Uvod u tenzore i mehaniku kontinuuma*. Zagreb: Golden marketing, 2003.

[120] T. Poinsot and D. Veynante, *Theoretical and Numerical Combustion*. Philadelphia: R.T. Edwards, Inc., 2001.

[121] T. Baritaud, T. Poinsot, and M. Baum, *Direct numerical simulation for turbulent reacting flows*.: Editions TECHNIP, 1996.

[122] M. Griebel, T. Dornseifer, and T. Neunhoeffer, *Numerical simulation in fluid dynamics: a practical introduction*, SIAM, Ed., 1998.

[123] A. W. Cook and J. J Riley, "Direct Numerical Simulation of a Turbulent Reactive Plume on a Parallel Computer," *Journal of Computational Physics*, vol. 129, pp. 263-283, 1996.

[124] W. Frost and T. H. Moulden, *Handbook of Turbulence*. New York: Plenum Press, 1977.

[125] D.C. Wilcox, *Turbulence modeling for CFD*.: DCW Industries, Inc., 1994.

[126] L.C. Berselli, T.Iliescu, and W.J. Layton, *Mathematics of large eddy*

simulation of turbulent flows, Springer, Ed., 2006.

[127] Q. Wang and K. D. Squires, "Large Eddy Simulation of Particle Laden Turbulent Channel Flow," *Physics of Fluids*, vol. 8, no. 5, pp. 1207-1223, 1996.

[128] M. P. Martin, U. Piomelli, and G. V. Candler, "Subgrid-scale models for compressible large-eddy simulations," *Theoretical and Computational Fluid Dynamics*, vol. 13, pp. 361-376, 2000.

[129] F. Ducros et al., "Large-Eddy Simulation of the Shock,/Turbulence Interaction," *Journal of Computational Physics*, vol. 152, pp. 517-549, 1999.

[130] S. Menon and W. H. Jou, "Large-eddy Simulations of Combustion Instability in an Axisymmetric Ramjet Combustor," *Combustion Science and Technology*, vol. 75, pp. 53-72, 1991.

[131] M. Baburić, R. Tatschl, and N. Duić, "Numerical simulation of jet diffusion flames with radiative heat transfer modeling," in *Proceedings of ASME Heat Transfer Conference*, USA, 2005.

[132] A.A. Ranjbar, K Sedighi, M. Farhadi, and M. Pourfallah, "Computational Study of the Effect of Different Injection Angle on Heavy Duty Diesel Engine Combustion," *Thermal Science*, vol. 13, no. 3, pp. 9-21, 2009.

[133] W. P. Jones and B. E. Launder, "The prediction of laminarization with a two-equation model of turbulence," *International Journal of Heat and Mass Transfer*, vol. 15, pp. 301-314, 1972.

[134] K. Hanjalic, M. Popovac, and M. Hadžiabdić, "A robust near-wall elliptic-relaxation eddy-viscosity turbulence model for CFD," *International Journal of Heat and Fluid Flow*, vol. 25, pp. 1047-1051, 2004.

[135] M. Popovac and K. Hanjalić, "Compound Wall Treatment for RANS Computation of Complex Turbulent Flows and Heat Transfer," *Flow Turbulence Combust*, vol. 78, pp. 177-202, 2007.

[136] W. Ghedhaifi, N. Darabiha, O. Gicquel, D. Veynante, and D. Pierrot, "A

Flame Surface Density Model Including Tabulated Chemistry," in *20th International Colloquium on the Dynamics of Explosions and Reactive Systems*, 2005.

[137] F. Halter, C. Chauveau, I. Gökalp, and D. Veynante, "Analysis of Flame Surface Density Measurements in Turbulent Premixed Combustion," *Combustion and Flame*, vol. 156, pp. 657-664, 2009.

[138] J. Michel, O. Colin, and D. Veynante, "Modeling ignition and chemical structure of partially premixed turbulent flames using tabulated chemistry," *Combustion and Flame*, vol. 152, no. 1-2, pp. 80-99, 2008.

[139] E.R. Hawkes and J.H. Chen, "Evaluation of models for flame stretch due to curvature in the thin reaction zones regime," *Proceedings of the Combustion Institute*, vol. 30, no. 1, pp. 647-655, 2005.

[140] E. Mastorakos, "Ignition of turbulent non-premixed flames," *Progress in Energy and Combustion Science*, vol. 35, no. 1, pp. 57-97, 2009.

[141] V. Knop and S. Jay, "Latest Developments in Gasoline Auto-Ignition Modelling Applied to an Optical CAI(TM) Engine," *Oil & Gas Science and Technology – Rev. IFP*, vol. 61, no. 1, pp. 121-137, 2006.

[142] V. Knop, A. Benkenida, S. Jay, and O. Colin, "Modelling of combustion and nitrogen oxide formation in hydrogen-fuelled internal combustion engines within a 3D CFD code," *International Journal of Hydrogen Energy.*, vol. 33, pp. 5083–5097, 2008.

[143] M. Baburić, D.R. Schneider, Ž. Bogdan, and N. Duić, "User function approach in combustion and radiation modelling in commercial CFD environment," *Transactions of FAMENA*, vol. 26, no. 2, pp. 1-12, 2002.

[144] P. Priesching, G. Ramusch, J. Ruetz, and R. Tatschl, "3D-CFD Modeling of Conventional and Alternative Diesel Combustion and Pollutant Formation – A Validation Study," SAE Paper 2007-01-1907 2007.

Curriculum Vitae

Name and family name:	Marko Ban
E-mail:	marko.ban@fsb.hr
Web:	http://powerlab.fsb.hr/ban

Date of birth:	24. August 1977.
Place of birth:	Zagreb, Croatia
Primary school:	1984. - 1994. Primary schools 'Medvedgrad'/Retkovec', Zagreb
High school:	1992. - 1996. XV. Gimnasium, Zagreb
Study:	1996. - 2004. University of Zagreb, Faculty of Mechanical Engineering and Naval Architecture
Post-graduate study:	2004. - .2011. University of Zagreb, Faculty of Mechanical Engineering and Naval Architecture, Department of Energy, Power Engineering and Environment
Occupation or position held:	February 2005. Research assistant at Faculty of Mechanical Engineering and Naval Architecture, Department of Energy, Power Engineering and Environment
Projects	2004 - .

	Research assistant at project 'Implementation of a New Oil Combustion model into the FIRE code', project leader prof..dr.sc. Neven Duić
Language:	English German (communicational level)
Membership:	European Research Community On Flow, Turbulence And Combustion Croatian Section of The Combustion Institute International Centre for Sustainable Development of Water, Energy and Environment System

---

Ime i prezime:	Marko Ban
E-mail:	marko.ban@fsb.hr
Web:	http://powerlab.fsb.hr/ban

Datum rođenja:	24. kolovoza 1977.
Mjesto rođenja:	Zagreb, Hrvatska
Osnovna škola:	1984. - 1992. Osnovna škola 'Medvedgrad'/'Retkovec', Zagreb
Srednja škola:	1992. - 1996. XV. Gimnazija, Zagreb
Studij:	1996. - 2004. Sveučilište u Zagrebu, Fakultet strojarstva i brodogradnje, studij strojarstva, procesno-enrgetski smjer

Poslijediplomski studij:	2004. – 2011. Sveučilište u Zagrebu, Fakultet strojarstva i brodogradnje, poslijediplomski studij strojarstva, procesno-energetski smjer
Zaposlenja:	Veljača 2005. znanstveni novak na Fakultetu strojarstva i brodogradnje, Zavod za energetska postrojenja, energetiku i ekologiju
Sudjelovanje na projektima	2004 - . Istraživač na projektu 'Implementation of a New Oil Combustion model into the FIRE code', nositelj projekta prof..dr.sc. Neven Duić
Znanje jezika:	Engleski Njemački (komunikacijska razina)
Članstva:	European Research Community On Flow, Turbulence And Combustion Croatian Section of The Combustion Institute